



2008-10-02

Design and Analysis of a Positively Engaged Continuously Variable Transmission

Brandon Levi Haupt

Brigham Young University - Provo

Follow this and additional works at: <https://scholarsarchive.byu.edu/etd>

 Part of the [Mechanical Engineering Commons](#)

BYU ScholarsArchive Citation

Haupt, Brandon Levi, "Design and Analysis of a Positively Engaged Continuously Variable Transmission" (2008). *All Theses and Dissertations*. 1917.

<https://scholarsarchive.byu.edu/etd/1917>

This Thesis is brought to you for free and open access by BYU ScholarsArchive. It has been accepted for inclusion in All Theses and Dissertations by an authorized administrator of BYU ScholarsArchive. For more information, please contact scholarsarchive@byu.edu, ellen_amatangelo@byu.edu.

CONCEPTUAL DESIGN AND ANALYSIS OF A POSITIVELY ENGAGED
CONTINUOUSLY VARIABLE TRANSMISSION

by

B. Levi Haupt

A thesis submitted to the faculty of

Brigham Young University

in partial fulfillment of the requirements for the degree of

Master of Science

Department of Mechanical Engineering

Brigham Young University

December 2008

Copyright © 2008 B. Levi Haupt

All Rights Reserved

BRIGHAM YOUNG UNIVERSITY

GRADUATE COMMITTEE APPROVAL

of a thesis submitted by

B. Levi Haupt

This thesis has been read by each member of the following graduate committee and by majority vote has been found to be satisfactory.

Date

Robert H. Todd, Chair

Date

Kenneth W. Chase

Date

Brian D. Jensen

BRIGHAM YOUNG UNIVERSITY

As chair of the candidate's graduate committee, I have read the thesis of B. Levi Haupt in its final form and have found that (1) its format, citations, and bibliographical style are consistent and acceptable and fulfill university and department style requirements; (2) its illustrative materials including figures, tables, and charts are in place; and (3) the final manuscript is satisfactory to the graduate committee and is ready for submission to the university library.

Date

Robert H. Todd
Chair, Graduate Committee

Accepted for the Department

Larry L. Howell
Graduate Coordinator

Accepted for the College

Alan R. Parkinson
Dean, Ira A. Fulton College of Engineering
and Technology

ABSTRACT

CONCEPTUAL DESIGN AND ANALYSIS OF A POSITIVELY ENGAGED CONTINUOUSLY VARIABLE TRANSMISSION

B. Levi Haupt

Department of Mechanical Engineering

Master of Science

With energy demands at an all time high, mechanical power systems are under great scrutiny. Substantial efforts are being made throughout the world to reduce energy use in common mechanical systems such as the internal combustion engine and transmission system. Eliminating or reducing efficiency losses in the transmission is a potential source of improving the efficiency of the system. To do so, various alternative types of transmissions are being investigated. At Brigham Young University, development of a Positively Engaged Continuously Variable Transmission (PECVT) is progressing.

In addition to the efficiency increases that would occur as a result of operating the engine at a more constant speed, a PECVT type transmission may reduce efficiency losses that occur in a standard transmission by eliminating the disengagement of involute gear sets to change gear ratios of the transmission. For a PECVT, this is done by maintaining engagement of the input and output members of the transmission, while

changing the gear ratio. Both of these types of losses are major contributing factors to the overall efficiency of the transmission and engine system, thus a PECVT is of great interest.

The investigation for developing a feasible PECVT began with the identification of a behavioral issue identified in all known PECVT embodiments. This behavioral issue, known as the Non-Integer-Tooth-Problem (NITP), is due to the geometry of an involute gear and prevents specific gear ratios from being achieved.

The research effort presented in this thesis returns to the conceptual design of a PECVT to address involutometry along with the NITP. A design tool entitled the Line-of-Action Model is developed which assists in quantifying how a conceptual solution can address the NITP using involutometry principles. As a result of the Line-of-Action Model, the Hybrid Involute Profile was discovered. Due to the simplicity of The Hybrid Involute Profile, it has proven to be an elegant solution to the NITP.

Validation of the Hybrid Involute Profile concept was conducted to ensure that this concept satisfies the objectives and requirements of a PECVT and solves the NITP. The validation was completed using two case studies and a theoretical analysis.

As a result of the validation, the Hybrid Involute Profile is declared a conceptual principal solution to the NITP. Fulfillment of the PECVT objectives, requirements list and elimination of the NITP by the Hybrid Involute Profile is also demonstrated.

With the Hybrid Involute Profile as the conceptual principle solution, the development of a commercially viable PECVT is believed to be attainable.

ACKNOWLEDGMENTS

It has been a great privilege to work on such a technical research project. I would like to express my appreciation to Vernier Moon Technologies who has sponsored this project. The faculty and administrators of Brigham Young University have been of great worth during this project. It has been a privilege to learn both spiritual and secular skills from such remarkable men and women. In particular Dr. Robert Todd, who has become a lifelong friend and mentor and has contributed to my education in countless ways. Also Dr. Ken Chase, Dr. Brian Jensen and Dr. Carl Sorensen have assisted in this research such that without their assistance the outcome would not have been achieved.

The support of my fellow student research colleagues Chris Lewis, Isaac Jones, and Ryan Dalling and have been of great worth. Their encouragement, insight and enthusiasm have progressed this work when at times the future seemed uncertain.

I express gratitude to my dearest friend and bride Torrie. Without her encouragement, support, and sacrifice this research would not have been possible. Her countless examples of diligence and sacrifice continue to strengthen me to this day.

Ultimately I express gratitude to my Savior Jesus Christ. Through this research I have learned of the innumerable ways in which he has blessed and shaped my life. In addition this research has taught me to rely on my savior for support in every endeavor I pursue.

TABLE OF CONTENTS

| | |
|---|-----------|
| LIST OF TABLES | ix |
| LIST OF FIGURES | xi |
| 1. Introduction..... | 1 |
| 1.1. PECVT History | 3 |
| 1.2. Desired PECVT Behavior | 4 |
| 1.3. Problem Statement | 5 |
| 1.4. Hypothesis | 5 |
| 1.5. Research Objectives | 6 |
| 1.6. Organization | 6 |
| 2. PECVT Technology | 9 |
| 2.1. PECVT Product Development Process | 10 |
| 2.2. Conceptual Design Limitations | 28 |
| 2.3. Assumption Rectifications | 32 |
| 3. Conceptual Design Method | 33 |
| 3.1. Technical Scope of the Conceptual Design Phase | 33 |
| 3.2. Conceptual Design Process Layout | 34 |
| 3.3. Embodiment Design Phase Concluding Remarks | 38 |
| 4. Involutometry | 41 |
| 4.1. Requirements List | 42 |
| 4.2. The Essential Problem and Functional Structures | 43 |
| 4.3. Working Principles | 44 |
| 4.4. Involute Curve Definitions | 44 |
| 4.5. Involute Curve Relationships | 47 |
| 4.6. Radius to the Involute Form | 51 |
| 4.7. Involute Curve Generation | 51 |
| 4.8. Involute Curve Properties | 51 |

| | | |
|-------------------|---|------------|
| 4.9. | Involotometry Significance | 64 |
| 5. | The Line of Action Model..... | 67 |
| 5.1. | Working Structures | 70 |
| 5.2. | Suitable Combinations and Firm Up..... | 91 |
| 5.3. | Line-of-Action-Model Validation and Case Studies..... | 96 |
| 5.4. | The Principal Solution..... | 105 |
| 6. | Conclusion and Recommendations | 107 |
| 6.1. | Conclusions | 107 |
| 6.2. | Recommendations | 111 |
| 7. | References | 116 |
| Appendix A | | 118 |

LIST OF TABLES

| | |
|--|-----|
| Table 2.1 The Non-Integer Tooth Problem Case Study Data..... | 13 |
| Table 2.2 PECVT Requirements List | 14 |
| Table 2.3 PECVT Design Specifications..... | 15 |
| Table 2.4 TRIZ Contradiction Matrix..... | 19 |
| Table 2.5 TRIZ Inventive Principles | 20 |
| Table 2.6 Seven Suggested Inventive Principles | 20 |
| Table 2.7 Concept Scoring Matrix..... | 21 |
| Table 2.8 Concept Scoring Matrix..... | 27 |
| Table 4.1 Revised Requirements List | 43 |
| Table 5.1 Case Study Parameters..... | 96 |
| Table 5.2 Profile Generation Case Study..... | 99 |
| Table 5.3 Paths of Contact Polynomials..... | 104 |

LIST OF FIGURES

| | |
|---|----|
| Figure 2.1 The Non-Integer Tooth Problem | 12 |
| Figure 2.2 Orientation Correction..... | 16 |
| Figure 2.3 Embodiment of Problem Elimination Class | 17 |
| Figure 2.4 The Triz Method..... | 18 |
| Figure 2.5 Cam-Follower Concept | 23 |
| Figure 2.6 Tension Rollers with Sprocket and Chain concept..... | 24 |
| Figure 2.7 Differential Concept | 25 |
| Figure 2.8 Preferred Meshing Location Concept..... | 26 |
| Figure 2.9 Dalling's Angular Correction..... | 29 |
| Figure 3.1 Conceptual Design Process | 34 |
| Figure 4.1 Traditional Involute Curve Generation Description..... | 44 |
| Figure 4.2 The Fundamental Involute Triangle | 46 |
| Figure 4.3 The Fundamental Involute Triangle & Base Circle | 46 |
| Figure 4.4 The Pressure Angle..... | 47 |
| Figure 4.5 The Subtended Arc | 48 |
| Figure 4.6 The Vectorial Angle | 49 |
| Figure 4.7 Radii of Curvature | 50 |
| Figure 4.8 Various Involute Curves..... | 52 |
| Figure 4.9 The Tangent Line | 54 |

| | |
|---|-----|
| Figure 4.10 The Pressure Angle Definition II | 55 |
| Figure 4.11 The Pressure Angle at the Pitch Point | 56 |
| Figure 4.12 The Path of Contact | 57 |
| Figure 4.13 Path of Contact Cartesian Coordinates..... | 58 |
| Figure 4.14 The Line of Action | 59 |
| Figure 4.15 The Line of Action and Path of Contact Relationship | 60 |
| Figure 4.16 Tangential Velocity | 62 |
| Figure 4.17 v_t Vector Components | 63 |
| Figure 5.1 Standard Transmission Transition..... | 67 |
| Figure 5.2 PECVT Transition..... | 68 |
| Figure 5.3 The Line of Action Model..... | 69 |
| Figure 5.4 Engagement Measurement Error | 75 |
| Figure 5.5 Length of Engagement | 76 |
| Figure 5.6 Engagement Time..... | 79 |
| Figure 5.7 Position Vector Triangles | 82 |
| Figure 5.8 Hybrid Involute Profile Angular Ring Velocity..... | 85 |
| Figure 5.9 Chordal Length T_c | 88 |
| Figure 5.10 Involute Profile Cartesian Coordinates | 88 |
| Figure 5.11 Cam Correction Transition | 93 |
| Figure 5.12 The Hybrid Involute Profile | 94 |
| Figure 5.13 Hybrid Involute Profile Transition | 95 |
| Figure 5.14 LOA Model Generated Profiles..... | 97 |
| Figure 5.15 Varying Base Radius | 100 |

| | |
|---|-----|
| Figure 5.16 Paths of Contact Slopes | 104 |
| Figure 6.1 Possible Hybrid Involute Profile Clash | 113 |

1. Introduction

The global demand for energy has never been greater. This demand is leading to the discovery of new energy sources as well as improvements in the efficiency of devices that use energy. As energy sources are discovered, a major challenge arises in converting non-mechanical energy into mechanical energy, a primary energy type in demand. The challenge of mechanical energy is the inherent frictional and coupling losses in mechanical systems. Specifically in an internal combustion engine and transmission system, a major loss of energy occurs from the disengagement of the engine from the load coupled to the transmission. This disengagement of the transmission is due to the operational behavior of a traditional clutch type method of connecting the engine to the transmission.

To allow the engine to operate in a desired performance range (rpm range) the transmission is employed to vary the torque and speed ratios between the engine and the load. The torque and speed ratios are governed by the diameter ratios between a pair of engaged gears. Typically the gears employ involute profile shapes on the surface of the gear teeth. The number of involute gear teeth is strictly governed by the diameter of the gear. By altering the diameter of one or both gears relative to one another the gear ratio as well as the speed and torque ratios are changed of the gearset. Efficiency losses are

introduced by disengaging and then engaging various gearset ratios in traditional transmissions.

The gear ratio in a traditional transmission is altered by substituting one or both of the gears of a gearset for another gear(s) of a different diameter size. Substitution is employed because there is no known method to dynamically change a mechanical component such as a gear while engaged with another gear under load. This required substitution generates losses in the transmission system. To substitute one gear for another, the input is briefly disconnected from the output. This brief disengagement decreases the efficiency of the transmission considerably. To improve the internal combustion engine and transmission mechanical system these losses in efficiency must be diminished or eliminated. One possible method to eliminate or substantially reduce these “gear shifting” losses would be to develop a Positively Engaged Continuously Variable Transmission (PECVT). If a PECVT could be developed, gearsets of different gear ratios could be engaged and disengaged without these clutching losses.

A PECVT would allow the gear ratio of a gearset to be altered without disengaging the engine from the load. This is done by maintaining engagement between the input and the output while the diameter of one of the gears of the gear pair is altered as well as the center distance of the gearset, allowing the gear ratio to change. In addition, PECVTs offer potentially improved wear characteristics and larger torque load capabilities in comparison with current friction based continuously variable transmissions (CVTs). These attributes result directly from the use of positively engaged gears during gear ratio changes.

1.1. PECVT History

The goal of developing a practical PECVT has been a continual pursuit by many research and industrial groups over many years. Brigham Young University and Vernier Moon Technologies (VMT) have conducted a joint research endeavor to investigate the feasibility of developing a functional PECVT. The initial research work was intended to evaluate a PECVT that was proposed by VMT.

The initial research work at BYU conducted by Brian Anderson identified the characteristic behaviors of PECVTs and resulted in the identification of the Non-Integer Tooth Problem (NITP). The NITP is a phenomenon that occurs in all known PECVT embodiments identified thus far.

The primary objective of a PECVT is to maintain engagement of the engine (input) to the load (output) while varying the gear ratio in the transmission without the use of clutches. To accomplish this, the objective a PECVT can be considered as containing an infinite number of gearsets at an infinite number of gear ratios. The NITP prevents an infinite number of gear ratios to occur since involute gear teeth profiles are different for different gear diameters. This mechanical trait of involute gears limits the available gear ratios to a finite number of radii with integer number of gear teeth. Hence the NITP arises when operating a PECVT between specific gear ratio diameters (diameters corresponding to non-integer numbers of teeth). In the case of the initial PECVT proposed by VMT, Anderson concluded the embodiment would not overcome the NITP [1]. The pursuit of a viable PECVT was continued by Ryan Dalling who furthered the work of Anderson. Dalling utilized the product development process described in *Product Design and Development* [2] to identify a conceptual kinematic

solution for a PECVT [3], which employed a corrective mechanism to overcome the NITP.

1.2. Desired PECVT Behavior

Various methods can be employed to vary the gear ratio in a PECVT; however, the initial work at BYU has shown a gear type engagement is most promising [1,3]. To accomplish the objective of a PECVT using a gear type engagement, several functional characteristics must be present. The functional characteristics include overcoming the NITP, maintaining involutometry properties of the gear teeth profiles, and maintaining conjugate action between the engaged gearset.

Addressing the NITP is critical to the development of a PECVT. With the NITP present, proper engagement between input and output members will not occur. The NITP is the first behavioral characteristic which should be addressed. Once this problem is addressed, the remaining behavioral characteristics can be considered.

Although a PECVT which does not maintain involutometry properties of the gears may function, the output kinematics of the device will be undesirable. Specifically, without involutometry properties satisfied, the desired efficiency gains will be negated by the energy losses resulting from increased friction between the engaged members. In addition, maintaining involutometry properties ensures conjugate action, action in which uniform rotary motion is transmitted through the gearset.

Conjugate action or the transfer of uniform rotary motion must be present between the engaged members of the gearset [4]. Without conjugate action considerable

oscillation of the output member in relation to the input will occur. These oscillations will ultimately lead to fatigue failures.

1.3. Problem Statement

The original intent of the research effort for this thesis was to continue the work of Dalling into the embodiment design phase. The work began with detailed analysis of the conceptual solution Dalling proposed. However, as a result of extensive additional analysis, it was determined that Dalling's solution incorporated assumptions which violate the fundamental laws of involutometry and hence, would not produce a kinematically viable solution.

1.4. Hypothesis

With the functional characteristics described in section 1.2 addressed the design space for a viable PECVT is defined. The pursuit of developing a commercially viable PECVT is based on utilizing the conceptual solution proposed by Dalling to address the NITP, while incorporating involutometry into the conceptual solution to ensure involutometry properties and conjugate action are satisfied. The design space will then be adequately defined to pursue the ideation of a PECVT, such that engagement of the input and output of the device will exist while varying the gear ratio by changing the diameter of one of the gears of the gearset relative to the other, as well as the center distance of the gearset.

1.5. Research Objectives

The objective of the research effort described in this thesis is to develop a conceptual, kinematically viable, solution for a PECVT. This conceptual solution will satisfy the functional characteristics of a PECVT and will channel the design space for developing a commercially viable PECVT embodiment.

1.6. Organization

This thesis is organized to guide the reader through the conceptual design phase of the product development process for the development of a conceptual kinematically viable PECVT. Chapter two provides a detailed literature review of the previous PECVT research relative to developing an understanding of the NITP and the kinematics of a PECVT. The literature review presented in chapter two centers on the work of Dalling; however, additional PECVT endeavors are discussed. Chapter two concludes with identification and implications of the assumptions made by Dalling.

Chapter three presents the methodology which will be used in the research effort. The methodology is structured after the conceptual design phase of a product development process, adapted from Paul, Bietz et al. [5].

Chapter four presents a second literature review detailing involutometry definitions, relationships and properties required to generate an involute curve. The literature search of chapter four is adapted from the various works of Earle Buckingham [4,6]. The involute properties described in chapter four are fundamental to the development of a design tool termed the Line-of-Action Model, which will assist in developing a conceptual, kinematically viable PECVT.

In Chapter five the Line-of-Action Model is developed. This design tool will identify the attributes that any PECVT embodiment must have to ensure that involutometry principles are satisfied in the components of the engaged gear teeth. Evaluation of the proposed conceptual solution by Dalling, along with a solution inherent in the Line-of-Action Model is presented as well. Validation of the Line-of-Action Model and a description of the proposed conceptual principle solution meeting these requirements conclude chapter five.

Chapter six concludes this thesis with a review of the work presented and recommendations for future work. The recommendations are not embodiment specific, but are noted observations and implications which may assist in the development of an embodiment which incorporates the requirements of the conceptual principle solution.

2. PECVT Technology

The concept of a positively engaged continuously variable transmission is not new. As traditional friction Continuously Variable Transmissions (CVTs) have become more mainstream the desire for a more efficient, larger torque load CVT arises. A PECVT may be a solution since a PECVT can provide both greater efficiency and torque load characteristics. Due to the potential benefits of a PECVT a practical PECVT has been sought for some time. Dalling identifies several previously patented embodiments, as well as evaluating the functionality of each embodiment [3].

In addition to the embodiments identified by Dalling, several other embodiment types have recently been developed. These include the Naudic rotorCVT and iCVT [7], and an IVT developed at Virginia Polytechnic Institute [8]. These embodiments however lack the qualifications to be classified as PECVTs. Specifically, although the Naudic iCVT utilizes positively engaged members, the transition between gear ratios is discontinuous (due to the use of a Geneva mechanism). The Naudic rotorCVT and the Virginia Tech IVT are more correctly classified as ratchet CVTs since a cam is utilized in both embodiments to rotate an incremental gear.

As the study of PECVTs has progressed, several considerations have been identified as being critical to the successful development of a PECVT. These considerations include the involutometry of gearsets [4, 6, 9, 10, 11], conjugate action

analysis [4, 6, 11], manufacturability [4, 6, 11, 12], and stress and fatigue analysis [4, 10, 12].

Upon evaluation of known PECVTs as well as closely related CVTs it has been determined that the product development process could prove to be highly beneficial in identifying a feasible PECVT embodiment.

2.1. PECVT Product Development Process

As the interest in developing a feasible PECVT has grown, research at Brigham Young University in conjunction with Vernier Moon Technologies has focused on the investigation of developing a PECVT through the use of the product development processes outlined in [2] and [5]. Since the product development process can include a range of phases and methods, a specific product development process has been selected for use to assist in the development of a feasible PECVT. The phases of the product development process which have been selected are conceptual design, embodiment design, and detailed design. The specific tasks and deliverables depend on each phase. In general, the deliverables of each phase are either virtual or physical prototypes.

2.1.1. Conceptual Design Phase

The initial phase of conceptual design in the product development process for developing a PECVT has been completed through prior work at Brigham Young University [3]. This work has focused on the identification of the essential problem, identification, development, and analysis of various conceptual solutions to the essential problem, and finally screening and evaluation of these concepts to arrive at a principal

conceptual solution. Prior to presenting the work of this research, the previous work in the conceptual design phase will be outlined.

2.1.1.1. Identification of the Essential Problem

From previous research, the essential problem of a PECVT has been identified as the non-integer tooth problem (NITP) [13]. The NITP is further described by Anderson [1]. However, the definition Anderson proposes is very embodiment specific. For this reason a more generic definition is given below.

2.1.1.1.1. The Non-Integer Tooth Problem

Previous research has proposed all PECVT embodiments to be considered as variable pitch gearsets where the input gear diametral pitch (P_d) is able to vary, while maintaining a constant number of teeth (N), and the output gear is a standard gear where P_d and N are fixed [1, 3]. From standard involutometry [10], the circular pitch (P_c) is defined in Equation 2.1 as:

$$P_c = \frac{\pi \cdot d}{N} \quad (2.1)$$

where d is the pitch diameter of the gear.

Also the diametral pitch (P_d) is defined in Equation 2.2 as:

$$P_d = \frac{N}{d} \quad (2.2)$$

Combining equations 2.1 and 2.2 yields Equation 2.3.

$$P_c = \frac{\pi}{P_d} \quad (2.3)$$

Thus, if N is held constant (to maintain the gear tooth profile) and d is varied P_d and P_c will change with d .

The change in the gear ratio (R) in a PECVT results from a change of the pitch diameter (d_{input}) of the input gear while the pitch diameter (d_{output}) of the output gear remains constant, as shown in Equation 2.4.

$$R = \frac{d_{input}}{d_{output}} \quad (2.4)$$

Thus the NITP arises when the diameter of the input (d_{input}) causes the initial current circular pitch (P_{c_o}) not to be evenly divisible by the current circular pitch (P_{c_i}). This is to say that as each individual tooth increases in its radial position, reorientation of the input gear is required in order for correct engagement to occur. Figure 2.1 illustrates the NITP phenomenon.

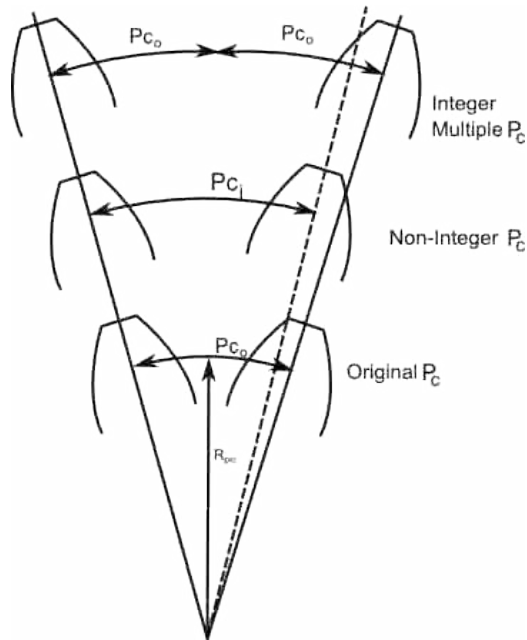


Figure 2.1 The Non-Integer Tooth Problem

To demonstrate the NITP, an arbitrary case study is presented in Table 2.1. In Table 2.1 the number of teeth (N) of the input and output are held constant (to maintain the size and shape of the gear teeth). These values as well as P_{c_o} , P_{d_o} , and d_{output} are shown as initial values. The diameter of the input, d_{input} is then varied and the corresponding P_{c_i} , P_{d_i} , as well as a ratio of P_{c_i} to P_{c_o} is also shown. This ratio correlates to the amount of reorientation required to align the tooth profile to the P_{c_o} . The input diameters that correspond to multiple P_{c_o} are highlighted to indicate no reorientation is required. The NITP is present at all locations where reorientation is required.

Table 2.1 The Non-Integer Tooth Problem Case Study Data

| Initial Values | | d_{input} | P_{d_i} | P_{c_i} | P_{c_i}/P_{c_o} | Reorientation Required (degrees) |
|------------------------------|------|-------------|-----------|-----------|-------------------|----------------------------------|
| N_{input} | 12 | 4 | 3.0 | 1.05 | 1.000 | 0 |
| N_{output} | 36 | 4.5 | 2.7 | 1.18 | 1.125 | 3.75 |
| P_{d_o} | 3 | 5 | 2.4 | 1.31 | 1.250 | 7.5 |
| P_{c_o} | 1.05 | 5.5 | 2.2 | 1.44 | 1.375 | 11.25 |
| d_{output} | 12 | 6 | 2.0 | 1.57 | 1.500 | 15 |
| Angular Tooth Spacing | 30 | 6.5 | 1.8 | 1.70 | 1.625 | 18.75 |
| | | 7 | 1.7 | 1.83 | 1.750 | 22.5 |
| | | 7.5 | 1.6 | 1.96 | 1.875 | 26.25 |
| | | 8 | 1.5 | 2.09 | 2.000 | Full Angular Tooth Spacing |
| | | 8.5 | 1.4 | 2.23 | 2.125 | 3.75 |
| | | 9 | 1.3 | 2.36 | 2.250 | 7.5 |
| | | 9.5 | 1.3 | 2.49 | 2.375 | 11.25 |
| | | 10 | 1.2 | 2.62 | 2.500 | 15 |
| | | 10.5 | 1.1 | 2.75 | 2.625 | 18.75 |
| | | 11 | 1.1 | 2.88 | 2.750 | 22.5 |
| | | 11.5 | 1.0 | 3.01 | 2.875 | 26.25 |
| | | 12 | 1.0 | 3.14 | 3.000 | Full Angular Tooth Spacing |

2.1.2. Design Specifications

Identification of the essential problem of a generic PECVT allows for the development of a requirements list. This list, adapted from [3], is presented as Table 2.2. Each requirement is assigned an importance rating, according to the requirement's contribution to the overall functionality of a PECVT. The ratings are based on the design team's heuristics, however item numbers one through four and ten *must* be satisfied for an embodiment to be classified and defined as a PECVT. If a specific application is desired, the requirements list for the PECVT would result in design specifications for the specific application. An example of resulting design specifications, again adapted from [3] are shown in Table 2.3 for a recreational vehicle application [14]. The design specifications and requirements list become the foundation to evaluate the feasibility of a possible PECVT concept throughout the development process.

Table 2.2 PECVT Requirements List

| Item number | Requirements | Importance |
|--------------------|--|-------------------|
| | The Transmission: | |
| 1 | ratio is continuously variable | 1 |
| 2 | transmits power solely through engaged members | 1 |
| 3 | provides positive engagement of the input and output | 1 |
| 4 | provides continuous engagement of the input and output | 1 |
| 10 | is able to vary the gear ratio under load | 1 |
| 16 | does not produce an oscillating output | 2 |
| 5 | can transmit high torque loads | 2 |
| 6 | is highly efficient | 2 |
| 9 | is not a complex system (preferably fully mechanical) | 3 |
| 7 | is light weight | 3 |
| 8 | is comprised of standard components | 3 |
| 12 | is adaptable to current applications | 3 |
| 11 | can provide a large gear ratio range | 4 |
| 13 | is simple to control | 4 |
| 14 | can be operated over wide range of RPMs | 4 |
| 15 | does not produce excessive vibrations | 4 |

Table 2.3 PECVT Design Specifications

| Metric Number | Requirement Number | Metric | Units | Marginal Value | Ideal Value |
|----------------------|---------------------------|------------------------------------|--------------|-----------------------|--------------------|
| 1 | 1, 4 | Continuously variable gear ratio | Binary | Yes | Yes |
| 2 | 2 | friction dependent | Binary | No | No |
| 3 | 3 | Positive engagement | Binary | Yes | Yes |
| 4 | 4, 10 | Continuous Engagement | Binary | Yes | Yes |
| 5 | 5 | Maximum torque load | ft-lbs | 30 | 40 |
| 6 | 6 | Efficiency | % | 90 | 95 |
| 7 | 7, 12 | Weight | lbs | <30 | <20 |
| 8 | 8 | Amount of non-standard components | # | <5 | 0 |
| 9 | 9 | Part count | # | <100 | 50 |
| 10 | 10 | Able to vary gear ratio under load | Binary | Yes | Yes |
| 11 | 11 | Maximum gear ratio | # :1 | 2.5 | 3 |
| 12 | 12 | Adaptable to current applications | Binary | Yes | Yes |
| 13 | 13 | Number of control sources | # | 1 | 1 |
| 14 | 14 | Maximum RPM | # | >5000 | >700 0 |
| 15 | 15 | Kinematic interference | Binary | No | No |
| 16 | 15 | Oscillating output | Binary | No | No |

2.1.3. Concept Generation

To initiate the generation of various concepts that will satisfy the design specifications, two sub-classes of PECVTs have been identified. The formulation of these sub-classes is founded on extensive research of all published CVTs (primarily patented embodiments) which can be classified as PECVTs. The sub-classes which have been identified are the problem correction class and the problem elimination class [3]. All known embodiments of PECVTs can be classified into these two sub-classes. Detailed case studies of these embodiment concepts are presented in [3]. A brief description of the types of embodiment concepts which fall within each sub-class is provided below.

2.1.3.1. Problem Correction Class

The problem correction class of PECVT's is very similar to traditional fixed ratio transmissions, meaning they are comprised of standard gearsets. In order to achieve a continuously variable gear ratio, the most common method of varying the gear ratio for the problem correction class utilizes a variable pitch gear. Such a gear maintains the appropriate number of gear teeth, while allowing for the pitch diameter to vary between various input gears. The non-integer tooth problem arises when the pitch of the gear changes the orientation due to the change in the circular pitch (as shown previously in section 2.1.1.1.1). The most common method of correction is through the use of a one-way clutch, as shown in Figure 2.2 [1]. The drawback to the use of a one-way clutch is the introduction of an oscillating output.

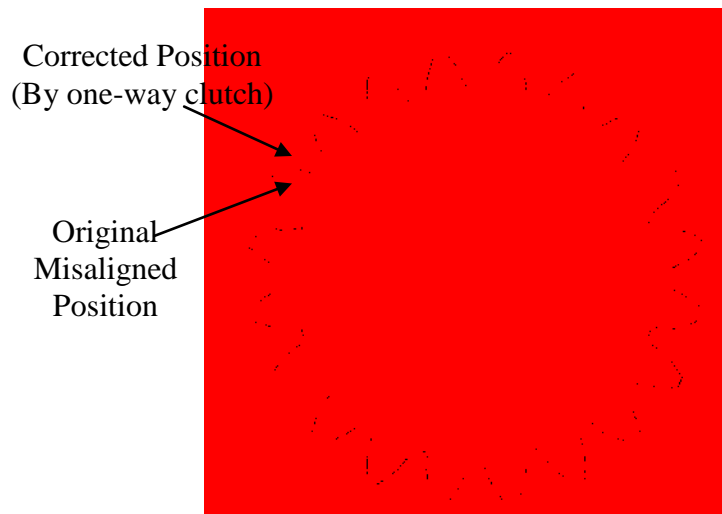


Figure 2.2 Orientation Correction

There are a number of alternatives to the one-way clutch solution; these alternatives, which employ problem correction without the use of one-way clutches, are detailed further in [3]. However, no known alternative to the one-way clutch solution has

successfully overcome the non-integer tooth problem without the introduction of an oscillating output.

2.1.3.2. Problem Elimination Class

Unlike the embodiments belonging to the problem correction class, embodiments classified under the problem elimination class use a device, mechanism, or other method to eliminate the non-integer tooth problem to ensure proper engagement. Embodiments in this class do not need any type of realignment correction because the characteristics of the members or devices that are engaged eliminate any misalignment *prior* to engagement. These embodiments employ tooth conforming or feedback loops to alter the meshing characteristics. Since these embodiments use meshing interfaces other than traditional involute gear teeth as shown in Figure 2.3, the non-integer problem is not present. However, all known embodiments of the problem elimination class lack the robustness to satisfy the design specifications (e.g. torque load capability) of a PECVT.

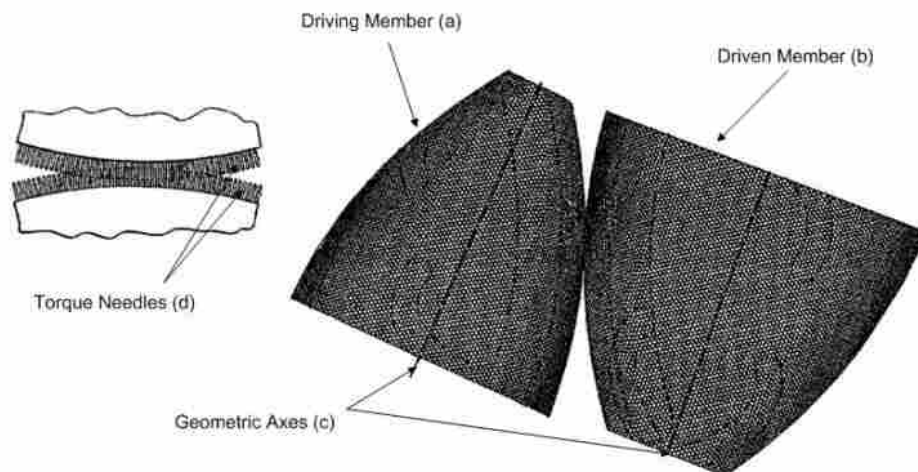


Figure 2.3 Embodiment of Problem Elimination Class
Using Torque Transmitting Needles (Retrieved from U.S. Patent No. 6964630)

2.1.3.3. Design Contradictions

An extensive analysis of literature including patents for all known PECVTs yielded no known functional PECVT. The failure to overcome the NITP, or lack of robustness resulting from complexity of the embodiment is the cause of the lack of practical functionality. During the review of proposed PECVT embodiments, a contradictory effect between the proposed solution to the NITP, and complexity/manufacturability of the devices required to overcome the NITP was noted. In order to resolve these contradiction(s) the TRIZ method [15] was utilized. The TRIZ method (developed by Genrich Altshuller in 1946) allows for the generation of abstract problems and solutions while identifying contradictions in potential or possible solutions. This approach is valuable in that contradictions can be identified and possibly eliminated, resulting in a specific inventive solution. Figure 2.4 adapted from [16] shows the TRIZ process as opposed to traditional problem solving techniques. The results of the TRIZ method will be further discussed in the concept evaluation phase (section 2.1.4) of this chapter.

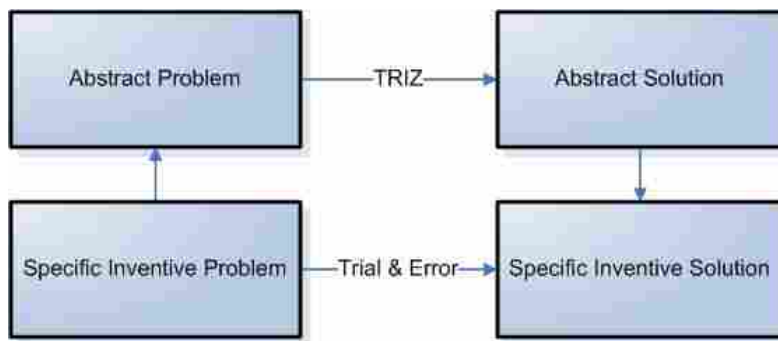




Figure 2.4 The Triz Method

2.1.4. Concept Evaluation

The TRIZ method first yields a contradiction matrix (Table 2.4 [3]) which includes all possible design contradictions that might exist for the specific design. The design team determined the parameters to include in the row headings of the matrix based on the parameters needing improvement in an ideal PECVT embodiment. In like manner, the column headings were also chosen based on the most probable inherent effects of the parameter features.

Table 2.4 TRIZ Contradiction Matrix

| | Worsening Feature  Improving Feature  | Speed | Shape | Stability of the object's composition | Duration of action of moving object | Loss of Information | Measurement accuracy | Object-generated harmful factors | Ease of manufacture | Adaptability or versatility | Device complexity | Difficulty of detecting and measuring |
|----|--|----------------|----------------|---------------------------------------|-------------------------------------|---------------------|----------------------|----------------------------------|---------------------|-----------------------------|-------------------|---------------------------------------|
| | | 9 | 12 | 13 | 15 | 24 | 28 | 31 | 32 | 35 | 36 | 37 |
| 12 | Shape | 35, 15, 34, 18 | + | 33, 1, 18, 4 | 14, 26, 9, 25 | | 28, 32, 1 | 35, 1 | 1, 32, 17, 28 | 1, 15, 29 | 16, 29, 1, 28 | 15, 13, 39 |
| 13 | Stability of the object's composition | 33, 15, 28, 18 | 22, 1, 18, 4 | + | 13, 27, 10, 35 | | 13 | 35, 40, 27, 39 | 35, 19 | 35, 30, 34, 2 | 2, 35, 22, 26 | 35, 22, 39, 23 |
| 15 | Duration of action of moving object | 3, 35, 5 | 14, 26, 28, 25 | 13, 3, 35 | + | 10 | 3 | 21, 39, 16, 22 | 27, 1, 4 | 1, 35, 13 | 10, 4, 29, 15 | 19, 29, 39, 35 |
| 23 | Loss of substance | 10, 13, 28, 38 | 29, 35, 3, 5 | 2, 14, 30, 40 | 28, 27, 3, 18 | | 16, 34, 31, 28 | 10, 1, 34, 29 | 15, 34, 33 | 15, 10, 2 | 35, 10, 28, 24 | 35, 18, 10, 13 |
| 24 | Loss of Information | 26, 32 | | | 10 | + | | 10, 21, 22 | 32 | | | 35, 33 |
| 35 | Adaptability or versatility | 35, 10, 14 | 15, 37, 1, 8 | 35, 30, 14 | 13, 1, 35 | | 35, 5, 1, 10 | | 1, 13, 31 | + | 15, 29, 37, 28 | 1 |
| 36 | Device complexity | 34, 10, 28 | 29, 13, 28, 15 | 2, 22, 17, 19 | 10, 4, 28, 15 | | 2, 26, 10, 34 | 19, 1 | 27, 26, 1, 13 | 29, 15, 28, 37 | + | 15, 10, 37, 28 |
| 37 | Difficulty of detecting and measuring | 3, 4, 16, 35 | 27, 13, 1, 39 | 11, 22, 39, 30 | 19, 29, 39, 25 | 35, 33, 27, 22 | 26, 24, 32, 28 | 2, 21 | 5, 28, 11, 29 | 1, 15 | 15, 10, 37, 28 | + |

The inventive principles (Table 2.5 [3]) suggested by TRIZ were applied to eliminate particular contradictions. From the contradiction matrix, seven inventive principles were identified which most commonly would eliminate design contradictions for this type of problem. The seven inventive principles are shown in Table 2.6 [3].

Table 2.5 TRIZ Inventive Principles

| <u>Inventive Principles of TRIZ</u> | |
|-------------------------------------|---|
| 1. Segmentation | 21. Rushing through |
| 2. Extraction | 22. Convert harm into benefit |
| 3. Local quality | 23. Feedback |
| 4. Asymmetry | 24. Mediator |
| 5. Combining | 25. Self-service |
| 6. Universality | 26. Copying |
| 7. Nesting | 27. An inexpensive short-lived object instead of an expensive durable one |
| 8. Counterweight | 28. Replacement of a mechanical system |
| 9. Prior counteraction | 29. Use of a pneumatic or hydraulic construction |
| 10. Prior action | 30. Flexible film or thin membranes |
| 11. Cushion in advance | 31. Use of porous material |
| 12. Equipotentiality | 32. Change the color |
| 13. Inversion | 33. Homogeneity |
| 14. Spheroidality | 34. Rejecting and regenerating parts |
| 15. Dynamicity | 35. Transformation of physical and chemical states of an object |
| 16. Partial or overdone action | 36. Phase transition |
| 17. Moving to a new dimension | 37. Thermal expansion |
| 18. Mechanical vibration | 38. Use strong oxidizers |
| 19. Periodic action | 39. Inert environment |
| 20. Continuity of useful action | 40. Composite materials |

Table 2.6 Seven Suggested Inventive Principles

| Inventive Principle Number | Inventive Principle Title | Inventive Principle Description |
|----------------------------|---------------------------|--|
| 35 | Parameter Changes | Change the degree of flexibility |
| | | Change the object's physical state (e.g. to gas, liquid, or solid) |
| 1 | Segmentation | Divide an object into independent parts |
| | | Increase the degree of fragmentation or segmentation |
| 10 | Preliminary Action | Perform, before it is needed, the required change of an object (either fully or partially) |
| | | Pre-arrange objects such that they can come in to action without losing time for their delivery |
| 28 | Mechanics Substitution | Replace a mechanical means with a sensory means |
| | | Use electric, magnetic and electromagnetic fields to interact with the object |
| 15 | Dynamics | Allow the characteristics of an object or process to change to be optimal or find an optimal operating condition |
| | | Divide an object into parts capable of movement relative to each other. |
| 13 | The other way around | Invert the action(s) used to solve the problem (e.g. instead of cooling an object, heat it) |
| | | Make moveable parts (or the external environment) fixed, and fixed parts movable |
| 29 | Pneumatics and Hydraulics | Use gas and liquid parts of an object instead of solid parts |

Upon inspection of the suggested inventive principles it is important to note some of the inventive principles imply solutions which violate the requirements of a PECVT. These are inventive principle 29: Pneumatics and Hydraulics, and inventive principle 35: Parameter Changes. In a similar manner, the remaining inventive principles must be implemented such that new contradictions are not created.

After implementation of the suggested inventive principles several potential concepts were developed. Each of these concepts are described in detail in [3]. To evaluate these potential concepts, a scoring and screening matrix (Table 2.7 [3]) was compiled. The scoring and screening matrix allows for a quantitative comparison of the various concepts based upon criteria extracted from the PECVT requirements list (Table 2.2).

Table 2.7 Concept Scoring Matrix

| | Concepts | | | | |
|--|--|------------------------------------|---|------------------------------|--|
| | A (Reference) | B | C | D | E |
| Selection Criteria | One way Clutches Between Driven Gears | Helical Gear Correction | Electric Actuator Correction | Cammed Correction | Constant Tooth and Pitch Embodiment |
| Does not produce an oscillating output | 0 | + | + | + | 0 |
| Can transmit high torque | 0 | 0 | 0 | + | - |
| Highly efficient | 0 | - | - | 0 | - |
| Not complex | 0 | 0 | - | + | - |
| Made of standard parts | 0 | 0 | 0 | 0 | - |
| Retrofit-able in current applications | 0 | 0 | 0 | 0 | 0 |
| Feasible | 0 | 0 | - | - | - |
| Robust | 0 | 0 | - | + | - |
| Net Score | 0 | 0 | -3 | 3 | -6 |
| Rank | 5 | 5 | 9 | 2 | 11 |
| Continue | NO | NO | NO | YES | NO |

Table 2.7 Concept Scoring Matrix Continued

| | Concepts | | | | | |
|--|---|---|--|---|-------------------------------------|---|
| | F | G | H | I | J | K |
| Selection Criteria | Shear Thickening/ Magneto-Rheological Fluid | Tension Rollers w/ Sprocket and Chain | Feedback using Reference Gear | Feedback using Differentials between Driven Gears | Resilient Material and Spikes | Preferred Meshing Location Embodiment |
| Does not produce an oscillating output | + | - | + | + | 0 | + |
| Can transmit high torque | - | + | 0 | 0 | - | 0 |
| Highly efficient | - | 0 | 0 | 0 | 0 | + |
| Not complex | - | 0 | 0 | - | + | - |
| Made of standard parts | - | + | 0 | 0 | - | 0 |
| Retrofit-able in current applications | 0 | - | 0 | 0 | 0 | + |
| Feasible | 0 | + | - | + | 0 | + |
| Robust | - | 0 | 0 | 0 | - | + |
| Net Score | -4 | 1 | 0 | 1 | -2 | 4 |
| Rank | 10 | 3 | 5 | 3 | 8 | 1 |
| Continue | NO | YES | NO | YES | NO | YES |

2.1.5. Concept Selection

From Table 2.7, four concepts which are most viable are identified through the “Continue” criteria. As mentioned previously the selection criteria for selecting the most viable concepts is based on the design specifications developed from the secondary and tertiary PECVT requirements provided in the requirements list (Table 2.2) of section 2.1.2. These concepts are D, G, I, and K are: the cam-follower correction concept, the tension rollers with sprocket and chain concept, the feedback using differentials between driven gears concept, and the preferred meshing location concept, respectively. These four concepts are detailed below. Note: the proceeding descriptions lack detailed information for a complete PECVT since conceptual designs solely address specific essential problems and are merely PECVT concepts, not actual embodiments.

2.1.5.1. Cam-Follower Correction Concept

As the pitch diameter of the input gear (d_{input}) is varied, this concept utilizes a cam-follower to correct the orientation of the driving teeth either by rotation or translation, as shown in Figure 2.5 [3] to overcome the NITP. The manner in which the cam is implemented into an embodiment can vary substantially depending on the actual embodiment of the concept. This method of correction fully address the NITP. The implementation of this concept; however, may be overly complex to be commercially viable.

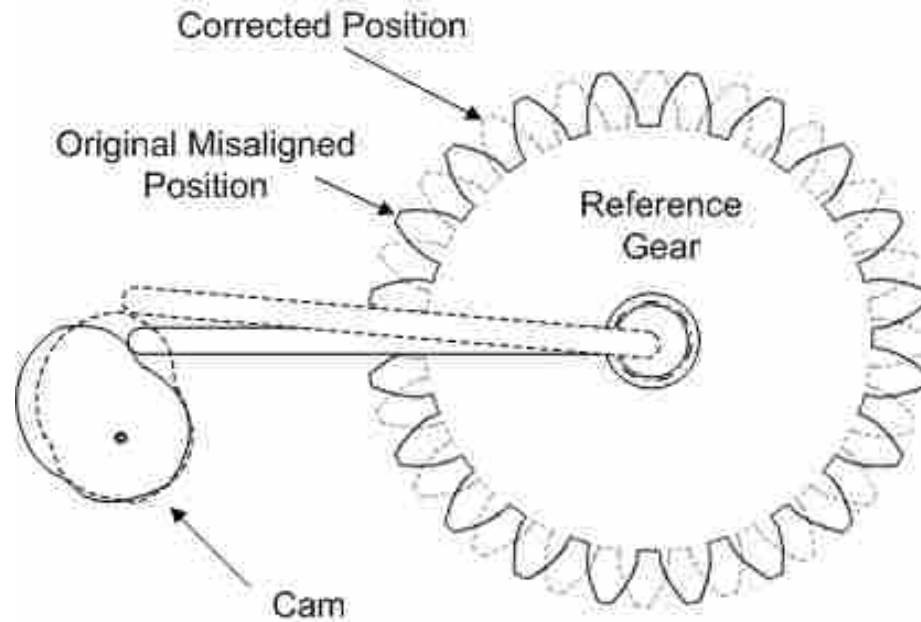


Figure 2.5 Cam-Follower Concept

2.1.5.2. Tension Rollers with Sprocket Chain Concept

This concept consists of a drive (a) and driven (b) portion of the embodiment which are connected by use of a chain (c). Each portion is composed of a segmented gear, using sprockets (d and e) in place of the gears. The sprockets (e), representing the driving portion of the embodiment, are allowed to change the effective diameter of the driving portion (a) and the effective transmission ratio. In addition, adjustable tension rollers (f) are also added to the driving portion (a) of the embodiment between each driving sprocket (e) that is meshed with the chain (c) to alter the effective P_c as shown in Figure 2.6 [3]. This method of correction also fully addresses the NITP, but is highly complex and does not satisfy tertiary design requirements.

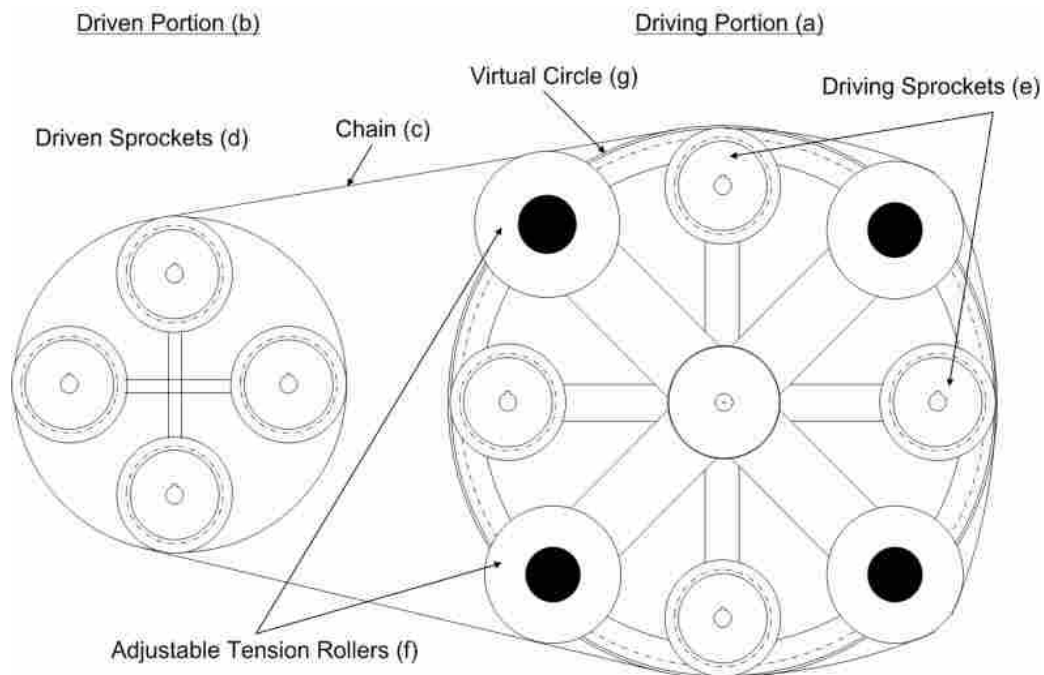


Figure 2.6 Tension Rollers with Sprocket and Chain concept

2.1.5.3. Feedback Using Differentials between Drive Gears Concept

This concept consists of using differential gearsets between the engaged and non-engaged driven gears (each engaged member is in a separate differential set) to provide relative rotational motion between them, thus eliminating the non-integer tooth problem. Both the TRIZ segmentation principle #1 and the preliminary action principle #10 are utilized in this design. Implementation of the differential gears is a somewhat feasible design, through duplicating and placing sets of planetary gears side by side out-of-plane on the same central axis. This configuration is shown in Figure 2.7, where each differential set consists of a ring and pinion. This concept does not fully address the NITP, but does address specific aspects of the NITP.

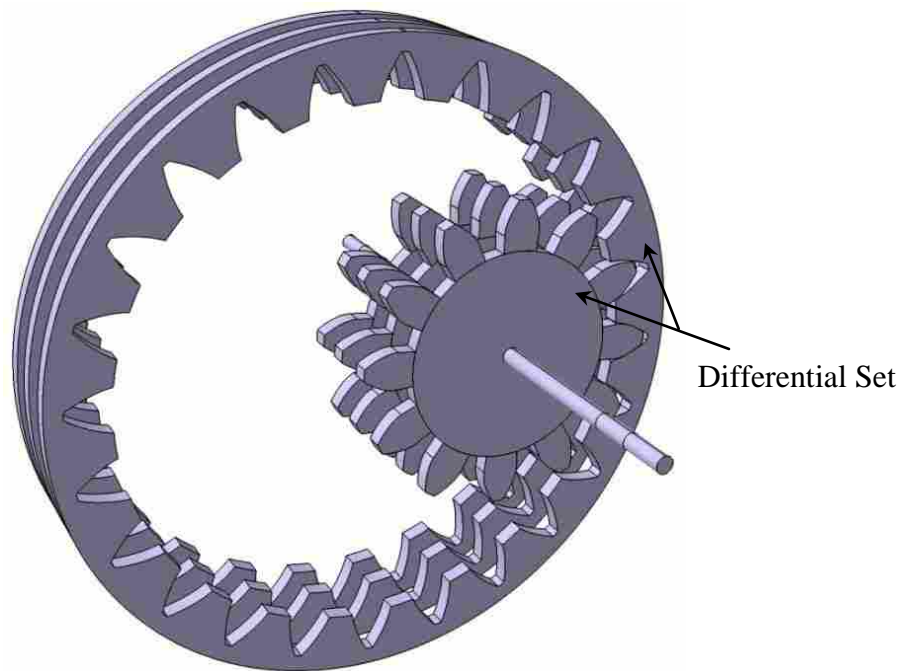


Figure 2.7 Differential Concept

2.1.5.4. Preferred Meshing Location Concept

This concept forces the PECVT to operate the majority of time at locations where the non-integer tooth problem does not exist (a). The NITP is still present in the correction regions (b), and the corrections required (no method for implementing the corrections is specified) to ensure proper meshing would only be applied while the transmission is transitioning from one “proper” meshing location to another. This greatly eliminates the number of corrections needed by a corrective device to correct the orientation of different members of the concept, which only occurs while transitioning through a range of RPM and gear ratios (b). The concept can continuously vary the RPM and gear ratios throughout the entire range of the transmission; however, the transmission generally operates at a specified set of operating ratios, and as a result, no correction is needed while operating at these preferred locations. The concept is shown in Figure 2.8 [3]. The NITP; however, is still present in the correction regions.

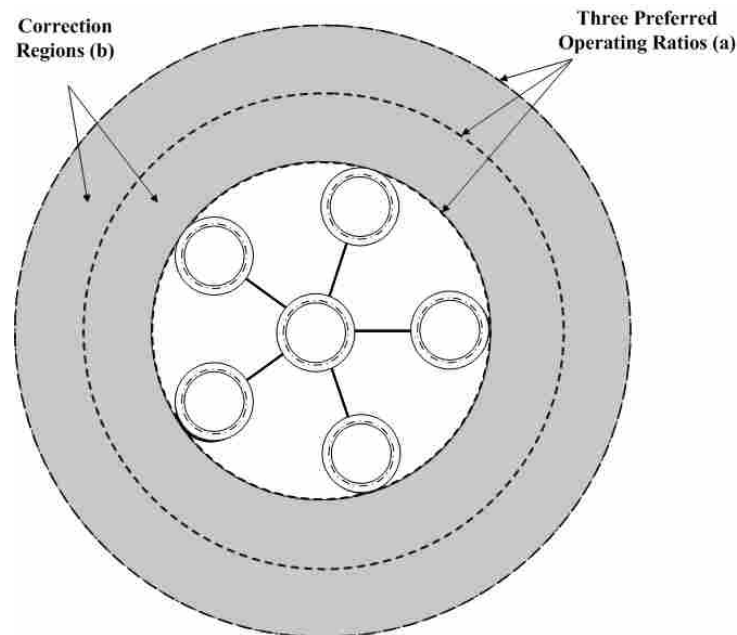


Figure 2.8 Preferred Meshing Location Concept

2.1.6. Concept Selection Results

Concept screening and scoring was again applied to the 4 potential principal solutions. The resulting matrix is shown in Table 2.8. Note the selection criteria are again taken from the requirements list (Table 2.2).

Table 2.8 Concept Scoring Matrix

| | | Cam Correction | | Tension Rollers w/ sprocket and Chain | |
|-------------------------------------|--------|-----------------------------|----------------|---------------------------------------|----------------|
| Selection Criteria | Weight | Rating | Weighted Score | Rating | Weighted Score |
| Does not produce oscillating output | 25% | 3 | 0.75 | 1 | 0.25 |
| Able to transmit high torque | 15% | 3 | 0.45 | 3 | 0.45 |
| Lack of Complexity | 10% | 3 | 0.3 | 2 | 0.2 |
| Standardized components | 5% | 2 | 0.1 | 3 | 0.15 |
| Ease of System Integration | 5% | 3 | 0.15 | 2 | 0.1 |
| Feasible | 25% | 4 | 1 | 3 | 0.75 |
| Robust | 15% | 3 | 0.45 | 3 | 0.45 |
| Weighted Score | | 3.2 | | 2.35 | |
| Rank | | 2 | | 4 | |
| | | | | | |
| | | Feedback using Differential | | Preferred Meshing Location | |
| Selection Criteria | Weight | Rating | Weighted Score | Rating | Weighted Score |
| Does not produce oscillating output | 25% | 3 | 0.75 | 3 | 0.75 |
| Able to transmit high torque | 15% | 3 | 0.45 | 3 | 0.45 |
| Lack of Complexity | 10% | 3 | 0.3 | 2 | 0.2 |
| Standardized components | 5% | 3 | 0.15 | 3 | 0.15 |
| Ease of System Integration | 5% | 3 | 0.15 | 4 | 0.2 |
| Feasible | 25% | 2 | 0.5 | 5 | 1.25 |
| Robust | 15% | 3 | 0.45 | 4 | 0.6 |
| Weighted Score | | 2.75 | | 3.6 | |
| Rank | | 3 | | 1 | |

2.1.7. Principal Conceptual Solution

From the selection criteria and the weighted scores (based on the design team's heuristics, and detailed further in [3]), the preferred meshing location embodiment was chosen as the most viable concept. The cam-follower correction concept and the feedback using differentials concepts ranked second and third, respectively. However, the preferred meshing location embodiment does not have a specified corrective device to make corrections while transitioning between optimal locations. Therefore, the cam-follower correction concept, which ranked second in the concept scoring process, could be combined with the preferred meshing locations concept to produce a more complete solution which would fully satisfy the design requirements (presented in section 2.1.2).

As noted in [3], this is solely a concept for a solution. Further refinement of this embodiment is certainly required. This is due to the complex nature of PECVTs, cam design, involutometry, and manufacturability. A diagram of the resulting specific embodiment is also not provided due to the nature of the detailed design phase which would need to follow in the product development process.

2.2. Conceptual Design Limitations

Prior to completing the discussion of the conceptual design phase, a discussion of the limitations of the conceptual design phase is required. During the development of the conceptual phase, several design assumptions were introduced to simplify the conceptual model. The introduction of assumptions into a complex model is appropriate, and is the case of the conceptual development of a PECVT. In the ensuing chapters of this thesis the assumptions will be validated or removed, based upon further knowledge of the behavior

of a PECVT. A discussion of each assumption is given below along with noted implications of these assumptions. The discussion will conclude with a brief description of how these assumptions will be addressed in order to continue the development of a PECVT.

2.2.1. Involutometry Assumptions

Dalling in [3], presents a mathematical model in which a theoretical angular correction is presented for the concept presented above. During the derivation of this angular correction of the input member termed C , Dalling makes several significant involutometry assumptions. The angular correction C is shown in Figure 2.9.

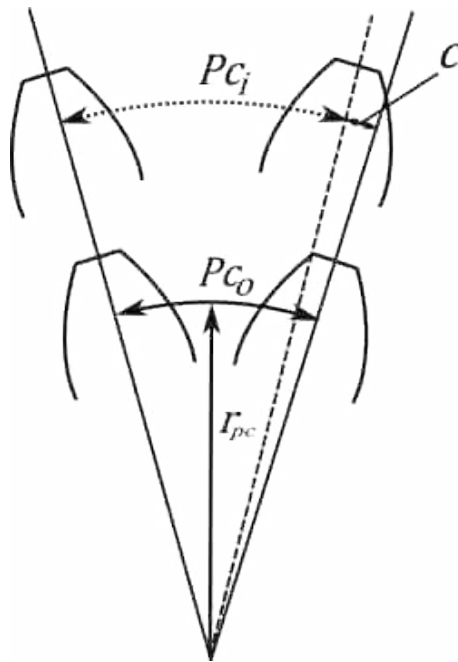


Figure 2.9 Dalling's Angular Correction

The most significant assumption Dalling makes is that the change in the size and shape of the involute profile which corresponds to the change in radius of the gear is insignificant. This however, is not the case. By not addressing the change in the involute

profile, unwanted oscillations are introduced into the output gear. In addition, since the arc length of the involute curve changes with the involute profile, the solution method Dalling proposes will alter the amount of rolling and sliding contact between the engaged teeth. This will result in a decreased efficiency of the engaged gear pair compared to standard involute gearsets, a direct contradiction of the objective of a PECVT.

In addition to the involute profile assumption, Dalling also overlooks the center-to-center distance relationship of the meshing gear pair in his analysis. Neglecting the center distance relationship dramatically alters the conceptual solution conclusion Dalling arrives at.

Finally Dalling assumes the angle of engagement consists of two equal and opposite components: the angle of approach and angle of recession. This assumption simplifies Dalling's equation of C , shown here as Equation 2.5 [3], which is the premise of his solution.

$$C = \frac{\Delta R_{orbit}(\theta_2^2 - \theta_1^2)}{4\pi} \quad (2.5)$$

Where ΔR_{orbit} is the change in the pinion radius, θ_1 is the original orientation of the gear tooth, and θ_2 is the new orientation of the gear tooth after reorientation.

With the angles of approach and recession never being equal, improper involute gear engagement will occur in the Dalling model, resulting in a loss of efficiency.

The investigation into the involutometry assumptions Dalling introduces is rather complex and will be addressed in subsequent chapters. However, it is sufficient to say the Dalling model will not function without correcting the involutometry assumptions.

2.2.2. Output Acceleration Assumption

During Dalling's kinematic analysis, another major assumption is made. In the initial description of the angular correction problem (section 5.2.3.1 [3]) Dalling describes two relative rotational motion scenarios. These two scenarios describe the relative motion between the gear tooth of the input drive member and the gear tooth of the output driven member. The first scenario consists of engagement at the pitch point, and the second is the scenario at any other engagement point. The unintentional assumption Dalling introduces into these scenarios results from the lack of consideration of the acceleration of the output member. Since the output will accelerate as the radius of the input gear tooth changes (Dalling's Δr_{orbit}), the output acceleration cannot be disregarded. From the second scenario, Dalling conceives an angular correction mathematical model [3]. Thus, since Dalling fails to consider the acceleration of the output member, the angular correction mathematical model will not provide the correction required for proper engagement.

2.2.3. Prescribed Angular Input Motion Assumption

In an effort to simplify the kinematic model, Dalling prescribes the angular input motion to be linear [3]. This motion is adequate; however, Dalling also assumed a linear angular input will produce a constant linear angular output motion [3]. This assumption breaks down when the acceleration of the output is considered. Since acceleration is a second order function, the output angular motion is not assured to be a constant or linear. Without prescribing the output acceleration (which Dalling does not do) the amount of angular correction required cannot be calculated.

2.3. Assumption Rectifications

Since the most significant assumptions (those of involutometry) are fundamental assumptions, the design efforts must return to the development of working principles in the conceptual design phase. By doing so, the working principles of involutometry will also be considered as a solution is developed. Also the angular acceleration of the output member must also be prescribed. By making these revisions the assumptions Dalling introduced will be rectified and a sufficient solution will be established.

These alterations to the selected concept will be achieved through the development of the Line-of-Action Model design tool. The Line-of-Action Model will be used to determine the amount of correction required to implement the cam-follower concept as a conceptual principal solution.

3. Conceptual Design Method

The return to the conceptual design phase is not unprecedented in the design process. Revisions and iterations should be anticipated in the development of a complex system. As revisions and iterations take place during the conceptual design phase, the requirements list should be revisited regardless of which step the revision or iteration returns to. This will allow for the requirements list to be modified based on new knowledge or constraints. For this reason this chapter will detail the conceptual design method which will be used to develop a conceptual solution which considers involutometry starting from the requirements list.

3.1. Technical Scope of the Conceptual Design Phase

The conceptual design work led by Dalling provided significant progress towards the development of a conceptual solution. For example, during the conceptual design phase significant patent and literature research was conducted to classify CVT embodiments as PECVTs. Although the current research efforts will return to the initial step of the conceptual design phase (that is, the establishment of the requirements list) not all stages of the conceptual design phase will be addressed. However, each stage will be described to provide a full understanding of the conceptual design phase.

In addition, significant concept generation will not be conducted since Dalling conducted extensive work in this area [3], alternatively, the most viable concepts Dalling generated will be re-evaluated based upon the new involutometry considerations.

The evaluation of potential conceptual solutions will be based primarily on kinematic considerations. Prior to indentifying and describing each individual stage of the conceptual design phase, a layout of the conceptual design phase will be presented in order to provide a broad perspective of the process.

3.2. Conceptual Design Process Layout

The conceptual design phase which will be used in this research effort is an adaptation from the product development process described in *Engineering Design, a Systematic Approach* by Pahl, Beitz, et al. [5]. The conceptual design phase is effectively described in [5] by a process flow diagram. Figure 3.1 depicts the conceptual design process diagram described in [5].



Figure 3.1 Conceptual Design Process

3.2.1. The Requirements List

As mentioned previously in section 2.1.2 the requirements list is a list of the required characteristics, parameters and objectives of the product. This list contains all of the needed parameters to identify and describe a solution which will meet the objectives of the product. Since this research is building upon the work of Dalling in [3], including returning to the requirements list to ensure the product objectives are accurately described, the requirements list Dalling established will be revised to incorporate new parameters which will ensure previous assumptions are addressed.

3.2.2. Essential Problem

In section 2.1.1.1 the essential problem of a PECVT was effectively described. The revision efforts of the current research will not analyze the essential problem in depth beyond what is discussed in section 2.1.1.1; however, due to the presence of assumptions which prevent the previous conceptual principal solution from meeting the objectives of a PECVT, the requirements list should be revised to include characteristics to address the known assumptions. With the new identification of requirements, the functional structures can be described.

3.2.3. Functional Structures

Functional structures are solution neutral descriptions of the relationship between energy, material or signal inputs and outputs [5]. Due to the very specific nature of a PECVT the functional structures are very well defined. The items contained in Dalling's requirements list (shown in section 2.1.2 as Table 2.2) that are given an importance rating

of one describe the functional structures of a PECVT. Since the functional structures are not affected by the revision of the requirements list, the functional structures will not be addressed in this research effort.

3.2.4. Working Principles

The core of the revision to the conceptual design phase of this research effort will focus on establishing additional working principles. Working principles are geometric and material characteristics that are fundamental to the physical function of the product [5]. Since the major assumption by Dalling is the absence of involutometry principles, which causes an infeasible conceptual principal solution to be arrived at the revision of the working principles will focus on considering the effects of involutometry. Once these additional working principles are established, working structures can be developed which satisfy the revised set of working principles.

3.2.5. Working Structures

Working structures are components or subsystems which satisfy specific working principles. In order to ensure that working principles are achieved by the product, working principles must be conveyed using working structures. These structures are developed in “system synthesis” [5]. This system synthesis, or the design of product components or subsystems is a highly iterative process, and in fact system synthesis encompasses the working structures, suitable combinations, firm up, and evaluation phases. If a working structure is found overly complex, or not commercially viable, the working structure will not be pursued in later phases of the conceptual design phase.

Likewise, a working structure may proceed in the conceptual design phase and then be deemed not commercially viable.

To establish working structures, in the case of the development of a PECVT, a design tool entitled the Line-of-Action Model will be developed to quantify the effect of the working principles (the NITP and involutometry) on the working structures proposed by Dalling, along with any newly developed working structures.

3.2.6. Suitable Combinations

The establishment of suitable combinations is a crucial step in the conceptual design phase. Once working structures have been developed, combinations of these structures will be developed to satisfy the requirements list in the most effective manner. As mentioned previously (section 2.1.3), Dalling has proposed two sub-classes of PECVTs. The working structures will be classified into these sub-classes to develop suitable combinations.

3.2.7. Firm Up

Due to the scope of this research effort, the most promising suitable combination of working structures will be selected to elaborate upon. The firming up of the concept is in preparation for evaluating the concept as the conceptual principal solution. The firming up of a concept will entail the development of needed elements, or components which were previously lacking to evaluate the concept.

3.2.8. Evaluation

Evaluation of the proposed concept will be carried out by conducting appropriate case studies and theoretical analyses. A combination of case studies and theoretical analyses will be used to ensure the potential conceptual solution overcomes the NITP and that involutometry principles are satisfied. Both the NITP and involutometry must be addressed in order to declare the concept the conceptual principal solution. If either the NITP or involutometry is not satisfied revisions to the conceptual design phase will again be required.

3.2.9. Principal Solution

Once the evaluation of the proposed concept is complete the concept will become the conceptual principal solution. The principal solution is the conceptual solution which fully addresses the essential problem, fulfills the objective and requirements lists, and is the most commercially viable concept.

To demonstrate the principal solution, a summary of the success of the proposed concept to fulfill the objective of a PECVT, design requirements, and a discussion of the commercial viability will be given.

3.3. Embodiment Design Phase Concluding Remarks

Previously, emphasis was placed on the conceptual design phase to solely address kinematic positioning of components to establish the feasibility of a PECVT (section 3.1). By ignoring the effects of stress, material properties, and manufacturability a kinematic solution may be sought which progresses the development of the PECVT

beyond currently published embodiments. However, in order to continue the development of a feasible PECVT beyond the conceptual design phase these effects must be addressed. Therefore, during the development of functional structures or “system synthesis” [5], consideration of these additional constraints will be secondary design objectives. By doing so, the resulting concept will have the greatest potential to succeed as a functional PECVT that will be commercially viable for end user applications.

4. Involutometry

The geometry of involute curves, or involutometry, has been a practical study for centuries [10]. Today worldwide associations have been established to standardize involute gear design [17]. The involute curve can be considered both simplistically beautiful, as well as remarkably complex. Due to the geometric complexity of the involute curve, world renowned industry experts in involute gear design were consulted to determine a definitive reference for studying involutometry principles [18]. The work of George Buckingham in *Analytical Mechanics of Gears* [4] has been selected as the primary reference for this research effort, based upon industry suggestions.

The use of the involute curve as the shape of the gear teeth in a gearset has several unique advantages. For this reason the involute gear profile has become the standard in gear design. The advantages of an involute shaped gear tooth however, diminish as the gear tooth profile deviates from the standard involute profile. From the initial efforts of this research, it was determined that the behavior of involute gears is desirable for a PECVT conceptual solution. For this reason emphasis is placed on developing involutometry principles that could be applied to a PECVT.

To include involutometry principles, the conceptual design process will return to the working principles stage. The working principles established by Dalling [3] will be expanded through a literature review of the work of Buckingham [4] to include

involotometry definitions, relationships, and subsequent principles. Ultimately, two involotometry principles in particular will prove to be fundamental to the development of a feasible PECVT solution. These principles are the line of action and path of contact principle relationship and the fundamental law of gearing principle requiring constant velocity along the line of action.

Prior to the development of these additional working principles the initial stages of the product development process will be evaluated for revision. As mentioned in chapter three, the revisions will begin with the requirements list. Also the essential problem and functional structures, conceptual design phases, will be examined for revision.

4.1. Requirements List

To address the involotometry assumptions made by Dalling the requirements list presented in section 2.1.2 was amended to include involotometry considerations. Specifically the engaged members utilized in the conceptual development of a PECVT must possess the kinematic characteristics of involute gears. This requirement does not necessarily require the engaged members to be involute gears, but rather requires that the engaged members behave, at a minimum, similar to involute gear profiles in terms of their contact behavior, kinematics, stress, and wear characteristics. Without these behaviors the engaged members will not satisfy involotometry principles. The revised requirements list which includes involute behavior is shown in Table 4.1. The additional requirement is highlighted in grey for convenience.

Table 4.1 Revised Requirements List

| Item number | Requirements | Importance |
|--------------------|--|-------------------|
| | The Transmission: | |
| 1 | ratio is continuously variable | 1 |
| 2 | transmits power solely through engaged members | 1 |
| 3 | provides positive engagement of the input and output | 1 |
| 4 | provides continuous engagement of the input and output | 1 |
| 10 | is able to vary the gear ratio under load | 1 |
| 17 | engaged members follow involutometry laws & behavior | 1 |
| 16 | does not produce an oscillating output | 2 |
| 5 | can transmit high torque loads | 2 |
| 6 | is highly efficient | 2 |
| 9 | is not a complex system (preferably fully mechanical) | 3 |
| 7 | is light weight | 3 |
| 8 | is comprised of standard components | 3 |
| 12 | is adaptable to current applications | 3 |
| 11 | can provide a large gear ratio range | 4 |
| 13 | is simple to control | 4 |
| 14 | can be operated over wide range of RPMs | 4 |
| 15 | does not produce excessive vibrations | 4 |

4.2. The Essential Problem and Functional Structures

The Essential Problem identified initially by Anderson, [1] and characterized by Dalling [3] is not altered with the addition of involutometry to the requirements list. This is the case since the NITP is present whenever a fixed gear profile is used. Additionally the NITP is described in section 2.1.1.1.1 utilizing an involute gear profile.

The functional structures selected previously are also not affected by the change in the requirements list. This is due to the fundamental objective of the design process which is to develop a positively engaged continuously variable transmission. The specification of positive engagement causes the functional structures to utilize engaged members to transfer the load, and thus the existing functional structures do not change with the addition of the new requirement.

4.3. Working Principles

Amending the working principles established by Dalling [3] is essential. To incorporate involutometry into the working principles, the development of an involute curve will be described. This will be done through identifying involutometry definitions, principles, and properties. As mentioned previously, sound understanding of the line of action and path of contact principle relationship and the fundamental law of gearing principle requiring a constant velocity along the line of action are essential to developing a viable PECVT.

4.4. Involute Curve Definitions

To generate an involute curve, several definitions must be established. These include the base circle, the global origin, the base radius, the fundamental involute triangle, and the pressure angle. In general, as the generation of the involute curve progresses, an involute curve can be thought of as a curve resulting from revolving a tangent line about a circle. This traditional description is depicted in Figure 4.1.

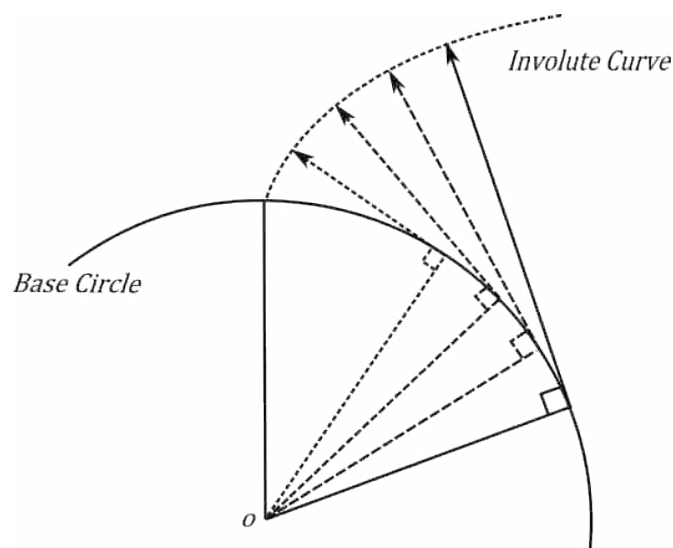


Figure 4.1 Traditional Involute Curve Generation Description

4.4.1. The Base Circle

The circle from which the involute is generated is termed the base circle. The base circle can be of any arbitrary size; however, the size of the involute curve is a function of the base circle. Thus the involute curve will change as the base circle is varied.

4.4.2. The Global Origin

The global origin is a point which will be defined as concentric with the center of the base circle. For convenience the global origin, or origin, will be termed O .

4.4.3. The Base Circle Radius

The base circle radius r_b , is the radius of the base circle, and is a function of other gear parameters which will be defined shortly. It is sufficient to define r_b of some arbitrary size for the generic generation of the involute.

4.4.4. The Fundamental Involute Triangle

To further understand the development of the involute curve a planar vector triangle termed the fundamental involute triangle is introduced, and shown in Figure 4.2. The legs of the vector triangle are $\overrightarrow{r_{inv}}$, whose magnitude is the radius of the involute form (r_{inv}), $\overrightarrow{r_c}$, whose magnitude is the radius of curvature at the involute form (r_c), and $\overrightarrow{r_b}$, whose magnitude is the base circle radius (r_b).

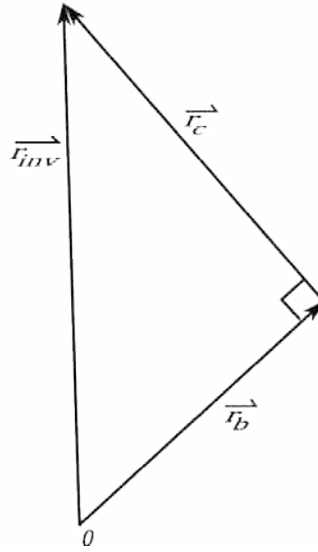


Figure 4.2 The Fundamental Involute Triangle

In relation to the base circle, the origin of the fundamental involute triangle is at O . Also r_c is tangent to the base circle. The scalar form of the fundamental triangle in relation to the base circle is shown in Figure 4.3.

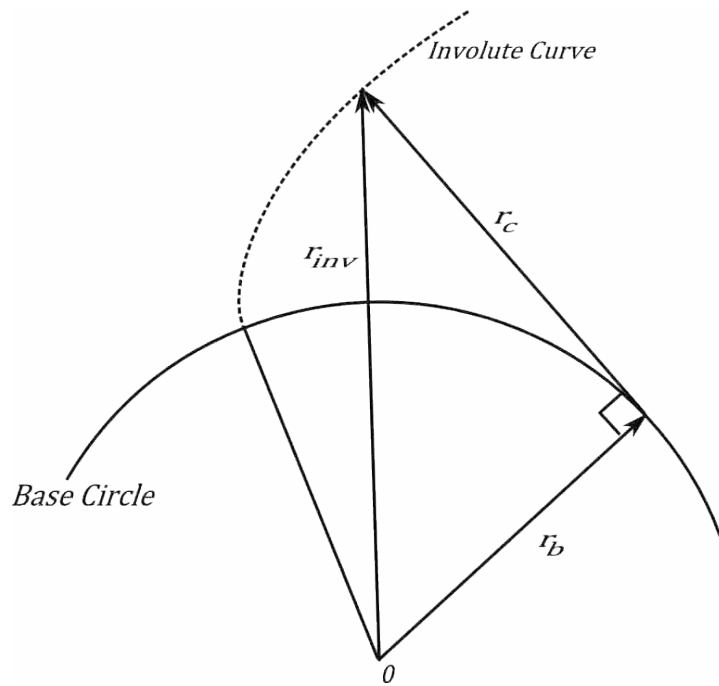


Figure 4.3 The Fundamental Involute Triangle & Base Circle

4.4.5. The Pressure Angle

Proper understanding of the pressure angle is essential to the development of the involute curve, and a PECVT. The pressure angle ϕ shown in Figure 4.4 can be found from several geometric configurations in involute profile generation. The primary definition of ϕ is the angle between r_{inv} and r_b as shown in Figure 4.4. Further discussion of the pressure angle will ensue as other geometric configurations are discussed.

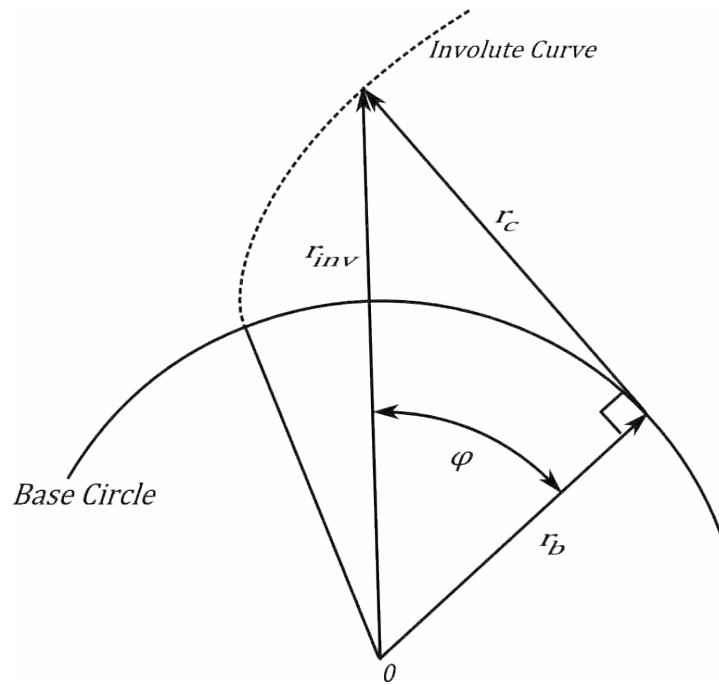


Figure 4.4 The Pressure Angle

4.5. Involute Curve Relationships

To generate an involute profile, additional definitions are required. These additional definitions are formed from the relationships of the previous set of involute definitions. These relationships define the subtended arc, the vectorial angle, r_c , and r_{inv} . Recall that the involute profile can be considered as a circumferential tangent line unwrapped about a base circle.

4.5.1. The Subtended Arc

The involute curve is based upon the amount the circumferential line r_c , is unwound. This subtended arc β , or the amount of the circumferential line has been unwound is shown in Figure 4.5.

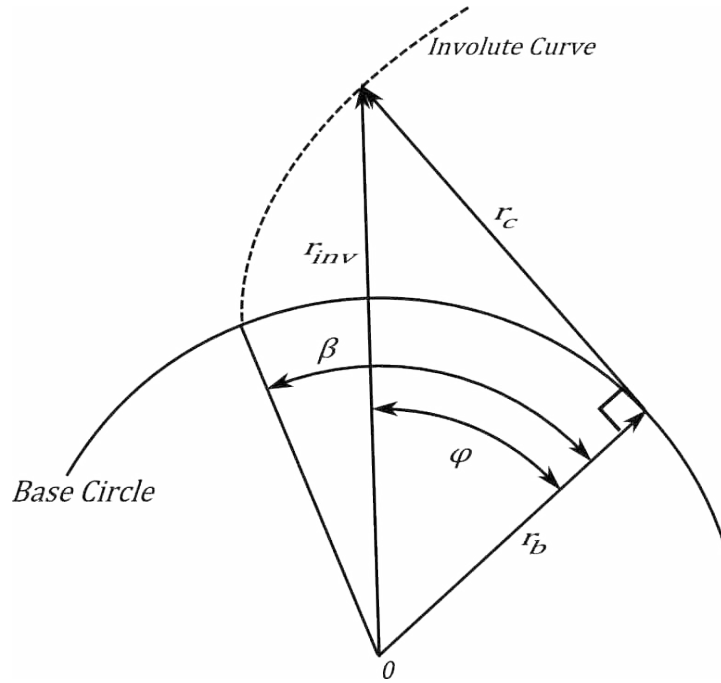


Figure 4.5 The Subtended Arc

The angle β is equal to the length of the circumference of the base circle that has been unwound [4] divided by the r_b , this relationship is shown in Equation 4.1.

$$\beta = \frac{\sqrt{r_{inv}^2 - r_b^2}}{r_b} \quad (4.1)$$

4.5.2. The Vectorial Angle

The vectorial angle θ , shown in Figure 4.6 is defined as the angle between r_{inv} and the origin of generation of the involute curve (a). Equation 4.2 describes θ from the geometry shown in Figure 4.6 [4].

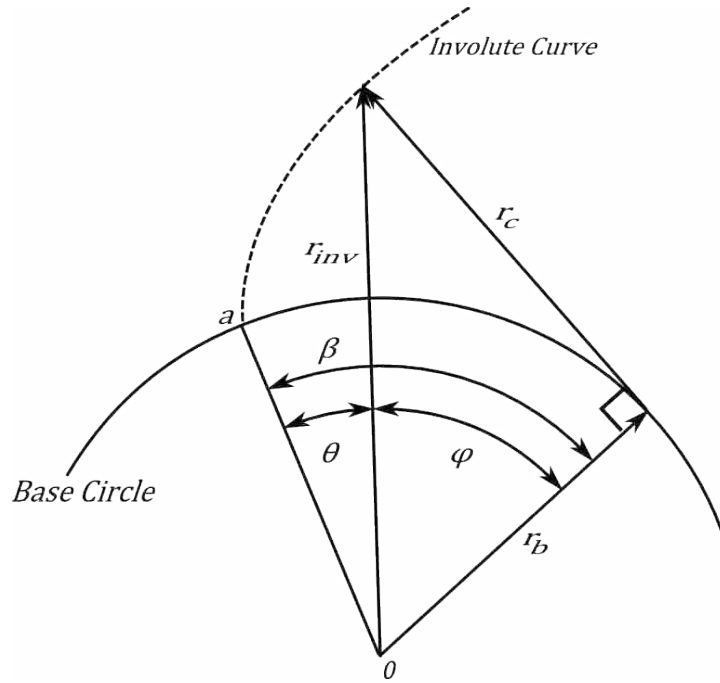


Figure 4.6 The Vectorial Angle

$$\theta = \beta - \tan^{-1} \frac{\sqrt{r_{inv}^2 - r_b^2}}{r_b} = \beta - \varphi \quad (4.2)$$

The most significant relationship involving θ is the relationship between θ and φ . Equation 4.3 depicts the geometrical relationship between θ and φ , the full derivation for this relationship can be found in [4].

$$\theta = \tan \varphi - \varphi = inv \varphi \quad (4.3)$$

The involute function of the pressure angle, termed $inv \varphi$ is more commonly used to describe the vectorial angle and is considered a fundamental relationship to the development of the involute curve [4].

4.5.3. The Radius of Curvature

Standard involutometry states that the length of the radius of curvature, r_c is the arc length along the base circle subtended by β [4]. This relationship is shown in Equation 4.4.

$$r_c = r_b \beta \quad (4.4)$$

When combining equations 4.2, 4.3, and 4.4, it can be seen that r_c is a function of φ , this implies as φ varies, so will r_c . Equation 4.5 depicts the relationship between r_c and φ . This relationship is also confirmed by examining the fundamental involute triangle of Figure 4.4.

$$r_c = r_b \tan \varphi \quad (4.5)$$

Figure 4.7 depicts several radii of curvature at various pressure angles. From this relationship, the points of the involute curve can be established.

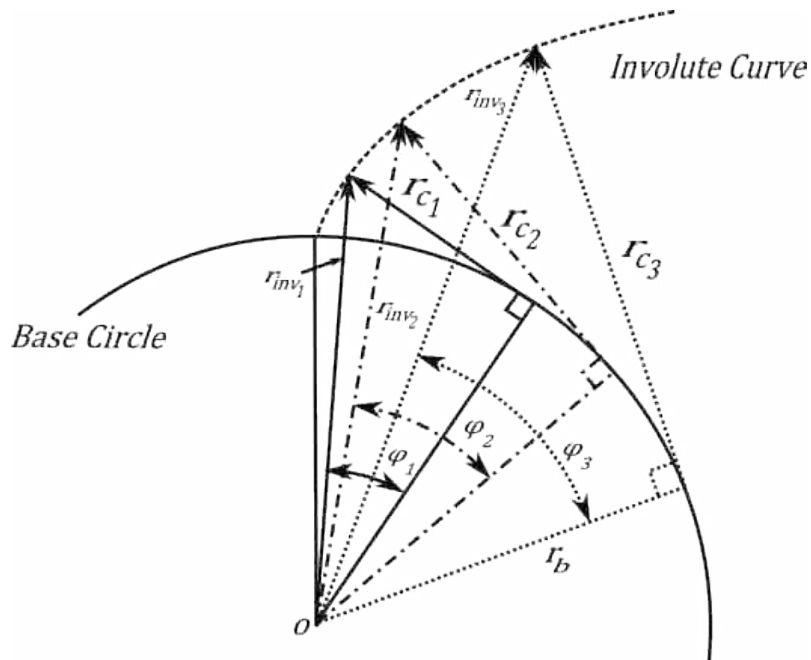


Figure 4.7 Radii of Curvature

4.6. Radius to the Involute Form

The radius to the involute form (r_{inv}) is the final relationship required before the involute curve can be generated in polar form. To derive r_{inv} recall the fundamental triangle with φ defined in Figure 4.4. From Pythagorean's Theorem r_{inv} is a function of φ as shown in Equation 4.6.

$$r_{inv}(\varphi) = \sqrt{r_b^2 + r_c^2} \quad (4.6)$$

4.7. Involute Curve Generation

With these additional definitions and relationships, the generation of the involute curve in polar coordinates can be understood. Initially r_{inv} and r_b are equal, implying r_c is equal to zero, since φ is equal to zero. Thus the involute curve is generated beginning at the base circle and is extended in the direction of rotation of φ . The points of the involute curve correspond to $r_{inv}(\varphi)$ at each instant as depicted in Figure 4.7. The involute curve will continue as φ is extended; however, φ is not extended beyond $\pi/2$.

4.8. Involute Curve Properties

As mentioned previously the involute curve exhibits several unique properties. In the development of a PECVT, the line of action and path of contact relationship and the constant velocity along the line of action property of the involute curve will be exploited to satisfy the behavioral requirements for a feasible PECVT. In order for these properties to be used in a nonstandard manner, a sound understanding of these properties is required.

The involute curve properties which are required to establish the line of action and path of contact relationship and the constant velocity along the line of action property are: the involute variation, the tangent line, the pressure angle, the path of contact, the line of action, the law of conjugate gear-tooth action, the fundamental law of gearing, and the mating gear tooth profile.

4.8.1. Involute Variation

From the definitions and relationships used to generate the involute profile the variation between involutes of various base radii is apparent. The relationship between the involute curve and the base radius is such that, as the base circle is varied the thickness and height of the involute will vary. Several involute profiles of varying r_b are shown in Figure 4.8 (arranged with the pitch radii tangent), to demonstrate the relationship between r_b and the shape of the involute profile.

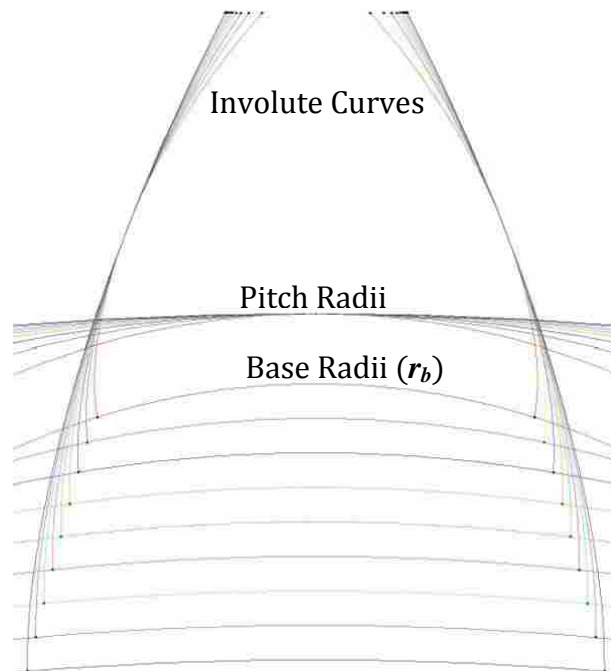


Figure 4.8 Various Involute Curves

Recall that the proposed PECVT conceptual solution by Dalling [3] allows the r_b to vary while maintaining a specified (fixed) involute profile. The preceding involutometry definitions and relationships discussed in sections 4.4 and 4.5 significantly increase the level of complexity for a fixed involute profile to behave as any other involute profile (an involute with a different r_b). This behavioral issue is a result of the change in arc length of the involute curve (the change in height and width) for two different base radii. In the case of a PECVT, this principle implies that no two involute curves will have the same engagement behavior (normal and sliding contact) with a common mating gear, because to change the gear ratio the base radii of the gears in the gear set must change, which in turn changes the size and shape of the profile. Thus, no single involute curve can be the foundation of the principal solution.

4.8.2. The Tangent Line

As with all curves, the point of contact between two mating involute curves is located at the singular point of tangency between the two curves [4, 12, 10]. This line of tangency (termed the tangent line and illustrated in Figure 4.9) at the point of contact is prominent in defining φ .

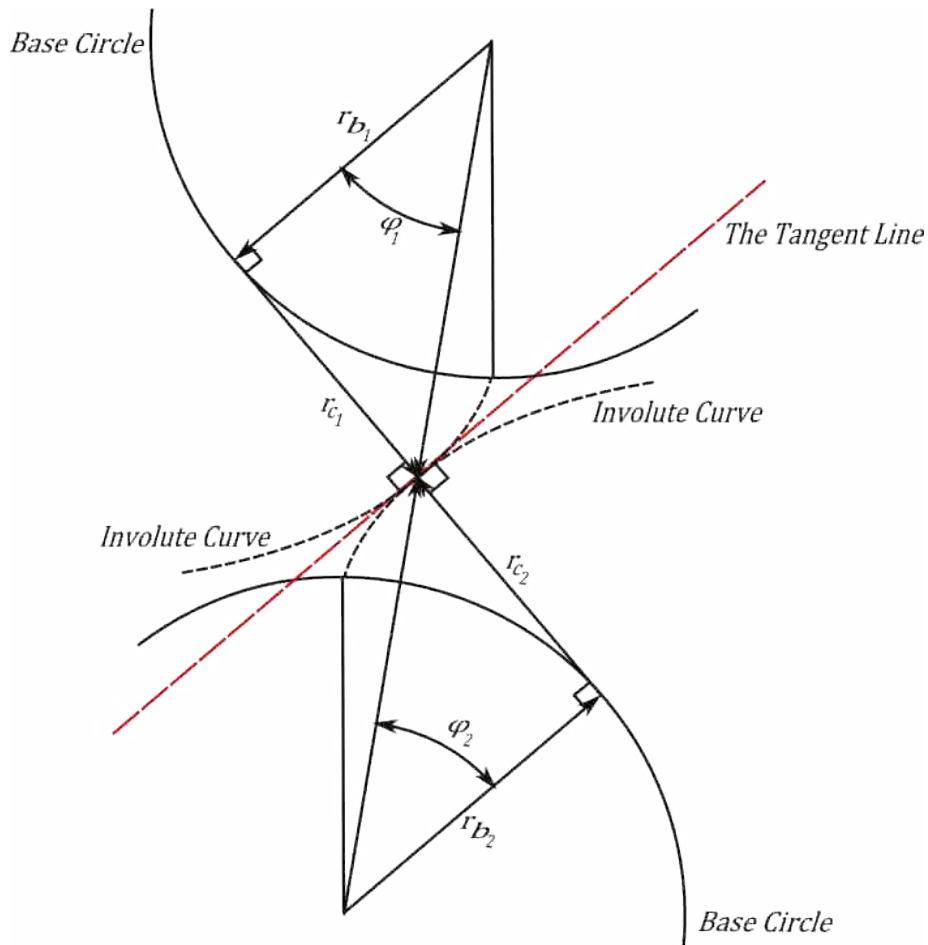


Figure 4.9 The Tangent Line

4.8.3. The Pressure Angle

Upon generation of the involute profile, an additional definition of φ is available. The pressure angle φ , is now also defined as the angle between r_{inv} and the tangent line to the curve at r_{inv} [4] and is shown in Figure 4.10. In the generation of an involute curve, this is the primary definition of φ , and is also the primary definition of φ that will be used in the development of a PECVT.

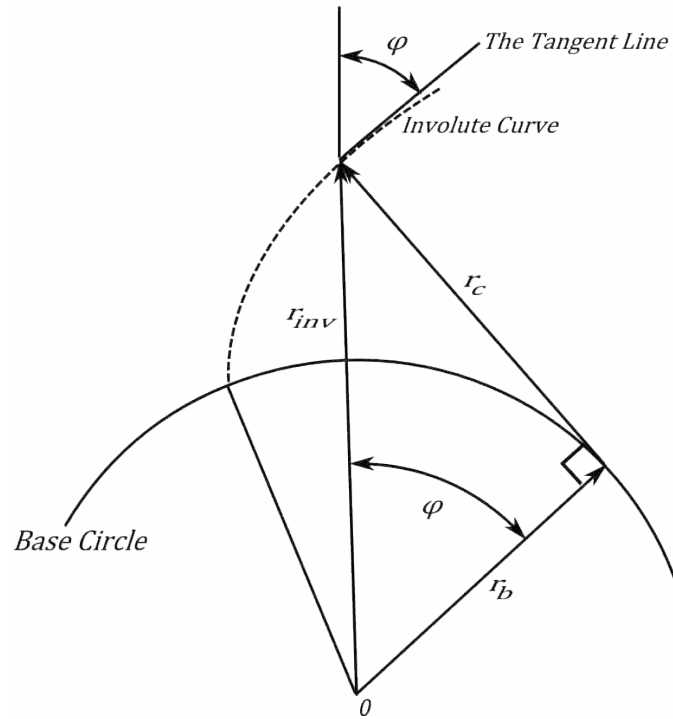


Figure 4.10 The Pressure Angle Definition II

4.8.3.1. Special Case of the Pressure Angle

With the introduction of the second definition of φ a special case of φ emerges. The pressure angle at the pitch radius φ_p , occurs exclusively at the pitch point (the point of contact (r_{inv}) between the mating involutes when contact occurs at the pitch radii, commonly referred to as the line of centers). In traditional involute gear design three design parameters are required, one of which is φ_p . For this reason φ_p is commonly generalized as φ . However, in the generation of an involute curve φ is varied, therefore this generality should be avoided. Thus φ_p is categorized as a special case of φ .

As shown in Figure 4.11 φ_p is defined as the angle between the tangent line to the base circles of an engaged involute gearset and the line normal to the line of centers at the pitch point [4].

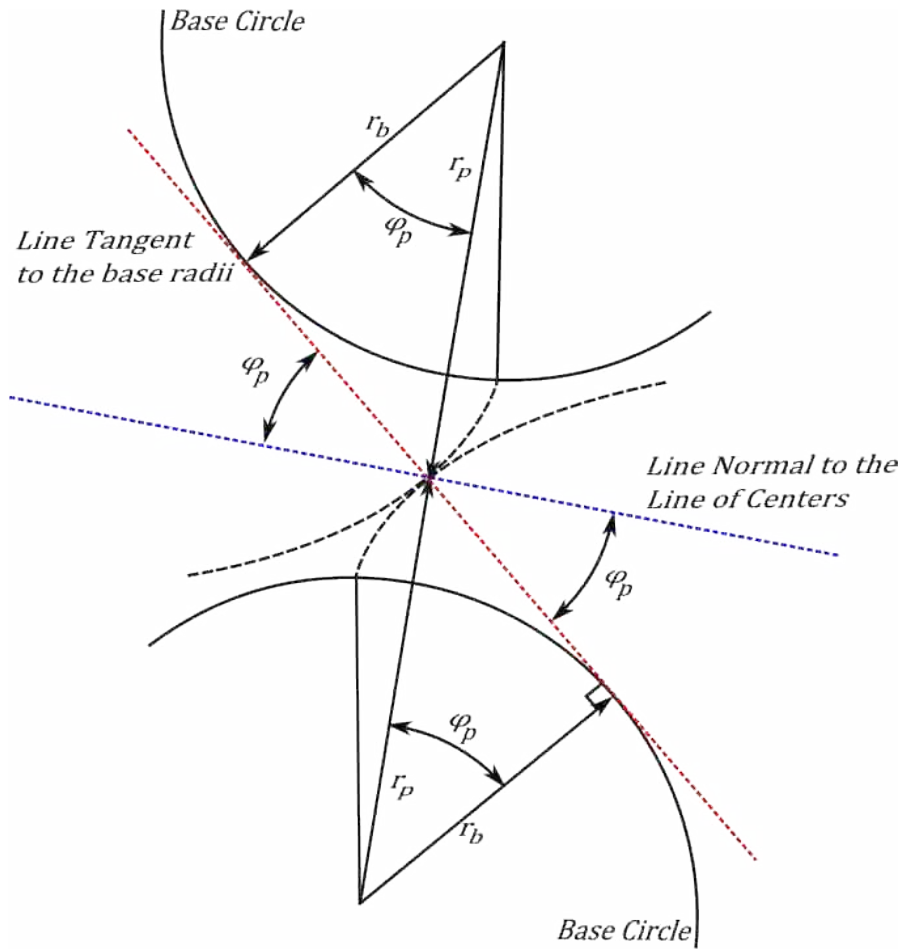


Figure 4.11 The Pressure Angle at the Pitch Point

4.8.4. The Path of Contact

The term, path of contact, is most accurately described by Buckingham, “when conjugate gear-tooth profiles act together, the point of contact between them will travel along a definite path, which is called the path of contact” [4]. A diagram illustrating the path of contact is shown in Figure 4.12.

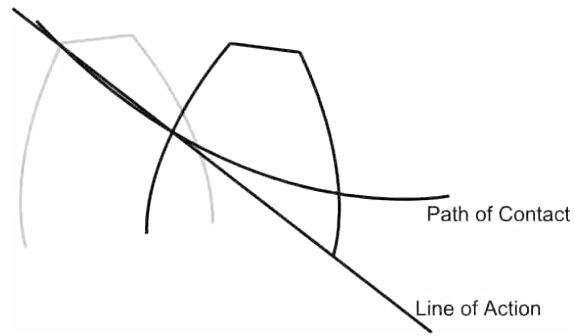


Figure 4.12 The Path of Contact

The Cartesian coordinates of the path of contact shown in Figure 4.13 can be found from the ordinate of the profile y , shown in Equation 4.7 and the abscissa of the path of contact x_p , shown in Equation 4.8. The full derivations for the coordinates of the path of contact can be found in [4].

$$y = r_{\text{inv}} \cdot \cos \theta' \quad (4.7)$$

$$x_p = \frac{-y}{\tan \varphi} \quad (4.8)$$

Where θ' is the vectorial angle θ with the Y axis at the centerline of the toothspace.

The path of contact is a characteristic of all conjugate action profiles, however, in the case of one involute profile acting on another involute profile, the path of contact lies on the common tangent to both base circles which is also illustrated in Figure 4.13.

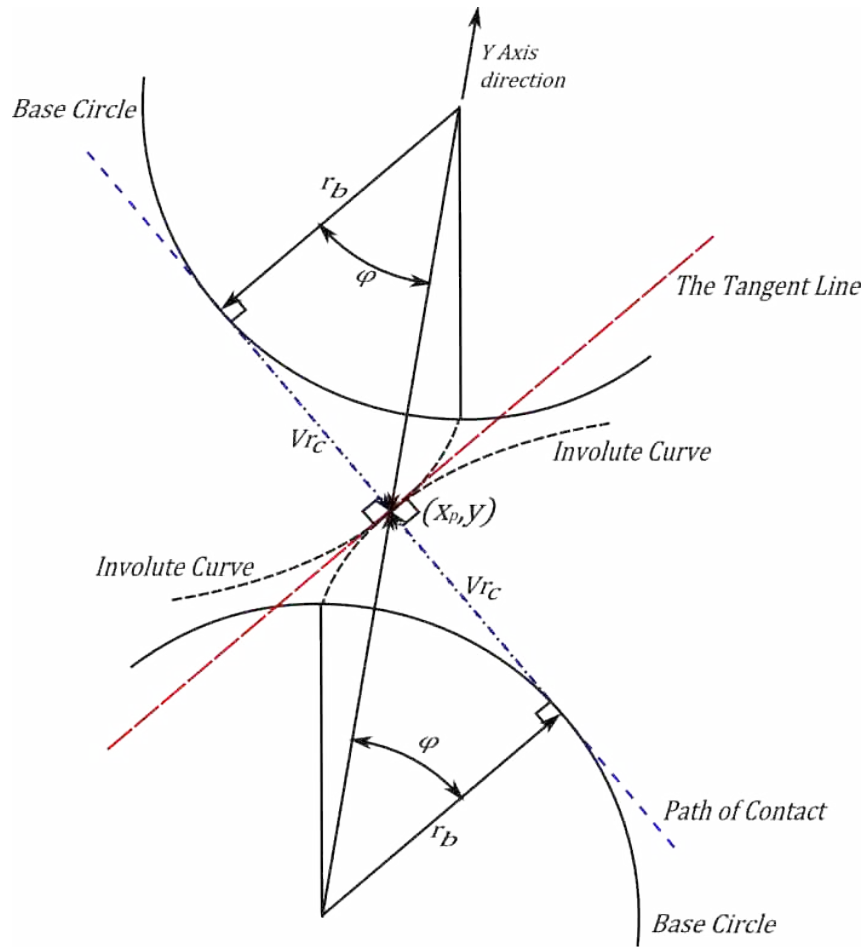


Figure 4.13 Path of Contact Cartesian Coordinates

4.8.5. The Line of Action

The line of action has several useful characteristics. The line of action is defined as the line normal to the tangent line at the point of contact (r_{inv}) and is illustrated in Figure 4.14. In the case of one involute profile acting on another involute profile, the line of action is tangent to the two base circles (r_b) of the mating profiles [4].

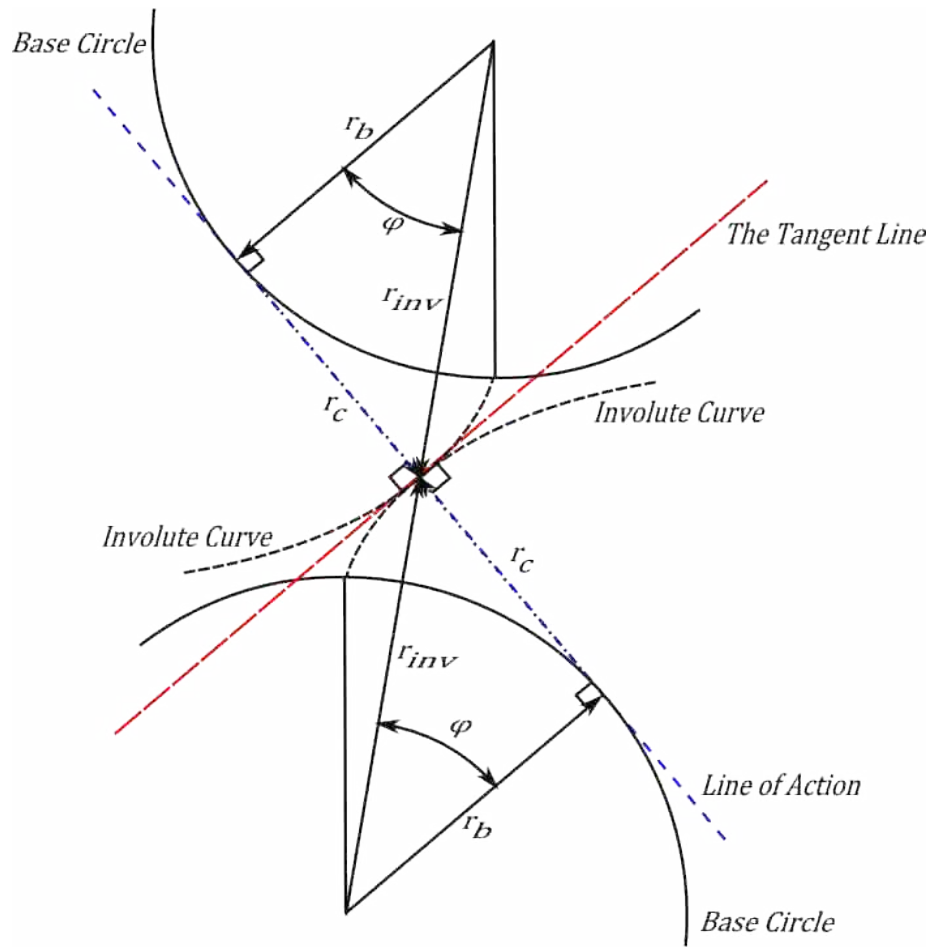


Figure 4.14 The Line of Action

The first fundamental property of involutometry which will be exploited in the development of a PECVT is a unique characteristic of the line of action. This characteristic is specific to the behavior of one involute profile acting on another involute profile. In this case, the path of contact and the line of action, are collinear since both lines are tangent to the base circle of the mating gears as illustrated in Figure 4.15 [4].

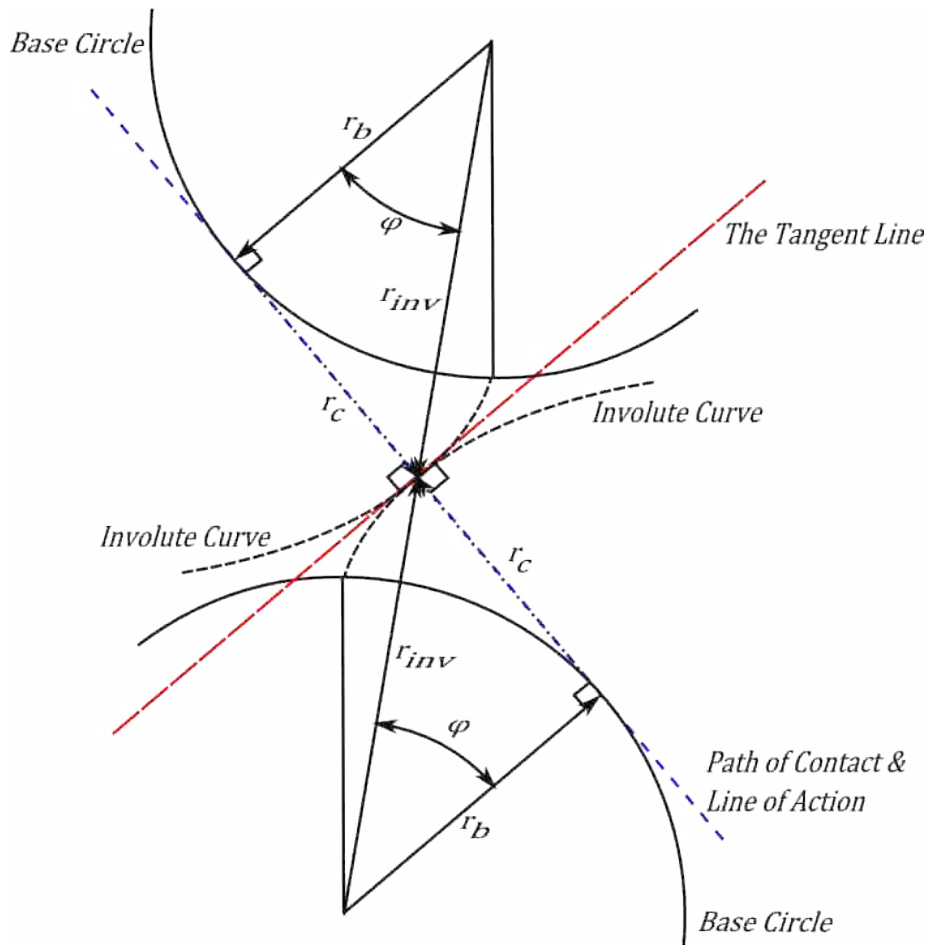


Figure 4.15 The Line of Action and Path of Contact Relationship

The second characteristic of the line of action is also unique to involute profile contact and is related to ϕ_p . Regardless of the size of the base radii (r_b), of the mating involute profiles, the line of action and the path of contact will not change [4]. This characteristic implies that the path of contact and line of action remain the same, regardless of the combination of two mating involute profiles with a common ϕ_p .

4.8.6. The Law of Conjugate Gear-Tooth Action

The common ϕ_p property in the line of action is supported by the law of conjugate gear-tooth action which states:

“To transmit uniform rotary motion from one shaft to another by means of gear teeth, the normals to the profiles of these teeth at all points of contact must pass through a fixed point in the common center line of the two shafts” [4].

Since the lines of action of each tooth size are collinear, the law of conjugate gear-tooth action remains valid and ensures involute profiles will provide conjugate action. In addition, the law of conjugate gear-tooth action provides a simple, yet essential, characteristic of gear motion. This law states that the contact point velocity at all points along the profile in the direction normal to the profile will pass through a fixed point.

4.8.7. The Fundamental Law of Gearing

The fundamental law of gearing is a property of the involute curve. The fundamental law of gearing is derived from the law of conjugate gear tooth-action. The fundamental law of gearing states:

“The angular velocity ratio between the gears of a gearset must remain constant throughout the mesh” [10] .

The angular velocity referenced in the fundamental law of gearing is shown in Equation 4.9 [10], and is derived from the tangential velocity \vec{v}_t , at the pitch radius (a unique radius along the involute profile). The tangential velocity \vec{v}_t is shown in Equation 4.10. A free body diagram of \vec{v}_t is shown in Figure 4.16.

$$\omega_{out} = \omega_{in} \frac{r_{in}}{r_{out}} \quad (4.9)$$

$$\mathbf{v}_t = r_{inv} \cdot \omega \quad (4.10)$$

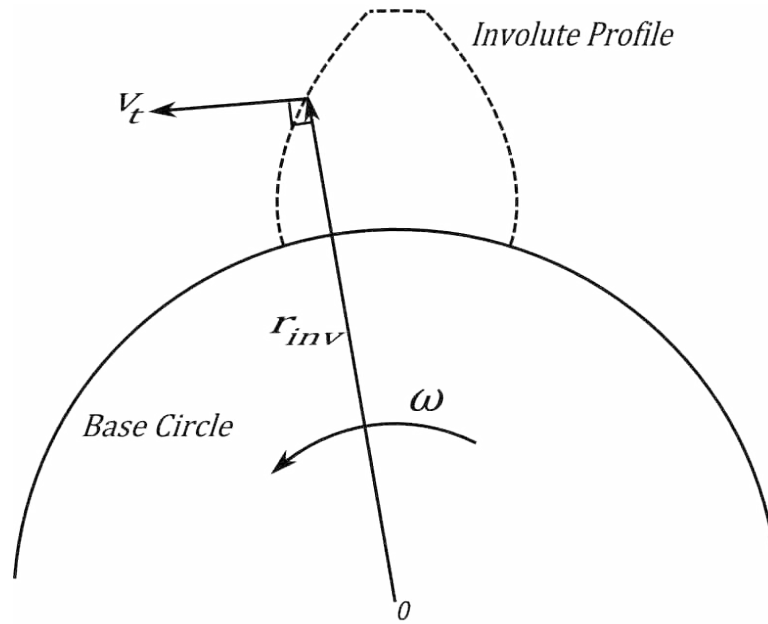


Figure 4.16 Tangential Velocity

Since the fundamental law of gearing is formulated at the pitch radius, further analysis of equation 4.10 is required to apply the fundamental law of gearing at all radii along the involute profile. At the pitch radius, the contact point lies on the line of centers. This property generates pure rolling contact only at this point. At all other radial locations along the involute profile, slipping occurs between the involute profiles of the gear teeth. Therefore, to generalize the fundamental law of gearing to all radii along the involute profile, the vectorial components of \vec{v}_t must be examined.

The tangential velocity vector components of the point of contact in terms of the involute profile, are the surface normal velocity \vec{v}_N in the direction normal to the involute profile at the point of contact, and the slip velocity \vec{v}_s in the direction tangent to the involute profile at the point of contact (the direction of the tangent line). Figure 4.17 shows the vector components of \vec{v}_t .

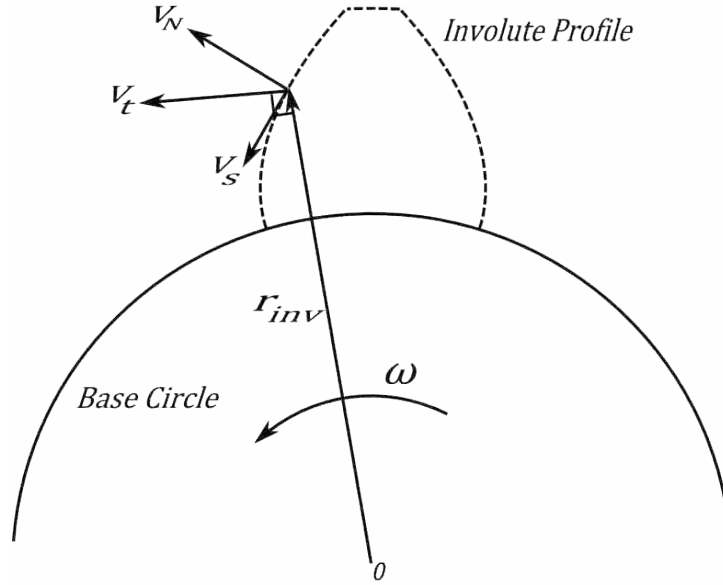


Figure 4.17 v_t Vector Components

Although both \vec{v}_t and \vec{v}_s change with r_{inv} due to the law of conjugate action and the use of rigid bodies, \vec{v}_N on both engaged members does not change. In fact, \vec{v}_N will be equal at all points along the involute profile. This relationship is the second fundamental property of involutometry which will be exploited in the development of a PECVT and is shown in Equation 4.11. Since the velocity in the normal direction lies on the line of action, \vec{v}_t will subsequently be termed the velocity along the line of action \vec{v}_{loa} .

$$\vec{v}_N = \vec{v}_{N_{input}} = \vec{v}_{N_{output}} = \vec{v}_{loa} = constant \quad (4.11)$$

4.8.8. Mating Gear Tooth Profile

With the path of contact, the law of conjugate gear-tooth action and the fundamental law of gearing established, an additional property of conjugate gear tooth systems is of significant use in the development of a feasible PECVT. This additional

property is known as the “Mating Gear-Tooth Profile” or “One Gear-Tooth Form Given” [4]. The *Mating Gear-Tooth Profile* states:

“Once a pitch line has been established for any given tooth profile, a definite path of contact exists along which contact with all conjugate gear-tooth profiles is made regardless of the number of teeth in these gears. The path of contact for any given conjugate gear-tooth system is the same for any two gears as it is for any one gear and the basic rack of the system.” [4]

This property is of great significance in that an infinite number of mating conjugate action involute gear teeth profiles can be generated (for different gearset ratios), once the path of contact is known.

The *One Gear-Tooth Form Given* is a special case of the *Mating Gear-Tooth Profile* in which a specific involute gear-tooth form is selected and the mating involute gear for a specific ratio can then be generated.

4.9. Involutometry Significance

The addition of the involutometry definitions, relationships, and properties to the working principles of the product development process for developing a feasible PECVT dramatically changes the landscape of a potential conceptual solution. This is done primarily through the path of contact, the line of action, the fundamental law of gearing and the *One Gear-Tooth Form Given* property.

As mentioned previously, the line of action and path of contact relationship and the fundamental law of gear gearing property of $\overline{v_{loa}}$ will be exploited in the development a kinematically feasible PECVT. These properties will be exploited while employing the *One Gear-Tooth Form Given* property. Doing so will enable the alterations of the previous conceptual solution to be quantified, as well as a new possible solution to be conceived and evaluated.

5. The Line-of-Action Model

The Line-of-Action Model (LOA model) should not be misconstrued as a conceptual embodiment. The Line-of-Action Model should rather be considered as a tool to aid in determining the details of a working structure or set of conditions where the working principles, including involutometry, are satisfied for enabling a functional PECVT to exist.

The Line-of-Action Model describes the conditions that must be met for one gear to be engaged with another as the gear ratio between the two is changing, as would be the case in a PECVT when the input to output ratio is changing. In a standard transmission this transition is a discontinuous step function, and is achieved via a clutching mechanism, allowing engaged gears to change discontinuously. A diagram of the transition between two gear ratios of a standard transmission is presented as Figure 5.1.

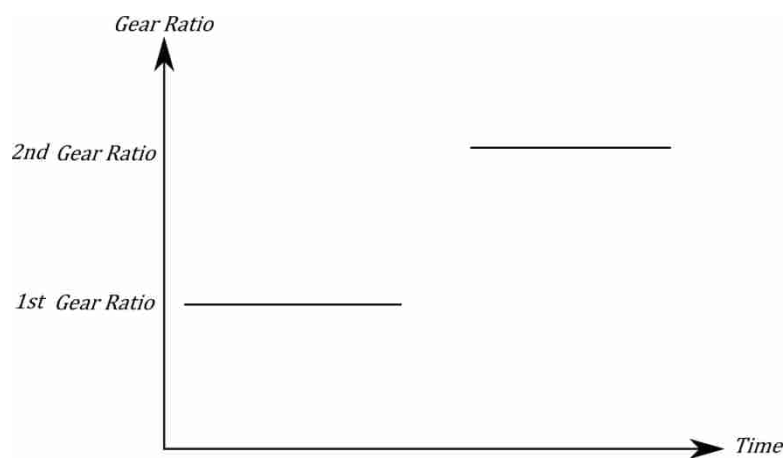


Figure 5.1 Standard Transmission Transition

The main objective of a PECVT is to make the transition between gear ratios continuous via positively engaged members. One possible transition of a PECVT between two gear ratios is shown in Figure 5.2. The Line-of-Action Model also serves as a tool to determine the involutometry alterations required for a specific gear tooth or set of teeth to enable this type of transition to occur.

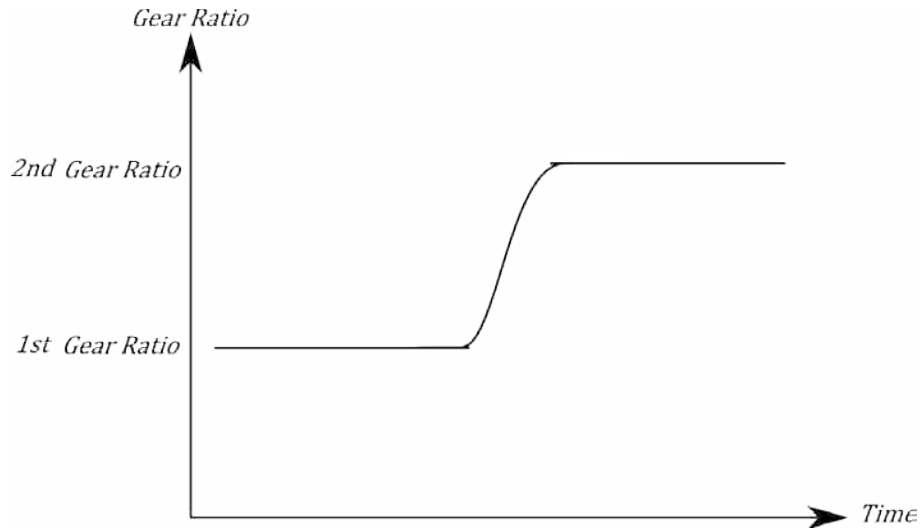


Figure 5.2 PECVT Transition

To identify the corrections required for the conceptual solution developed by Dalling [3] an external spur pinion and an internal spur, ring gearset, will be utilized to show the development of the Line-of-Action Model.

As mentioned previously the line of action and path of contact relationship and fundamental law of gearing property ($\overline{v_{loa}}$) have powerful implications in the development of a PECVT. These two properties coupled with the one gear-tooth form given property, are the foundation of the Line-of-Action Model.

The output ring member of the gearset will act as the one gear-tooth form given, and the spur pinion, input member, involute profile will be generated using the Line-of-Action Model. This is done by determining r_{inv} and φ of the pinion member at each

incremental location along the line of action from the one gear tooth-form given property, while maintaining an instantaneous velocity along the line of action ($\overline{v_{loa}}$). This is illustrated in Figure 5.3, a kinematic diagram depicting the fundamental law of gearing and the line of action to illustrate the line-of-action-model. In Figure 5.3 for a standard involute gearset, the radius of the involute form of the ring gear r_{inv_r} , is specified, and then the radius of the involute form of the pinion gear r_{inv_p} , as well as the center distance CD , are determined so that $\overline{v_{loa}}$ remains constant.

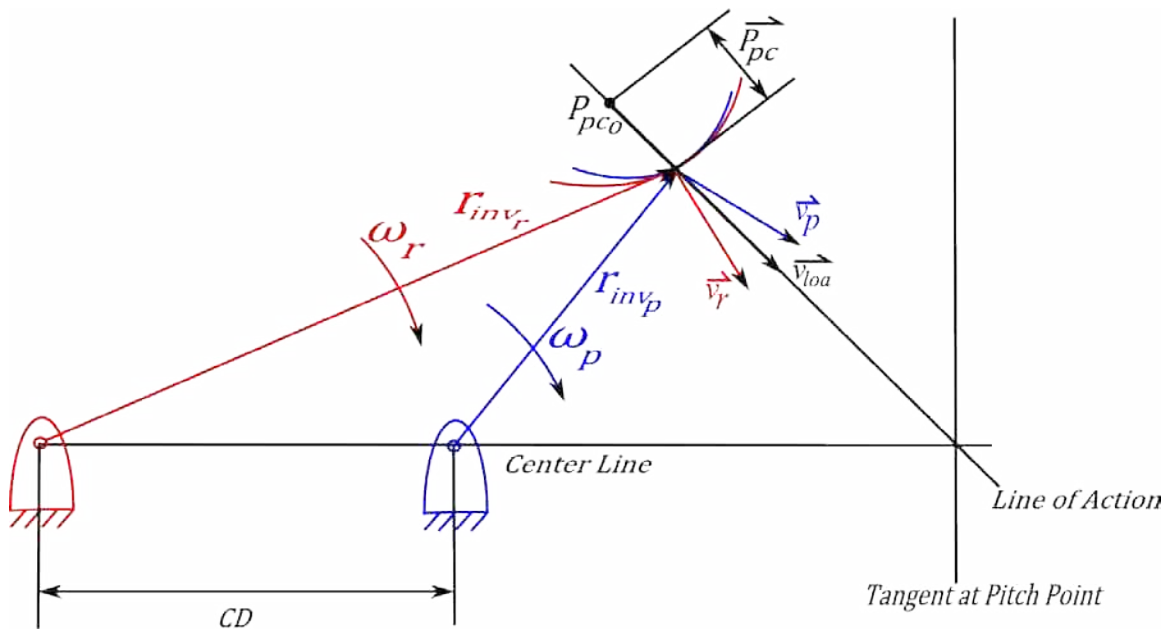


Figure 5.3 The Line of Action Model

Where:

- CD Center Distance of Gearset
- ω_r Angular Velocity of Ring Gear
- ω_p Angular Velocity of Pinion Gear
- r_{inv_r} Radius of Involute Form for Ring Gear
- r_{inv_p} Radius of Involute Form for Pinion Gear

| | |
|----------------------|--|
| \overline{v}_r | Tangential Velocity of Ring Gear |
| \overline{v}_p | Tangential Velocity of Pinion Gear |
| \overline{v}_{loa} | Velocity along the line of action |
| P_{pc_0} | Initial position of the Point of Contact |
| \overline{P}_{pc} | Position of the Point of Contact |

Once the LOA model is established, the working structures determined from the LOA model will be arranged in suitable combinations. The practicality of the generated suitable combinations will also be quantified by the LOA model. The suitable combinations will then be firmed up prior to validation. The firm up phase will determine any additional detail required prior to validation. Finally, case studies and a theoretical analysis will be used to validate the potential conceptual solution, and the conceptual solution will be described.

5.1. Working Structures

With the full set of working principles established, which include involutometry, the product development process can proceed to establish working structures. The working structures do not need to represent any conceptual embodiment in particular. Rather, the working structures are developed as methods to ensure that the working principles are satisfied. The main working structure to be established is a quantification of the required angular and radial correction of a specific involute tooth profile to perform the gear ratio transition of the two engaged gears. This is accomplished with the use of the Line-of-Action Model tool. The transition corrections will be encapsulated in what is called a “Hybrid Involute Profile” since the one gear-tooth form given principle

will generate an array of radii to the involute r_{inv} , and pressure angle ϕ , sets. This modified involute profile will be shown to maintain involutometry laws and behavior, but the velocity along the line of action ($\overline{v_{loa}}$) and the center distance CD , will not be constant since the Hybrid Involute Profile will function during the transition between gear ratios, the region where the gear ratio is continually changing.

5.1.1. Involutometry Design Parameters

The first phase of the development of the Line-of-Action Model is to identify traditional involutometry design parameters. These parameters were not defined previously in chapter 4 since knowledge of these parameters is relatively well understood by gear designers. In addition, no manipulation or exploitation will be done to these parameters; whereas the involutometry described in chapter four for the development of a PECVT will undergo some manipulation and exploitation, and thus were defined in detail in chapter four. As with the involutometry discussion noted in chapter four these parameters are taken from the work of Buckingham; however, these parameters are taken from Buckingham's *Revised Manual of Gear Design* [6].

Previously a spur pinion and ring gearset was identified as the gearset configuration which will be utilized to develop the Line-of-Action Model (with a common pressure angle at the pitch radius ϕ_p , and diametral pitch). If another gearset configuration was used, the LOA model would be altered; however, the development of the LOA model would follow the same phases.

Since the involute gear tooth profile of the output gear is the one gear-tooth form given, only a single set of parameters is required for the output ring. However; since the

spur pinion gear tooth profile is the generated member, the gear ratio boundary conditions of the gearset will be driven by the pinion. Therefore, two sets of parameters must be selected for the two limiting pinion gear teeth, an initial pinion and a final pinion which will be utilized for the ratio transition.

The standard involutometry parameters required for the development of the line of action are:

| | |
|------------|--|
| N | Number of Gear Teeth |
| D_p | Diametral Pitch |
| r_p | Pitch radius |
| r_a | Addendum Radius |
| r_b | Base Radius |
| ω_r | Angular velocity of the ring |
| ω_p | Angular Velocity of the Pinion |
| T_p | Circular Tooth Thickness at Pitch Radius |

The initial two parameters, N and D_p are selected design parameters, and the final two parameters, ω_p and T_p can be addressed in general terms. Due to the functional structures previously specified, ω_p is simply a selected design parameter and is a constant value for both the initial and final pinions. By definition, T_p is the same at the pitch radius for all internal and external spur gears. T_p is presented in Equation 5.1.

$$T_p = \frac{\pi}{2 \cdot D_p} \quad (5.1)$$

The parameters for the gear teeth profile of the ring are distinguished from the gear teeth profile of the pinion parameters through the use of a second subscript such as

r_{xr} and r_{xp} . The pinions are distinguished by a secondary subscript of o or f to indicate the initial or final pinion profiles respectively.

5.1.1.1. Initial Pinion Involutometry

The standard involutometry parameters for the initial pinion are presented as Equations 5.2, 5.3 and 5.4

$$r_{pp_o} = \frac{N_{p_o}}{2 \cdot D_p} \quad (5.2)$$

$$r_{ap_o} = r_{pp_o} + \frac{1}{D_p} \quad (5.3)$$

$$r_{bp_o} = r_{pp_o} \cdot \cos \varphi_p \quad (5.4)$$

5.1.1.2. Final Pinion Involutometry

The standard involutometry parameters for the final pinion are presented as Equations 5.5, 5.6 and 5.7. Note these parameters are identical to those of the initial pinion, except for the secondary subscript, which is critical to maintain.

$$r_{pp_f} = \frac{N_{p_f}}{2 \cdot D_p} \quad (5.5)$$

$$r_{ap_f} = r_{pp_f} + \frac{1}{D_p} \quad (5.6)$$

$$r_{bp_f} = r_{pp_f} \cdot \cos \varphi_p \quad (5.7)$$

5.1.1.3. Ring Involotometry

The standard involotometry parameters for the final pinion are presented as Equations 5.8, 5.9, 5.10, 5.11, 5.12, and 5.13. Note that in ring gear design, an additional radius termed the internal ring radius r_{ir} and ω_{r_o} and ω_{r_f} are also required.

$$r_{pr} = \frac{N_r}{2 \cdot D_p} \quad (5.8)$$

$$r_{ar} = r_{pr} + \frac{1}{D_p} \quad (5.9)$$

$$r_{br} = r_{pr} \cdot \cos \phi_p \quad (5.10)$$

$$r_{ir} = \frac{(N_r - 1.2)}{2 \cdot D_p} \quad (5.11)$$

$$\omega_{r_o} = \omega_{p_o} \cdot \frac{r_{pp_o}}{r_{pr}} \quad (5.12)$$

$$\omega_{r_f} = \omega_{p_f} \cdot \frac{r_{pp_f}}{r_{pr}} \quad (5.13)$$

5.1.2. Lengths of Contact and Angles of Engagement

The second phase in the development of the LOA model is to determine the length along the line of action a particular gear pair will be engaged, as well as the angular amount of engagement along the line of action. In standard involotometry, the length along the line of action is termed *The Length of Action* [10, 12]. The angle of engagement (with respect to the ring) is segmented into an angle from the initial point of contact to the pitch point termed, *The Angle or Arc of Approach* [4, 6, 10, 12], and an angle from the pitch point to the final point of contact is termed, *The Angle or Arc of Recess* [4, 6, 10, 12]. The derivations for the length of action, angle of approach and angle of recess are well defined; however, the definitions contain critical elements which

prevent incorporating the derivations into the Line-of-Action Model directly. These elements pertain to the location along the involute profile where the measurement is taken for the initial and final points of contact. The measurements are not measured from r_b and r_a , but rather from r_p . This small change in location, shown in Figure 5.4 results in a change in the length of action and angles of approach and recess. These minor changes will alter the length of the generated pinion profile in the Line-of-Action Model, if they are used.

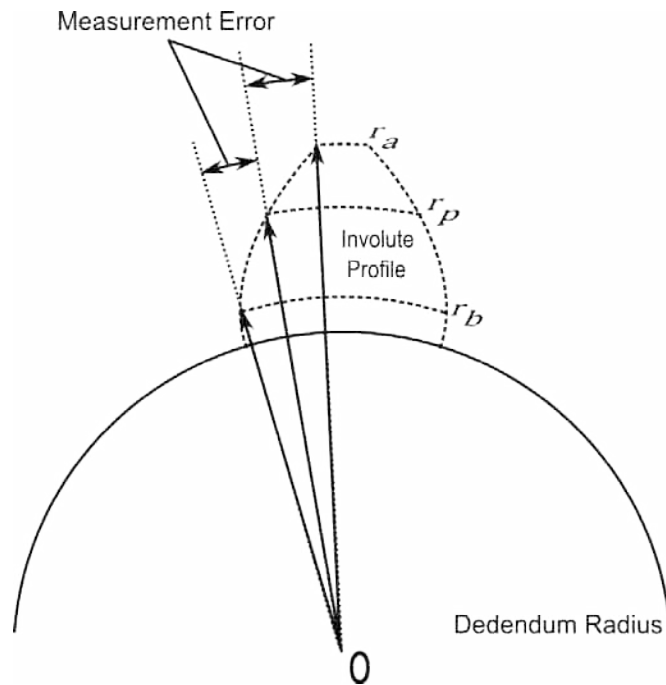


Figure 5.4 Engagement Measurement Error

These measurement errors can be rectified through the use of Figure 6-6 from [4], which is shown here as Figure 5.5.

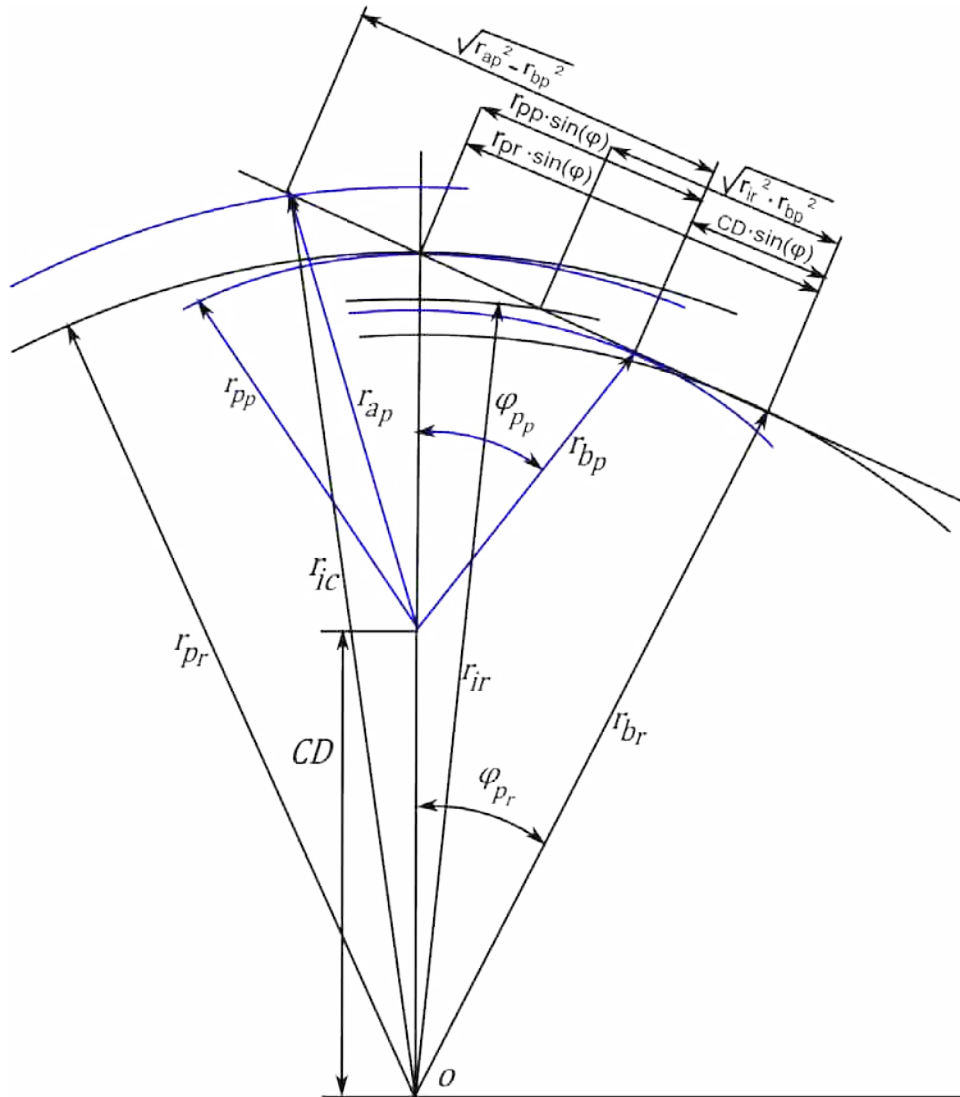


Figure 5.5 Length of Engagement

The geometric configuration of the pinion radii and ring radii shown in Figure 5.5 is employed to determine:

- L_a Length of Approach
- η_a Angle of Contact through Approach
- L_r Length of Recession
- η_r Angle of Contact through Recession
- r_{ic} Initial Radius to the Point of Contact along the Involute Form

Since the ring is the driven member, L_a and η_a are constants regardless of the pinion geometry of the gearset. Thus L_a and η_a are shown in Equations 5.14 and 5.15 respectively. The derivations of L_a and η_a from Figure 5.5, employ the trigonometric law of cosines and are left to the reader. In addition, L_a and η_a will be presented again for initial and final pinion teeth to maintain continuity.

$$L_a = r_{pr} \cdot \sin(\varphi_p) - \sqrt{r_{ir}^2 - r_{br}^2} \quad (5.14)$$

$$\eta_a = \cos^{-1} \left(\frac{-L_a + r_{ir}^2 + r_{pr}^2}{2 \cdot r_{ir} \cdot r_{pr}} \right) \quad (5.15)$$

As with the standard involutometry equations presented in section 5.2 the initial pinion equations are differentiated from the final pinion equations with the use of the secondary subscripts o and f respectively.

5.1.2.1. Initial Pinion Lengths of Contact and Angles of Engagement

The lengths of contact and angles of engagement for the initial pinion are presented as Equations 5.16, 5.17, 5.18, 5.19, and 5.20. Note, r_{ic_o} (equation 5.19) is also derived from the law of cosines, and is left to the reader.

$$L_{a_o} = r_{pr} \cdot \sin(\varphi_p) - \sqrt{r_{ir}^2 - r_{br}^2} \quad (5.16)$$

$$\eta_{a_o} = \cos^{-1} \left(\frac{-L_{a_o} + r_{ir}^2 + r_{pr}^2}{2 \cdot r_{ir} \cdot r_{pr}} \right) \quad (5.17)$$

$$L_{r_o} = \sqrt{r_{ap_o}^2 - r_{bp_o}^2} - r_{pp_o} \cdot \sin(\varphi_p) \quad (5.18)$$

$$r_{ic_o} = \sqrt{r_{pr}^2 + L_{r_o}^2 - 2 \cdot r_{pr} \cdot L_{r_o} \cdot \cos(\varphi_p + \pi/2)} \quad (5.19)$$

$$\eta_{r_o} = \cos^{-1} \left(\frac{-L_{r_o} + r_{ic_o}^2 + r_{pr}^2}{2 \cdot r_{ic_o} \cdot r_{pr}} \right) \quad (5.20)$$

5.1.2.2. Final Pinion Lengths of Contact and Angles of Engagement

The lengths of contact and angles of engagement for the final pinion are presented as Equations 5.21, 5.22, 5.23, 5.24, and 5.25. As with r_{ic_o} (equation 5.19), r_{ic_f} (equation 5.25) is also derived from the law of cosines, and is left to the reader.

$$L_{a_f} = r_{pr} \cdot \sin(\varphi_p) - \sqrt{r_{ir}^2 - r_{br}^2} \quad (5.21)$$

$$\eta_{a_f} = \cos^{-1} \left(\frac{-L_{a_f} + r_{ir}^2 + r_{pr}^2}{2 \cdot r_{ir} \cdot r_{pr}} \right) \quad (5.22)$$

$$L_{r_f} = \sqrt{r_{ap_f}^2 - r_{bp_f}^2} - r_{pp_f} \cdot \sin(\varphi_p) \quad (5.23)$$

$$r_{ic_f} = \sqrt{r_{pr}^2 + L_{r_f}^2 - 2 \cdot r_{pr} \cdot L_{r_f} \cdot \cos(\varphi_g + \pi/2)} \quad (5.24)$$

$$\eta_{r_f} = \cos^{-1} \left(\frac{-L_{r_f} + r_{ic_f}^2 + r_{pr}^2}{2 \cdot r_{ic_f} \cdot r_{pr}} \right) \quad (5.25)$$

5.1.3. Radii of Contact

The third phase in the development of the line-of-action-model is to determine the radii of contact along the involute profile (r_{inv}). To do so, an incremental time unit is required.

Once the incremental time is determined, the instantaneous radius of contact along the involute profile can be determined by implementing the fundamental law of gearing principle, that is, the constant velocity along the line of action $\overline{v_{loa}}$.

5.1.3.1. Incremental Time

For convenience, time will be the incremental unit. Since the unit of time is dependent on the angular velocity of the pinion, or in effect the gear ratio, the total engagement time (t) will vary depending on the pinion size. For this reason three engagement times will be determined: the engagement time of the initial pinion (t_o), the engagement time of the Hybrid Involute Profile pinion (t_h), and the engagement time of the final pinion (t_f).

To determine the time of engagement consider Figure 5.6, which is an adaptation of Figure 5.3 with the addition of L_a and L_r . Since $\overline{v_{loa}}$ is a constant for standard involute gears, the times of engagement for the initial and final pinions can be derived from the length along the line of action and $\overline{v_{loa}}$ as shown in Equation 5.26. Note, r_{br} is used to determine the tangential velocity, since the initial point of contact of the ring r_{inv_r} equals

r_{br} .

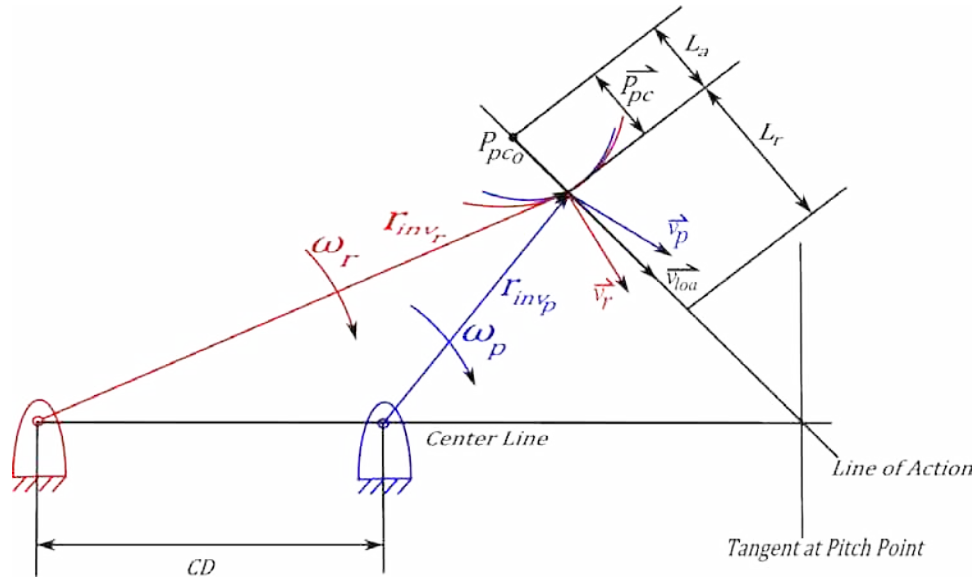


Figure 5.6 Engagement Time

$$t = \frac{L_a + L_r}{\omega_r \cdot r_{br}} \quad (5.26)$$

5.1.3.1.1. Initial Pinion Time Increment

The time of engagement of the initial pinion (t_o) is shown in Equation 5.27.

$$t_o = \frac{L_{a_o} + L_{r_o}}{\omega_{r_o} \cdot r_{br}} \quad (5.27)$$

5.1.3.1.2. Hybrid Involute Profile Pinion Time Increment

To derive the time of engagement of the Hybrid Involute Profile pinion (t_h) additional relationships are required. These relationships concern the acceleration of the point of contact ($\overline{A_{pc}}$) and $\overline{v_{loa}}$ for the Hybrid Involute Profile. For simplicity of the model, $\overline{A_{pc}}$ is assumed to be a constant. Thus, $\overline{A_{pc}}$ and t_h can be derived from solving the system of kinematic velocity equations presented as Equations 5.28 and 5.29.

$$\overline{v_f} = \overline{A_{pc}} \cdot t_h + \overline{v_o} \quad (5.28)$$

$$\overline{P_{pc}} = \overline{A_{pc}} \cdot \frac{t_h}{2} - \overline{v_o} \cdot t_h + \overline{P_o} \quad (5.29)$$

Where:

$\overline{v_f}$ Final $\overline{v_{loa}}$

$\overline{v_i}$ Initial $\overline{v_{loa}}$

$\overline{P_{pc}}$ Position of the Point of Contact

$\overline{P_o}$ Initial Position of the Point of Contact

And

$$\overline{v_f} = \omega_{r_f} \cdot r_{br} \quad (5.30)$$

$$\overline{v_o} = \omega_{r_o} \cdot r_{br} \quad (5.31)$$

$$\overline{P_{pc}} = L_{a_o} + L_{r_f} \quad (5.32)$$

5.1.3.1.3. Final Pinion Time Increment

Similar to t_f the time of engagement of the final pinion is determined by the constant angular velocity of the ring (in this case ω_{r_f}). The time of engagement is shown in Equation 5.33.

$$t_f = \frac{L_{a_f} + L_{r_f}}{\omega_r \cdot r_{br}} \quad (5.33)$$

5.1.3.2. Radii of Contact

The instantaneous radius of contact or instantaneous radius of the involute form along the involute profile of the pinion (r_{inv_p}) is derived through exploitation of $\overline{v_{loa}}$.

To exploit $\overline{v_{loa}}$ several derivations are required; these include:

$\overline{V_o}$ Initial Velocity along the Line of Action

$\overline{V_{pc}}$ Velocity of the Point of Contact

$\overline{P_{pc}}$ Position of the Point of Contact

r_{inv_r} Ring Radius of Point of Contact

\overline{CD} Center Distance of Gear Pair

r_{inv_p} Pinion Radius of Point of Contact

At $\overline{V_o}$, $\overline{v_{loa}}$ is simply the tangential velocity of the ring or the pinion (since in a ring-pinion gearset contact is initiated at the base circles of both profiles). The derivation of $\overline{V_o}$ is shown in Equation 5.34 in polar form.

$$\overline{V_o} = \omega_r \cdot r_{br} \cdot i \cdot e^{i \cdot \varphi_p} \quad (5.34)$$

For the initial and final pinion gearsets (where the gear ratio is fixed) $\overline{\mathbf{V}}_{pc}$ is equal to $\overline{\mathbf{V}}_o$ and is shown in Equation 5.35.

$$\overline{\mathbf{V}}_{pc} = |\overline{\mathbf{V}}_o| \cdot e^{i \cdot \psi} \quad (5.35)$$

Where:

$$\psi = \varphi_p - \frac{\pi}{2} \quad (5.36)$$

The integration of $\overline{\mathbf{V}}_{pc}$ in terms of time yields $\overline{\mathbf{P}}_{pc}$. The integration of $\overline{\mathbf{V}}_{pc}$ is shown in Equations 5.37 and 5.38.

$$\overline{\mathbf{P}}_{pc} = \int \overline{\mathbf{V}}_{pc} \cdot dt \quad (5.37)$$

$$\overline{\mathbf{P}}_{pc} = \overline{\mathbf{V}}_{pc} \cdot t + \overline{\mathbf{P}}_o \quad (5.38)$$

To derive, $\overline{\mathbf{r}}_{inv_r}$, consider the position vector triangle $\overline{\mathbf{r}}_{br}$, $\overline{\mathbf{P}}_{pc}$, $\overline{\mathbf{r}}_{inv_r}$ shown in Figure 5.7. Equation 5.39 depicts $\overline{\mathbf{r}}_{inv_r}$ from $\overline{\mathbf{r}}_{br}$, $\overline{\mathbf{P}}_{pc}$, $\overline{\mathbf{r}}_{inv_r}$, where γ_r is the angle between $\overline{\mathbf{r}}_{inv_r}$ and the pitch point.

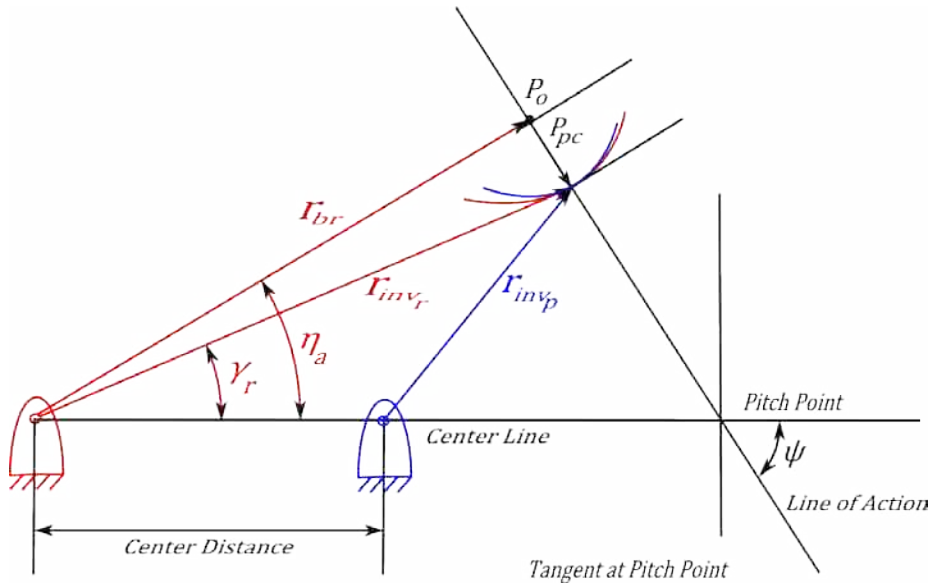


Figure 5.7 Position Vector Triangles

$$\overline{\mathbf{r}}_{inv_r} = r_{ir} \cdot e^{i \cdot \eta_a} + \overline{\mathbf{P}}_{pc} \quad (5.39)$$

The standard involutometry equation for center distance \overline{CD} [4, 6, 10, 12], applies and is shown in polar form in Equation 5.40.

$$\overline{CD} = (r_{pr} - r_{pp}) \cdot e^{i \cdot 0} \quad (5.40)$$

With $\overline{r_{inv_r}}$ and \overline{CD} defined, $\overline{r_{inv_p}}$ can be derived from the position vector triangle $\overline{r_{inv_r}}, \overline{CD}, \overline{r_{inv_p}}$, also shown in Figure 5.7. The derivation of $\overline{r_{inv_p}}$ is shown in Equation 5.41.

$$\overline{r_{inv_p}} = \overline{r_{inv_r}} - \overline{CD} \quad (5.41)$$

As with the derivations of time in section 5.4.1 the derivations of the initial and final involute profiles will be differentiated by the subscripts o and f respectively.

5.1.3.2.1. Initial Pinion Radii of Contact

The derivations of the initial involute profile composed of the initial contact radii are shown in equations 5.42, 5.43, 5.44, 5.45 and 5.46.

$$\overline{V_{o_o}} = \omega_{r_o} \cdot r_{br} \cdot i \cdot e^{i \cdot \varphi_p} \quad (5.42)$$

$$\overline{V_{pc_o}} = |\overline{V_{o_o}}| \cdot e^{i \cdot \psi} \quad (5.43)$$

$$\overline{P_{pc_o}} = \overline{V_{pc_o}} \cdot t + \overline{P_o} \quad (5.44)$$

$$\overline{r_{inv_{r_o}}} = r_{ir} \cdot e^{i \cdot \eta_{a_o}} + \overline{P_{pc_o}} \quad (5.45)$$

$$\overline{r_{inv_{p_o}}} = \overline{r_{inv_{r_o}}} - \overline{CD} \quad (5.46)$$

5.1.3.2.2. Hybrid Involute Profile Pinion Radii of Contact

To develop the radii of contact of the Hybrid Involute Profile, a physical description is beneficial. The Hybrid Involute Profile can be described as an involute profile that behaves as the initial pinion profile at the first point of contact, and behaves as the final pinion profile at the final point of contact. Between these points of contact, the Hybrid Involute Profile will behave like an infinite number of intermediate involute profiles in order to maintain the involute properties of $\overline{v_{loa}}$ and φ . With this in mind, $\overline{V_{oh}}$ is defined to be equal to $\overline{V_{oo}}$ (equation 5.42), and is shown in Equation 5.47.

$$\overline{V_{oh}} = \omega_{r_o} \cdot r_{br} \cdot i \cdot e^{i \cdot \varphi_p} \quad (5.47)$$

As mentioned previously, after the initial point of contact $\overline{V_{oh}}$, $\overline{V_{pc_h}}$ is governed by the rate of change of the gear ratio, or $\overline{A_{pc}}$. This relationship of $\overline{V_{pc_h}}$ is shown in Equation 5.48.

$$\overline{V_{pc_h}} = \overline{A_{pc}} \cdot t + \overline{V_{oh}} \quad (5.48)$$

Integrating $\overline{V_{pc_h}}$ will yield $\overline{P_{pc_h}}$, and is shown in Equations 5.49 and 5.50.

$$\overline{P_{pc_h}} = \int (\overline{A_{pc}} \cdot t + \overline{V_{oh}}) \cdot dt \quad (5.49)$$

$$\overline{P_{pc_h}} = \frac{\overline{A_{pc}} \cdot t^2}{2} + \overline{V_{oh}} \cdot t + \overline{P_o} \quad (5.50)$$

Since $\overline{r_{invr_h}}$ is derived at the initial point of contact, $\overline{r_{invr_h}}$ will be equal to $\overline{r_{invr_o}}$ (equation 5.45), as shown in Equation 5.51.

$$\overline{r_{invr_h}} = r_{ir} \cdot e^{i \cdot \eta_{a_o}} + \overline{P_{pc_o}} \quad (5.51)$$

As shown in Figure 5.7 γ_r is the angle between $\overline{r_{invr_h}}$ and the pitch point.

Prior to determining \overline{CD}_h for the Hybrid Involute Profile tooth, two additional terms are required. This is due to the absence of a constant pitch radius (r_{pp_h}). The first term, the angular velocity of the ring (ω_{r_h}) can be derived from the kinematic diagram Figure 5.8, and shown in Equation 5.52.

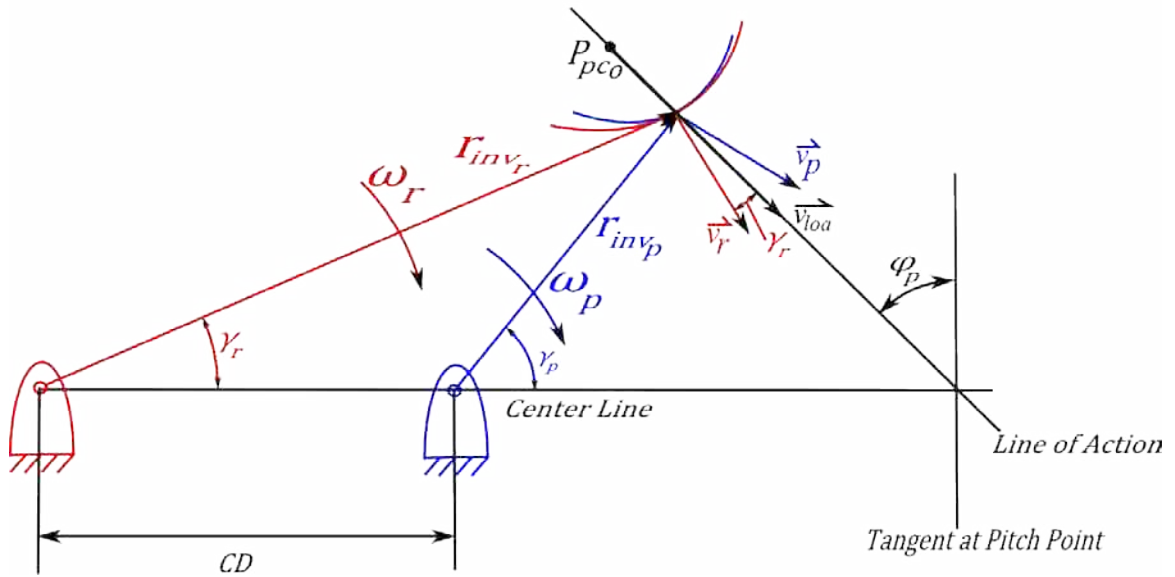


Figure 5.8 Hybrid Involute Profile Angular Ring Velocity

$$\omega_{r_h} = \frac{\overline{v_{pc_h}}}{\overline{r_{invr_h}} \cdot \cos(\varphi - \gamma_r)} \quad (5.52)$$

The second term, the instantaneous pitch radius of the Hybrid Involute Profile (r_{pp_h}) is derived directly from the fundamental law of gearing equation 4.9. The derivation of r_{pp_h} is shown in Equation 5.53.

$$r_{pp_h} = r_{pr} \cdot \frac{\omega_{r_h}}{\omega_p} \quad (5.53)$$

With r_{pp_h} established, \overline{CD}_h is derived and shown in Equation 5.54.

$$\overrightarrow{CD_h} = (r_{pr} - r_{pp_h}) \cdot e^{i \cdot 0} \quad (5.54)$$

Finally, $\overrightarrow{r_{invp_h}}$ shown in Equation 5.55, is derived from the position vector triangle $\overrightarrow{r_{invr_h}}$, $\overrightarrow{CD_h}$, $\overrightarrow{r_{invp_h}}$, also shown in Figure 5.8.

$$\overrightarrow{r_{invp_h}} = \overrightarrow{r_{invr_h}} - \overrightarrow{CD_h} \quad (5.55)$$

5.1.3.2.3. Final Pinion Radii of Contact

Similar to the initial pinion profile, the derivations of the final involute profile composed of the final contact radii are shown in equations 5.56, 5.57, 5.58, 5.59, and 5.60. Note the constant angular velocity ω_{r_f} .

$$\overrightarrow{V_{of}} = \omega_{r_f} \cdot r_{br} \cdot i \cdot e^{i \cdot \varphi_p} \quad (5.56)$$

$$\overrightarrow{V_{pcf}} = \left| \overrightarrow{V_{of}} \right| \cdot e^{i \cdot \psi} \quad (5.57)$$

$$\overrightarrow{P_{pcf}} = \overrightarrow{V_{pcf}} \cdot t + \overrightarrow{P_o} \quad (5.58)$$

$$\overrightarrow{r_{invr_f}} = r_{ir} \cdot e^{i \cdot \eta_{af}} + \overrightarrow{P_{pcf}} \quad (5.59)$$

$$\overrightarrow{r_{invp_f}} = \overrightarrow{r_{invr_f}} - \overrightarrow{CD} \quad (5.60)$$

5.1.4. Mating Gear-Tooth Profile

Buckingham presents additional involutometry terms in [6]. Combining several of these common involutometry terms, a simplistic method to determine the Cartesian coordinates of an involute profile can be derived. With the involute profile centered about the Y axis, the derivations at each instant along the involute profile required to determine the Cartesian coordinates are:

| | |
|-----------------------|---|
| φ | The Pressure Angle |
| $\text{inv } \varphi$ | The Involute Function of the Pressure Angle |
| T | The Circular Tooth Thickness |
| T_c | The Chordal Tooth Thickness |
| X | The Cartesian X-Coordinate |
| Y | The Cartesian Y-Coordinate |

In [6] Buckingham presents a relationship between one set of r and φ to another set of r and φ on the same involute gear profile. This relationship, shown in Equation 5.61, can be exploited to determine φ at each r_{inv} when r_p and φ_p are used as the first set of r and φ . Rearranging equation 5.61 will yield φ , and is shown in Equation 5.62.

$$\cos \varphi_2 = \frac{r_1 \cdot \cos(\varphi_1)}{r_2} \quad (5.61)$$

$$\varphi = \cos^{-1} \left(\frac{r_{pp} \cdot \cos(\varphi_p)}{r_{inv}} \right) \quad (5.62)$$

The derivation of $\text{inv } \varphi$ is not altered from equation 4.3. The instantaneous circular tooth thickness (T) is also derived in [6] and presented here as Equation 5.63.

$$T = 2 \cdot r_{inv} \cdot \left(\frac{T_p}{2} + \text{inv}(\varphi_p) - \text{inv}(\varphi) \right) \quad (5.63)$$

The chordal length (T_c) is “the length of the chord subtended by the circular thickness arc” and is shown in Figure 5.9 [6]. The derivation of T_c is also adapted from [6] and is shown in Equation 5.64.

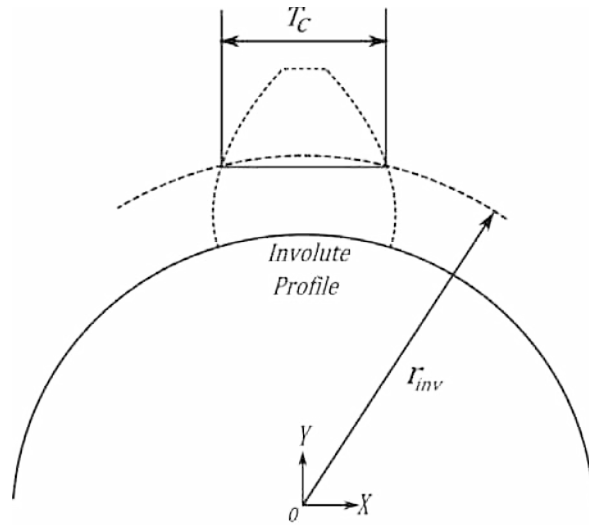


Figure 5.9 Chordal Length T_c

$$T_c = 2 \cdot r_{inv} \cdot \sin\left(\frac{T_p}{2 \cdot r_{inv}}\right) \quad (5.64)$$

With the involute profile centered about the Y axis the Cartesian X Coordinate is simply half of T_c . The Cartesian coordinates are shown in Figure 5.10. Equation 5.65 depicts the Cartesian X coordinate.

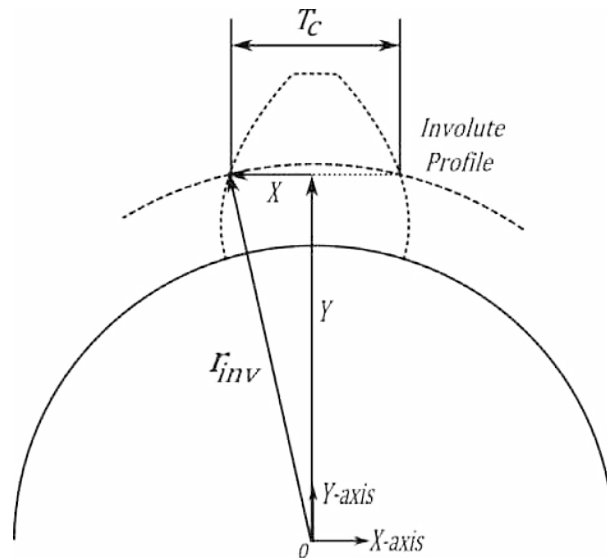


Figure 5.10 Involute Profile Cartesian Coordinates

$$X = \frac{T_c}{2} \quad (5.65)$$

From Pythagorean's Theorem the Cartesian Y Coordinate shown in Equation 5.66 can be determined.

$$Y = \sqrt{r_{inv}^2 - X^2} \quad (5.66)$$

As with the previous derivations sets, to maintain consistency, the derivation sets of the initial, Hybrid Involute, and final involute profiles will be presented as sets and will be differentiated by the subscripts o , h and f respectively.

5.1.4.1. Initial Pinion Involute Tooth Profile

The Cartesian Coordinates of the initial involute profile are derived from Equations 5.67, 5.68, 5.69, 5.70, 5.71, and 5.72.

$$\varphi_o = \cos^{-1} \left(\frac{r_{pp_o} \cdot \cos(\varphi_p)}{r_{inv_o}} \right) \quad (5.67)$$

$$inv \varphi_o = \tan(\varphi_o) - \varphi_o \quad (5.68)$$

$$T_o = 2 \cdot r_{inv_o} \cdot \left(\frac{T_p}{2} + inv(\varphi_p) - inv(\varphi_o) \right) \quad (5.69)$$

$$T_{c_o} = 2 \cdot r_{inv_o} \cdot \sin \left(\frac{T_o}{2 \cdot r_{inv_o}} \right) \quad (5.70)$$

$$X_o = \frac{T_{c_o}}{2} \quad (5.71)$$

$$Y_o = \sqrt{r_{inv_o}^2 - X_o^2} \quad (5.72)$$

5.1.4.2. Hybrid Involute Profile Pinion Involute Tooth Profile

The Cartesian Coordinates of the Hybrid Involute Profile are derived from Equations 5.73, 5.74, 5.75, 5.76, 5.77, and 5.78.

$$\varphi_h = \cos^{-1} \left(\frac{r_{pp_h} \cdot \cos(\varphi_p)}{r_{inv_h}} \right) \quad (5.73)$$

$$inv \varphi_h = \tan(\varphi_h) - \varphi_h \quad (5.74)$$

$$T_h = 2 \cdot r_{inv_h} \cdot \left(\frac{T_p}{2} + inv(\varphi_p) - inv(\varphi_h) \right) \quad (5.75)$$

$$T_{c_h} = 2 \cdot r_{inv_h} \cdot \sin \left(\frac{T_h}{2 \cdot r_{inv_h}} \right) \quad (5.76)$$

$$X_h = \frac{T_{c_h}}{2} \quad (5.77)$$

$$Y_h = \sqrt{r_{inv_h}^2 - X_h^2} + (r_{pp_f} - r_{pp_o}) \quad (5.78)$$

Depending on the difference in the boundary conditions, a comparison of the Hybrid Involute Profile may be challenging. For this reason equation 5.78 is amended from the standard involute equation to allow for a comparison of the Hybrid Involute Profile to the final profile. This alteration is equivalent to maintaining tangency of the pitch radii. It is important to note this is solely done for a comparison and that without this compensation, an active change in CD while the Hybrid Involute Profile tooth is engaged, is required.

5.1.4.3. Final Pinion Involute Tooth Profile

The Cartesian Coordinates of the final involute profile are derived from Equations 5.79, 5.80, 5.81, 5.82, 5.83, and 5.84.

$$\varphi_f = \cos^{-1}\left(\frac{r_{ppf} \cdot \cos(\varphi_p)}{r_{invf}}\right) \quad (5.79)$$

$$inv \varphi_f = \tan(\varphi_f) - \varphi_f \quad (5.80)$$

$$T_f = 2 \cdot r_{invf} \cdot \left(\frac{T_p}{2} + inv(\varphi_p) - inv(\varphi_f)\right) \quad (5.81)$$

$$T_{cf} = 2 \cdot r_{invf} \cdot \sin\left(\frac{T_f}{2 \cdot r_{invf}}\right) \quad (5.82)$$

$$X_f = \frac{T_{cf}}{2} \quad (5.83)$$

$$Y_f = \sqrt{r_{invf}^2 - X_f^2} \quad (5.84)$$

5.1.5. Resulting Working Structures

The formulation of the line-of-action-model completes the development of working structures. Two working structures will be further developed in the conceptual design process. The first is a problem correction class solution; the previous conceptual solution (cam correction concept) which employs a fixed profile input member. The second is a problem elimination class solution and is inherent in the Line-of-Action Model; this is the Hybrid Involute Profile which contains the required r_{inv} and φ for the transition from an initial pinion size to a final pinion size.

5.2. Suitable Combinations and Firm Up

Suitable combinations can be quantified in terms of the level of complexity required to ensure the working principles are met by means of the Line-of-Action Model. The previous gear ratio transition description of a PECVT (Figure 5.2) is useful in quantifying the complexity of the working principles.

5.2.1. Fixed Profile Cam Correction Working Structure

Recall that the hypothesis of this thesis is to build upon the principal solution proposed by Dalling. Dalling's previous conceptual solution is described as a combination of the cam-follower concept and the preferred meshing location concept [3]. However, the preferred meshing location cannot satisfy the involute property: involute tooth shape variation as the gear diameters change. Therefore the working structure will be modified and will solely employ the cam-follower concept. Dalling describes the conceptual solution employing six input gear teeth [3], thus six input members will be considered for comparison. For this concept to satisfy the working principles, each of these input members (or fixed profile teeth) will require a mechanism to provide an angular correction (φ) and a mechanism to provide the radial correction (r_{inv}) during transition as well as to operate at the second gear ratio (due to the involute variation property). The transition and second operating gear ratio will be segmented into six segments corresponding to the number of input members. Since each gear tooth profile will mesh with the output member at a different r_{inv} , each profile will require two radial correction cams (one for the transition and one for the operation gear ratio). Similarly each gear tooth profile will require two angular correction cams. Thus for a single transition between operating gear ratios 24 cams would be required. The complexity of the cam correction working structure can be seen in the transition diagram for this concept, and is illustrated in Figure 5.11.

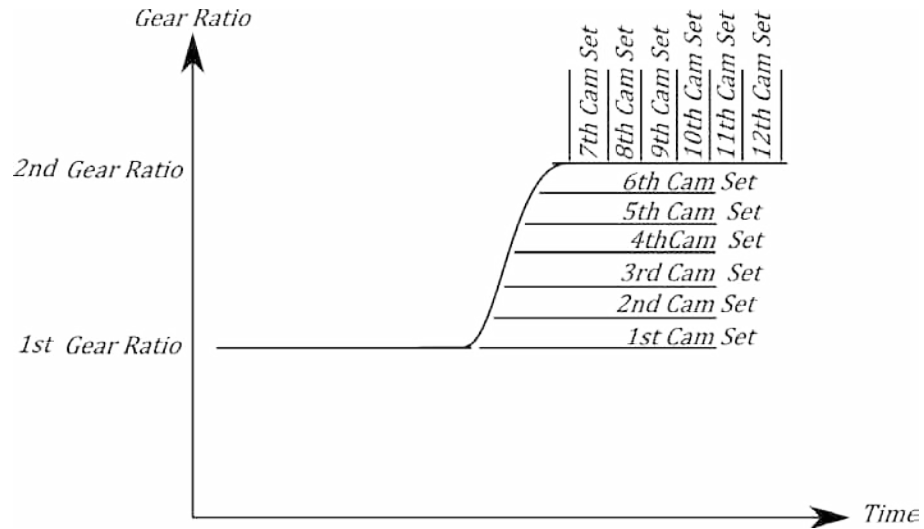


Figure 5.11 Cam Correction Transition

The use of such a large number of cam profiles introduces significant complications. In addition to the complexity of the cam position profiles shown in Figure 5.11, ensuring the velocity, acceleration and jerk profiles of each cam are appropriate, as well as ensuring these profiles are continuous from one cam profile to another is required for this suitable combination to succeed. Developing these complicated profiles are a monumental task. In addition to the complexity of the profiles, the wear characteristics of these cam profiles are of concern. This is due to the transfer of the torque load from the gear teeth to the cam profile since the cams essentially will be load bearing members. System integration is also an issue. With additional operating gear ratios, the system integration complexity becomes immense. For these reasons alone the cam correction working structure is not a suitable combination, nor a commercially viable PECVT solution, and will not be pursued further.

5.2.2. Hybrid Involute Profile Working Structure

It is believed that the inherent Hybrid Involute Profile of the line-of-action-model depicted in Figure 5.12 along with the boundary condition, standard involute profiles, is an elegant working structure.

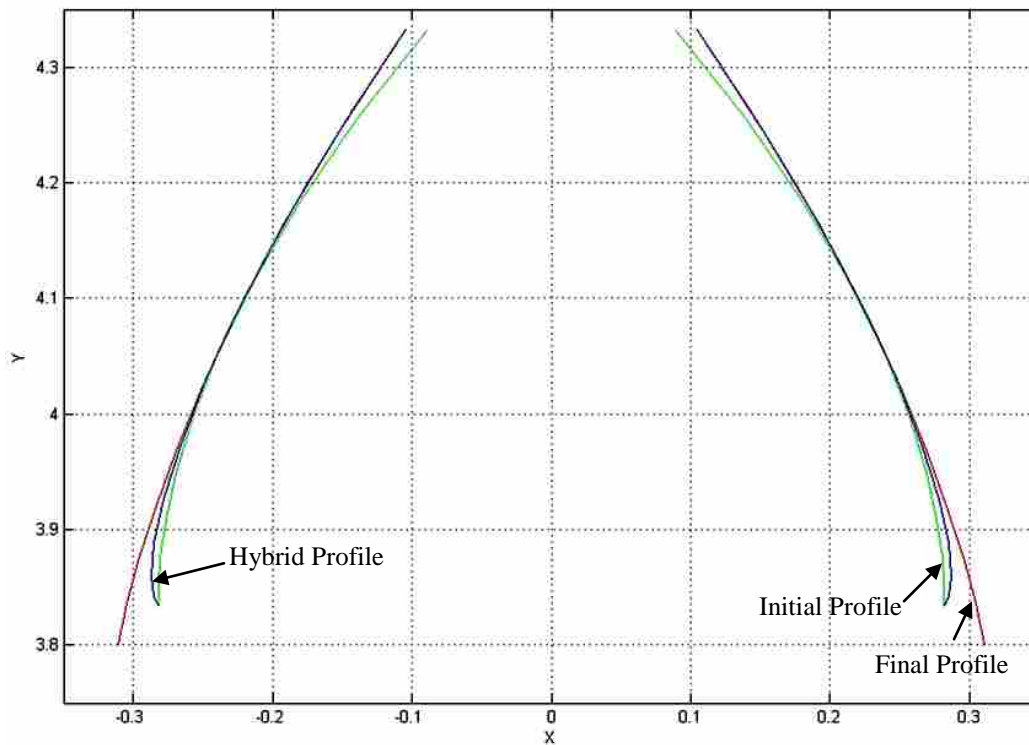


Figure 5.12 The Hybrid Involute Profile

The elegance is carried over into a suitable combination. With the line-of-action-model generating the Hybrid Involute Profile, the transition between two operating gear ratios is fully addressed with a single Hybrid Involute Profile. This allows for standard involute gears to be employed at fixed operating gear ratios. The simplicity of the Hybrid Involute Profile working structure is conveyed in the transition diagram depicted in Figure 5.13

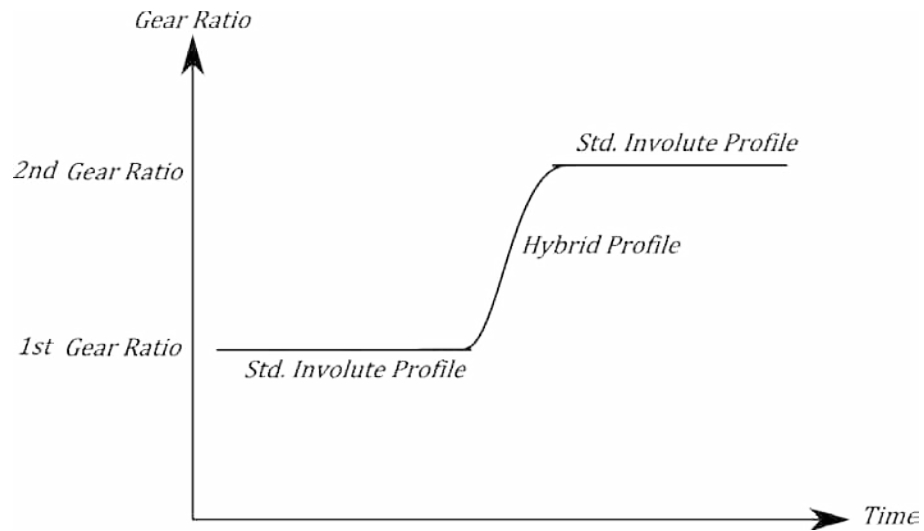


Figure 5.13 Hybrid Involute Profile Transition

If the transition time is desired to be elongated beyond the engagement time of a single tooth, this suggests that the Hybrid Involute Profile be segmented across multiple gear teeth and a helical angle could possibly be added to increase the contact ratio beyond 1.0 [18].

In comparison to the cam correction working structure, the Hybrid Involute Profile can be thought of as an involute profile with the cam corrections imbedded into the profiles of the teeth themselves. However, none of the complications of the cam correction working structure are present in the Hybrid Involute Profile concept. This is due to the simplicity of the Hybrid Involute Profile and as a result of adherence to the Line-of-Action Model.

The simplicity and elegance of the Hybrid Involute Profile working structure are encouraging factors to the viability of the working structure. Therefore, the Hybrid Involute Profile will be pursued further into the validation stage of the conceptual design phase.

5.3. Line-of-Action-Model Validation and Case Studies

Multiple validation methods will be used to validate the line-of-action-model. Multiple validation methods are used since no single validation method can validate both r_{inv} and ϕ simultaneously. The validation methods are a combination of case studies and a theoretical validation to ensure the Line-of-Action Model is robust.

The previous derivations of the Line-of-Action Model have been arranged in a Matlab .m file. The Matlab code is included in Appendix A. To allow for a wide range of analyses the .m file is fully parametric. The input parameters and arbitrary values of the case studies for the .m file are shown in Table 5.1.

Table 5.1 Case Study Parameters

| Parameter Description | Acronym | Value |
|---|------------|-------------|
| <i>Initial Pinion Number of Teeth</i> | N_{po} | 12 |
| <i>Final Pinion Number of Teeth</i> | N_{pf} | 24 |
| <i>Ring Number of Teeth</i> | N_r | 36 |
| <i>Diametral Pitch</i> | DP | 3 |
| <i>Pressure Angle at the Pitch Radius</i> | ϕ_g | 22.5° |
| <i>Initial Position of the Point of Contact</i> | P_{pco} | 0 |
| <i>Angular Velocity of the Pinion</i> | ω_p | -12 rad/sec |
| <i>Number of Time Increments (n-1)</i> | T_{step} | 9 |

The resulting initial, Hybrid Involute and final involute profiles of the .m file are shown in Figure 5.14 configured with the pitch radii tangent. Note that the Hybrid Involute Profile begins at the initial profile and ends at the final profile.

The resulting profiles will be validated via three methods. The first two methods will analyze r_{inv} . The first is a r_{inv} case study, and is founded on a comparison of the generated involute profiles. The second is a theoretical analysis of the Hybrid Involute Profile base radii. The third validation method is a case study which addresses ϕ and will validate the paths of contact of the engaged involute profiles.

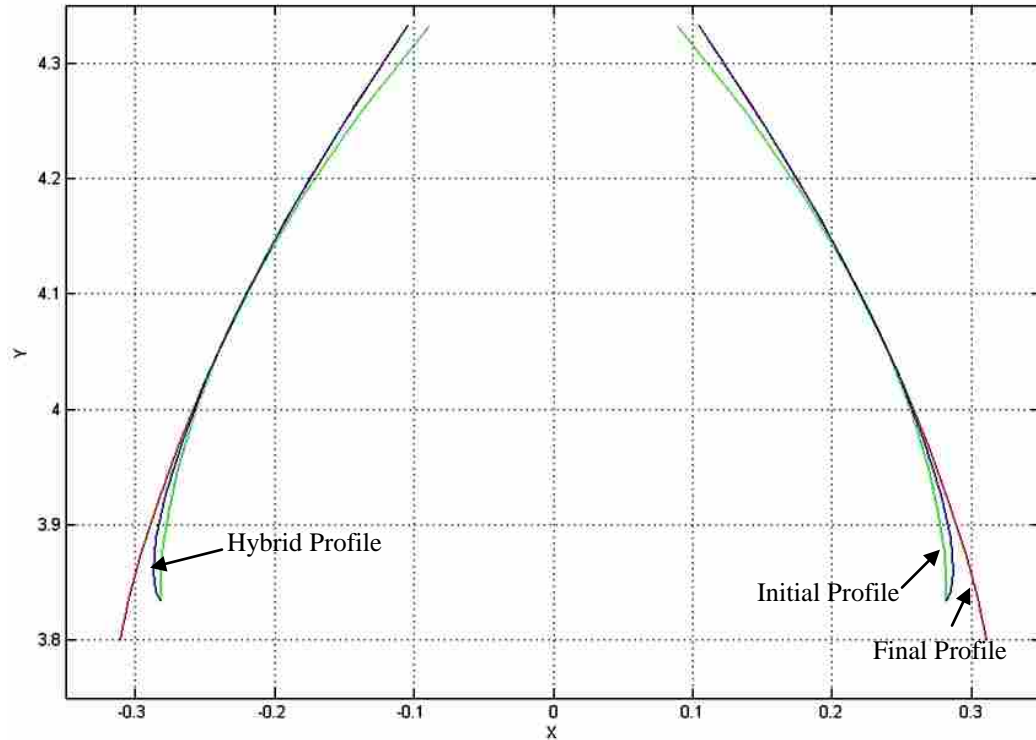


Figure 5.14 LOA Model Generated Profiles

5.3.1. Profile Generation Case Study

The profile generation case study will validate the initial and final involute profile Cartesian coordinates generated from the Line-of-Action Model. The Hybrid Involute Profile will not be evaluated by this method since the Hybrid Involute Profile is non-standard. Rather, the Hybrid Involute Profile will be evaluated by the base radii method. The Cartesian coordinates will be compared to the Cartesian Coordinates generated for involutes of the same size from Buckingham's method in [4].

The Buckingham method of determining Cartesian Coordinates is initiated by determining ϕ at the radius of interest. This is done through the use of Buckingham's equation 5-4 from page 80 of [4], shown here as equation 5.85.

$$\cos(\varphi) = \frac{r_b}{r} \quad (5.85)$$

Where r_b is the base radius and r is the radius of interest.

Also required are r_p (both for the initial and final pinions), $inv \varphi$, and T_p which can be determined from equations 5.2, 5.5, 4.2, and 5.1 respectively. With r_p , $inv \varphi$, T_p , and φ known, the vectorial angle from the centerline of the profile (θ'') is now required, and can be determined through Buckingham's equation 5-6 from page 81 of [4], shown here as Equation 5.86.

$$\theta'' = \frac{T_p}{2 \cdot r_{pp}} + inv \varphi_p - inv \varphi \quad (5.86)$$

The Cartesian Coordinates can now be determined via Buckingham's equations 1-5 and 1-6 from page 5 of [4]. The X coordinate is determined by equation 1-5 shown here as Equation 5.87. The Y coordinate is determined by equation 1-6 shown here as Equation 5.88.

$$X = r \cdot \sin (\theta'') \quad (5.87)$$

$$Y = r \cdot \cos (\theta'') \quad (5.88)$$

Using the case study parameters shown in Table 5.1, Table 5.2 shows the comparison of the Cartesian Coordinates determined from the Line-of-Action Model and from Buckingham's method.

Table 5.2 Profile Generation Case Study

| Steps | Buckingham X | Buckingham Y | LOA X | LOA Y | % Error X | % Error Y |
|-----------------|--------------|--------------|--------|--------|-----------|-----------|
| Initial Profile | | | | | | |
| 1 | 0.281278 | 1.8347 | 0.2813 | 1.8347 | -0.01% | 0.00% |
| 2 | 0.281577 | 1.8530 | 0.2816 | 1.8531 | -0.01% | 0.00% |
| 3 | 0.279912 | 1.8819 | 0.2799 | 1.8819 | 0.00% | 0.00% |
| 4 | 0.274746 | 1.9207 | 0.2747 | 1.9208 | 0.02% | 0.00% |
| 5 | 0.264530 | 1.9694 | 0.2645 | 1.9694 | 0.01% | 0.00% |
| 6 | 0.247827 | 2.0271 | 0.2478 | 2.0271 | 0.01% | 0.00% |
| 7 | 0.223179 | 2.0932 | 0.2232 | 2.0932 | -0.01% | 0.00% |
| 8 | 0.189308 | 2.1667 | 0.1893 | 2.1667 | 0.00% | 0.00% |
| 9 | 0.144960 | 2.2466 | 0.1450 | 2.2466 | -0.03% | 0.00% |
| 10 | 0.089071 | 2.3316 | 0.0890 | 2.3316 | 0.08% | 0.00% |
| Final Profile | | | | | | |
| 1 | 0.3111 | 3.8008 | 0.3111 | 3.8008 | -0.01% | 0.00% |
| 2 | 0.3035 | 3.8403 | 0.3035 | 3.8404 | 0.02% | 0.00% |
| 3 | 0.2931 | 3.8854 | 0.2931 | 3.8853 | 0.00% | 0.00% |
| 4 | 0.2794 | 3.9355 | 0.2794 | 3.9355 | -0.01% | 0.00% |
| 5 | 0.2619 | 3.9906 | 0.2619 | 3.9906 | 0.00% | 0.00% |
| 6 | 0.2403 | 4.0505 | 0.2403 | 4.0505 | -0.02% | 0.00% |
| 7 | 0.2141 | 4.1148 | 0.2141 | 4.1148 | -0.02% | 0.00% |
| 8 | 0.1829 | 4.1834 | 0.1829 | 4.1834 | 0.01% | 0.00% |
| 9 | 0.1464 | 4.2560 | 0.1464 | 4.256 | 0.01% | 0.00% |
| 10 | 0.1043 | 4.3320 | 0.1043 | 4.3321 | -0.01% | 0.00% |

With the Buckingham method as the true value and the LOA model results as the estimated value, the percent error of the LOA model is negligible. Thus the LOA model is validated in being able to generate standard involute profiles. Also the initial and final involute profiles serve as boundary conditions for the Hybrid Involute Profile. Therefore the Hybrid Involute Profile can be considered valid within these bounds.

5.3.2. Base Radius Theoretical Analysis

A validation of the base radii (r_b) is an alternate theoretical method to validate the Hybrid Involute Profile. The validation of the base radii also provides a second description of the Hybrid Involute Profile. In addition to the line-of-action-model the Hybrid Involute Profile can be thought of as an involute profile which is generated from a varying base circle. This concept is shown in Figure 5.15.

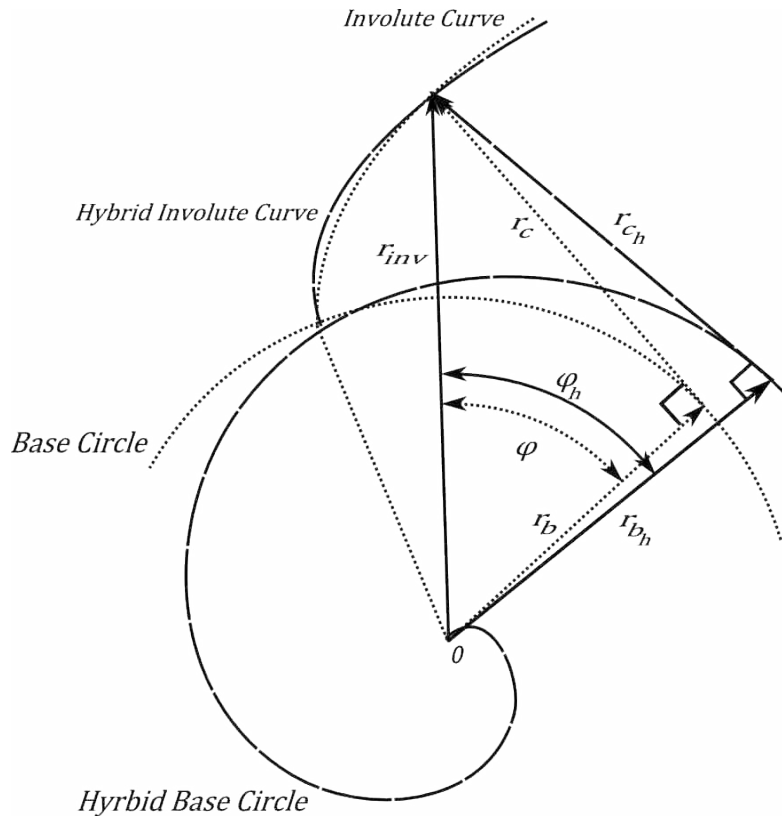


Figure 5.15 Varying Base Radius

To evaluate the how the base radii of the Hybrid Involute Profile (r_{b_h}) vary, the base radii of the Hybrid Involute Profile, r_{b_h} is required to be derived. The relationship of the base radius of the Hybrid Involute Profile, r_{b_h} to the pitch radius of the Hybrid Involute Profile, r_{p_h} is identical the radii relationship presented in equation 5.61. In fact,

Buckingham derives the relationship described by equation 5.61 from the base radius.

The relationship of r_{b_h} to r_{p_h} is shown in equation 5.89.

$$r_{b_h} = \frac{r_{pp_h} \cdot \cos(\varphi_p)}{\cos(\varphi_h)} \quad (5.89)$$

It is important to note that φ_h at r_{b_h} is equal to zero. Also since r_{pp_h} is an array of pitch radii for each r_{inv} , there will exist a unique r_{b_h} for each r_{pp_h} . From equation 5.89 the rate at which r_{b_h} varies can be seen as the same rate at which r_{pp_h} varies. This relationship is also the standard involutometry relationship of r_b and r_p [6, 10, 11, 12] which is valid for the initial and final involute profiles; and is shown in equation 5.90. With the rate of change of r_{b_h} shown to hold through standard involutometry, the base radii validation is complete.

$$r_b = r_{pp} \cdot \cos(\varphi_p) \quad (5.90)$$

To conclude, for a specified rate of change in r_{pp_h} , the rate of change of r_{b_h} is also specified and the Hybrid Involute Profile can be generated.

5.3.3. Paths of Contact Case Study

To solely validate r_{inv} is not sufficient to conclude that the required involute behavior for a functional PECVT is present in the Hybrid Involute Profile. In addition to the change in r_{inv} , the change in φ must also be validated to ensure the desired behavior, and is done through a case study.

The involute property, *the Path of Contact*, discussed in section 4.7.4 can prove the correct φ is present at each r_{inv} in the Line-of-Action Model. This is done through demonstrating the line of action and path of contact relationship discussed in section

4.7.5 which addresses the scenario of one involute profile acting against another is valid for each of the profiles generated by the LOA model. The line of action and path of contact relationship states that the line of action and path of contact are collinear, or in other words the line of action and path of contact have the same slope. This property can be demonstrated by calculating the slopes of the lines of action of each profile generated by the LOA model. Since it has been established that the initial and final profiles are involute profiles (section 5.3.1), the Hybrid Involute Profile will maintain involute behavior and thus be comprised of the correct φ and r_{inv} if the slopes of the lines of action of the three profiles are shown to be collinear.

The path of contact abscissa (x_p) and ordinate (y) previously discussed in section 4.7.4 can be determined for an involute profile through Buckingham's equations 1-16 and 1-15 from page 10 of [4], shown here as Equations 5.91 and 5.92.

$$x_p = r_{inv} \cdot \sin(\varphi - \varphi_p) \quad (5.91)$$

$$y = r_{pp} - r_{inv} \cdot \cos(\varphi - \varphi_p) \quad (5.92)$$

5.3.3.1. Initial Pinion Path of Contact

The equations of the path of contact for the initial profile are shown as Equations 5.93 and 5.94.

$$x_{p_o} = r_{inv_o} \cdot \sin(\varphi_o - \varphi_p) \quad (5.93)$$

$$y_o = r_{pp_o} - r_{inv_o} \cdot \cos(\varphi_o - \varphi_p) \quad (5.94)$$

5.3.3.2. Hybrid Involute Profile Pinion Path of Contact

The equations of the path of contact for the Hybrid Involute Profile are shown as Equations 5.95 and 5.96.

$$x_{p_h} = r_{inv_h} \cdot \sin(\varphi_h - \varphi_p) \quad (5.95)$$

$$y_h = r_{pp_h} - r_{inv_h} \cdot \cos(\varphi_h - \varphi_p) \quad (5.96)$$

5.3.3.3. Final Pinion Path of Contact

The equations of the path of contact for the final profile are shown as Equations 5.97 and 5.98.

$$x_{p_f} = r_{inv_f} \cdot \sin(\varphi_f - \varphi_p) \quad (5.97)$$

$$y_f = r_{pp_f} - r_{inv_f} \cdot \cos(\varphi_f - \varphi_p) \quad (5.98)$$

5.3.3.4. Paths of Contact Profile Validation

The equations of the path of contact for the initial, Hybrid Involute, and final profiles are contained in the .m file, and are fully validated in the .m file. The validation is performed by fitting the x_p and y vectors to a 1st order polynomial (any other order polynomial would also be acceptable) in order to determine the slopes of the paths of contacts. The slopes of the paths of contact are shown in Figure 5.16 and the calculated slopes are shown in Table 5.3. The percent error of the polynomial fits in comparison to each other is significantly less than .01%.

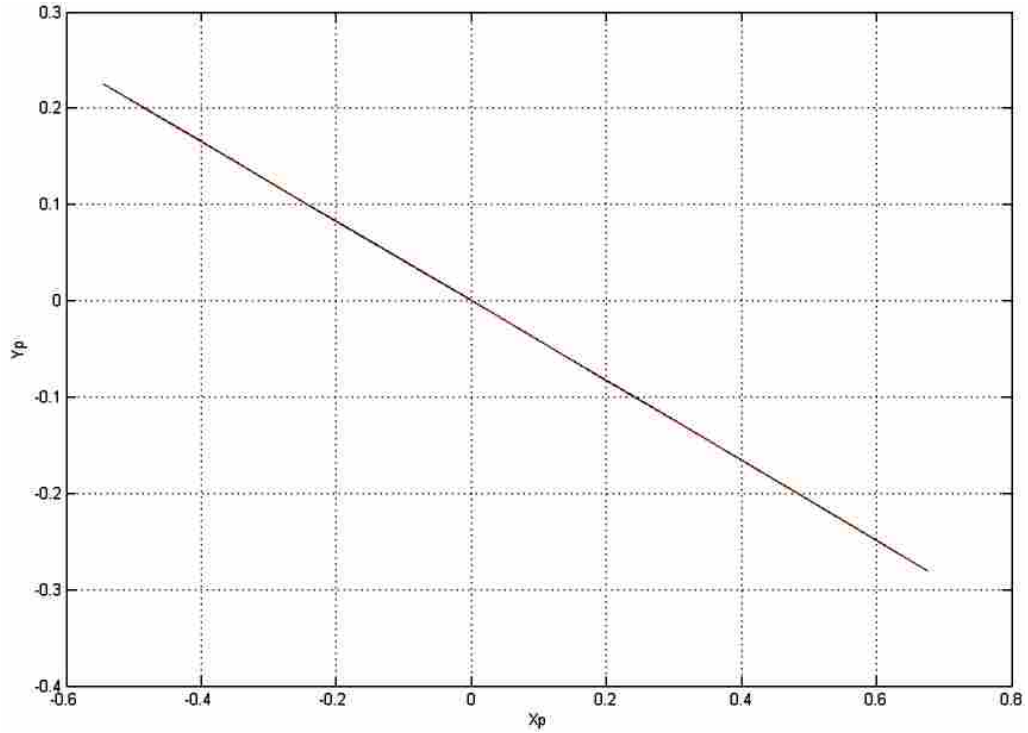


Figure 5.16 Paths of Contact Slopes

Table 5.3 Paths of Contact Polynomials

| Path of Contact | 1 st order Polynomial |
|--------------------------|----------------------------------|
| Initial Involute Profile | $y = -0.4142x + o$ |
| Hybrid Involute Profile | $y = -0.4142x + o$ |
| Final Involute Profile | $y = -0.4142x + o$ |

With the paths of contact of the three profiles being collinear, the ϕ at each r_{inv} is validated.

5.3.4. Validation and Case Study Results

The completion of the validations and case studies has resulted in the identification of the required correction in both ϕ and r_{inv} for the Hybrid Involute Profile to provide involute behavior while engaged. This was done by employing the Line-of-Action Model. With the Hybrid Involute Profile determined by the Line-of-Action

Model, the Hybrid Involute Profile working structure is sufficiently developed to be declared a viable conceptual principal solution.

5.4. The Principal Solution

As the conceptual principal solution, the Hybrid Involute Profile will be discussed in terms of satisfying the objectives of a PECVT, overcoming the NITP, and satisfying the requirements list. These three prerequisites are essential for the embodiment design phase to be initiated in the product development process.

The objective of a PECVT described in Figure 5.2 is to have the input and output remain positively engaged while transitioning between gear ratios. This objective is met by the Hybrid Involute Profile due to the line-of-action-model. With the boundary conditions of the Hybrid Involute Profile being the standard profiles at the operating gear ratios, the Hybrid Involute Profile is engaged throughout the entire transition.

As a problem elimination class, PECVT solution the Hybrid Involute Profile not only fully addresses the NITP; the NITP is eliminated. This is a substantial benefit in that the operating gear ratios are not constrained to be at multiples of the original profile's P_c (section 2.1.1.1.1).

The Hybrid Involute Profile, conceptual principal solution, fulfills the primary, secondary, tertiary, and quaternary requirements of the requirements list (Table 4.1) for a PECVT. By fulfilling all of the requirements of a PECVT in such a simplistic manner, the Hybrid Involute Profile, conceptual principal solution, appears to be commercially viable and truly an elegant solution.

6. Conclusion and Recommendations

6.1. Conclusions

The conceptual development of a viable Positively Engaged Continuously Variable Transmission, which will maintain engagement of the input and output gear members of the transmission while changing the gear ratio via the change in the diameter of one gear and the change in the center distance of the gearset, has been described in this thesis. The development began with detailed analysis and review of the previous conceptual principal solution proposed by Dalling. The work of Dalling concluded that a cam correction type mechanism would overcome the Non-Integer-Tooth-Problem (NITP), and would lead to a viable PECVT. However, critical assumptions, which were appropriate at the time, prevents the solution Dalling developed, from actually leading to a viable PECVT. The assumptions which hinder Dalling's methodology are:

- Involutometry Assumptions
 - Involute Profile Size assumption
 - The Center Distance assumption
 - The Angles of Approach and Recession Relationship Assumption
- Output Acceleration Assumption
- Prescribed Angular Input Motion Assumption

To rectify these assumptions, it was hypothesized that a commercially viable PECVT should utilize the conceptual solution proposed by Dalling to address the NTIP, while incorporating involutometry principles so that conjugate action is satisfied. This hypothesis has been rejected in light of the development of the Hybrid Involute Profile, which satisfies the objective of the research effort in a more simplistic and elegant manner.

To test the hypothesis, the research effort returned to the working principles stage of the conceptual design phase of the product development process. Additional working principles were identified through a literature review of involutometry. This literature review primarily drew upon the collective works of Earl Buckingham [4, 6]. Definitions, relationship and principles of involutometry were discussed, and ultimately, two involutometry principles proved fundamental to developing a design tool entitled the Line-of-Action Model and the Hybrid Involute Profile. The fundamental involutometry principles for the development of a feasible PECVT are the line of action and path of contact relationship, and the fundamental law of gearing principle.

The test of the hypothesis continued in the conceptual design stage through the determination of working structures. Working structures, which are components or subsystems which satisfy specific working principles, were developed with the use of the Line-of-Action Model design tool.

The Line-of-Action Model design tool was established through a combination of the line of action and path of contact relationship, the fundamental law of gearing principle, the path of contact principle, and the one-gear tooth form given principle of involutometry. The Line-of-Action Model uses a given output involute gear and specified

gear ratio of the gear set to, determine the involute profile of the input gear required to satisfy the involute gear profile behavior of the gearset. The Hybrid Involute Profile arises when the specified gear ratio is changed while the gearset is engaged.

The Hybrid Involute Profile is the non-standard involute profile that is generated by the Line-of-Action Model for a specific gear ratio change. The establishment of the Hybrid Involute Profile is an elegant working structure that encapsulates the objectives of a feasible PECVT.

The test of the hypothesis is concluded with the suitable combination stage of the conceptual design phase. Two combinations of the working structures were investigated. These combinations are the previous conceptual solution of the hypothesis and the Hybrid Involute Profile concept inherent in the Line-of-Action Model. While developing the suitable combination of the hypothesis solution or cam correction concept, insurmountable complications arose. These complications were associated with the number and complexity of the cam profiles required to implement the concept. In contrast, the Hybrid Involute Profile concept did not display any of the complications of the cam correction concept. In fact, the simplicity and elegance of the Hybrid Involute Profile concept emerged during the development of working structures for the cam correction concept. For these reasons, the concept of the hypothesis was rejected and replaced by the Hybrid Involute Profile.

According to Pahl, solely disproving a hypothesis does not fulfill the objectives of the research effort. To develop a conceptual, kinematically, viable, PECVT the conceptual design phase was continued through the evaluation and principal solution phases.

The evaluation stage of the conceptual design phase entailed conducting two case studies and a theoretical analysis to ensure the Hybrid Involute Profile concept overcame the NITP as well as satisfied involutometry principles. The first case study was conducted to demonstrate that the Line-of-Action Model would generate an involute profile. Two standard involute profiles (the boundary condition profiles of the gear ratio change) were generated by the Line-of-Action Model. The Cartesian coordinates of these profiles were compared to the standard method of generating Cartesian coordinates for involute profiles presented in [4] to demonstrate the appropriate r_{inv} was present. The percent error of the Line-of-Action Model involute profile, in comparison with standard involute profiles was shown to be less than .1%, a negligible amount. This case study concluded that the Line-of-Action Model can produce standard involute profiles, and that the Hybrid Involute Profile is also valid between two given standard involute profile bounds.

The theoretical analysis that was conducted confirmed that the Hybrid Involute Profile maintains involutometry principles for a set of involute curves acting against one another. This was accomplished by considering the Hybrid Involute Profile as an involute profile generated from a varying base radius. The base radius of the Hybrid involute was then derived using involutometry relationships described in [4]. The relationship between the pitch radius and base radius of the Hybrid Involute Profile was then shown to be identical to the pitch radius and base radius relationship of a standard involute gear. The identification of this fundamental relationship adequately shows that the Hybrid Involute Profile maintains involutometry principles.

The second case study evaluated the pressure angle ϕ , of the profiles generated by the Line-of-Action Model through analysis of the paths of contact of each profile. Since

the first case study demonstrated that standard involute profiles are generated by the Line-of-Action Model. Demonstrating that the slope of the path of contact of the Hybrid Involute Profile is identical to the slope of the path of contact of a standard involute of the same ϕ_p will complete the validation of the Hybrid Involute Profile concept. The comparison of the slopes revealed a percent error significantly less than .01%. Thus the appropriate ϕ is generated by the Line-of-Action Model for a Hybrid Involute Profile.

With the Hybrid Involute Profile concept fully validated the Hybrid Involute Profile was declared the conceptual principal solution, and a foundation for creating a feasible PECVT. In doing so the Hybrid Involute Profile concept was discussed in terms of satisfying the objectives of a PECVT, overcoming the NITP, and satisfying the requirements list. The Hybrid Involute Profile fully satisfies the objective of a PECVT, eliminates the NITP, and fulfills the primary, secondary, tertiary, and quaternary requirements of the requirements list (Table 4.1) for a PECVT. With fulfillment of the objectives required for a feasible PECVT, the Hybrid Involute Profile is envisioned as being a truly elegant solution.

6.2. Recommendations

The identification of the elegant Hybrid Involute Profile, conceptual, principal solution, concludes the conceptual design phase and initiates the embodiment design phase of the product development process. It is recommended that the embodiment design phase be commenced using the Hybrid Involute Profile, as the foundation for all pursuing all possible embodiments.

To implement the Hybrid Involute Profile in the embodiment design phase several modifications are required to the Line-of-Action Model and the secondary design objectives discussed in section 3.3 must now become primary objectives. The modifications will transform the Hybrid Involute Profile from a conceptual solution to a practical solution. These modifications of the Line-of-Action Model include:

- Segmenting the diameter change (or gear ratio change) over several gear teeth
- Expanding the model into three dimensional space to produce a helical gear
- Applying a non-constant A_{pc} in the hybrid profile of the LOA model

Segmenting the diameter change over several gear teeth will have multiple benefits. Currently if the diameter or gear ratio change (the difference in the size of the initial and final pinions) is significant, the Hybrid Involute Profile will “clash” with the mating output ring gear, an example the clash is depicted in Figure 6.1.

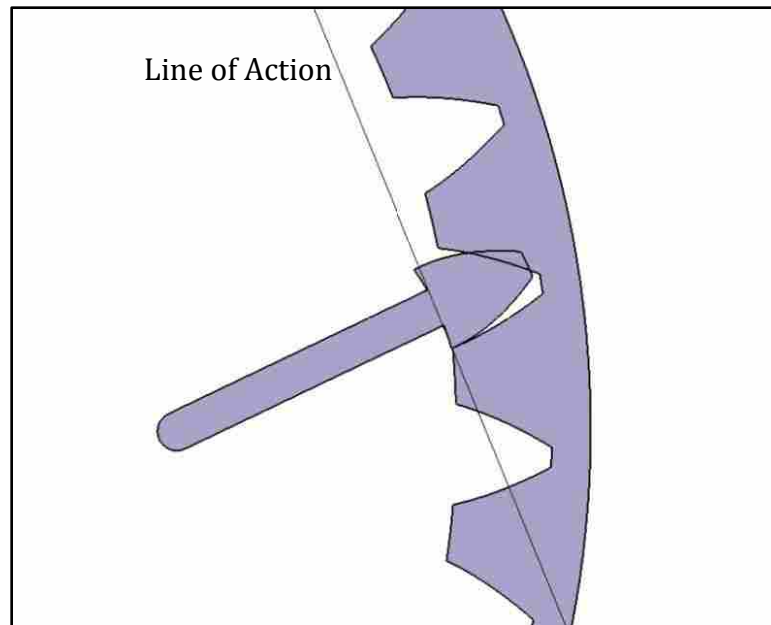


Figure 6.1 Possible Hybrid Involute Profile Clash

This is the case since the center to center distance, (CD) of the mating gears, is only correct for the point which is in contact, and not the proceeding points of contact. By allowing the Hybrid Involute Profile to be segmented over multiple gear teeth, the relative change in CD of each hybrid profile will be diminished so that “clash” will be eliminated. Furthermore, to eliminate clash, segmenting the gear will increase the contact ratio of the gearset. With the Hybrid Involute Profile encompassed on a single gear tooth the contact ratio is restricted to be 1.0. Segmenting the gear will increase the contact ratio above 1.0 depending on the segmentation. Finally segmenting the gear may improve the transition between the use of the standard gear and the Hybrid Involute Profile Gear.

To assist with the elimination of clash as well as improve the contact ratio, the use of a helical gear is recommended. A helical gear would have several benefits; primarily the helical gear will improve the contact ratio due to its helix angle. Also the helical gear may improve the wear characteristics of the Hybrid Involute Gear.

Applying a non-constant acceleration of the point of contact (A_{pc}) in the hybrid profile resulting from the LOA model is recommended as well, for wear and stress characteristics. Currently the constant A_{pc} assumption in the Hybrid Involute Profile will cause the Hybrid Gear be susceptible to the dynamic response of the gear pair. This is a direct result of the constant A_{pc} , in that the derivative of A_{pc} , or the jerk of the Hybrid Involute profile is infinite at the initial and final points of contact (the locations of the discontinuous change in A_{pc}). A non-constant A_{pc} will create a finite jerk profile and will improve the wear and stress characteristics of the Hybrid Involute Gear.

In addition to modifying the Line-of-Action Model it is recommended that a mechanism be developed which will govern the required change in CD while the hybrid

profile is engaged. Also it is recommended that the PECVT embodiment consist of a differential or planetary gearset type of configuration. This is recommended to optimize the ratio of the number of gears (both standard and hybrid) to the number of available operating gear ratios. A differential or planetary gearset configuration would allow for a smaller ratio to exist while utilizing standard transmission components such as brake bands and synchronizers.

Addressing the secondary objectives of section 3.3 is essential to the commercial viability of a PECVT, and it is appropriate to address these issues in the embodiment design phase. The previous secondary objectives include:

- Manufacturability
- Stress Analysis
- Material Properties

Beyond the embodiment design phase, stress analysis of the Hybrid Involute Profile is recommended as well as an investigation of feasible manufacturing methods to manufacture the Hybrid Involute Profile. The stress analysis and manufacturing of the Hybrid Involute Profile will vary from standard involute stress analysis and manufacturing because of the changing base radius. While developing an embodiment of the Hybrid Involute Profile, consideration of material properties of the gear will also need to be considered.

As the efforts to develop a commercially viable PECVT continue, the success or failure of any embodiment may be highly dependent on the design parameters of the Hybrid Involute Profile and its use in a transmission. Parameters such as the diametral pitch, engine conditions such as rpm range, torque and hp, as well as the size of the gear

ratio change between operating standard gear ratios, will have a profound effect on the resulting embodiment. For this reason it is recommended that great care be taken when selecting these parameters, and that any embodiment which is pursued be analyzed for various parameter settings to determine the viability of the PECVT embodiment.

7. References

- [1] **Anderson, Brian S.** *An Investigation of a Positive Engagement, Continuously Variable Transmission.* Department of Mechanical Engineering, Brigham Young University. Provo : Brigham Young University, 2007.
- [2] **Ullrich, Karl and Steven, Eppinger.** *Product Design and Development Third Edition.* New York : McGraw Hill, 2003 . 9780072471465.
- [3] **Dalling, Ryan R.** *An Investigation of Positive Engagement Continuously Variable Transmissions.* Department of Mechanical Engineering, Brigham Young University. Provo : Brigham Young University, 2008.
- [4] **Buckingham, Earle.** *Analytical Mechanics of Gears.* New York : McGraw Hill, 1949.
- [5] **Pahl, G., et al.** *Engineering Design a Systematic Approach 3rd Edition.* London : Springer, 2007. 9781846283185.
- [6] **Buckingham, Earle and Buckingham, Eliot K.** *Revised Manual of Gear Design.* New York : Industrial Press, 1981. 0831131160.
- [7] *Barloworld.* [Online] [Cited: March 4, 2008.] <http://www.barloworld-cvt.com/barloworld/products>.
- [8] *The Operation and Kinematic Analysis of a Novel Cam-based Infinitely Variable Transmission.* **Lahr, Derek and Hong, Dennis W.** Philadelphia : ASME, 2006. DETC2006-99634.
- [9] **Vogel, Werner F.** *Involutometry and Trigonometry.* Michigan : Michigan Tool Company, 1945.
- [10] **Norton, Robert L.** *Machine Design an Integrated Approach 3rd Edition.* Upper Saddle River : Pearson Prentice Hall, 2006. 0131481908.
- [11] **Cleghorn, W. L.** *Mechanics of Machines.* New York : Oxford University Press, 2005. 9780195154528.
- [12] **Norton, Robert L.** *Design of Machinery 4th Edition.* New York : McGraw Hill, 2008. 9780073121581.
- [13] *A Survey of Positively Engagement, Continuously Variable Transmissions.* **Anderson, Brian S., Dalling, Ryan R. and Todd, Robert H.** Las Vegas : ASME, 2007. DETC2007-34856.
- [14] **McArdle, Pat.** "Frequently Asked Questions". *Polaris SAE Team.* [Online] February 9, 2008. http://www.polarissuppliers.com/sae_team/faq.htm.
- [15] **Ladewig, Gunter.** "The Theory of Inventive Problem Solving (TRIZ)". [Online] [Cited: April 25, 2007.] <http://www.primaperformance.com/triz.htm>.

- [16] **Souchkov, Valeri.** TRIZ: A Systematic Approach to Innovative Design. *Knowledge Base*. [Online] Insytec. [Cited: January 15, 2008.] <http://www.insytec.com/TRIZApproach.htm>.
- [17] History of AGMA. *American Gear Manufacturers Association*. [Online] [Cited: August 9, 2008.] <http://www.agma.org/Content/NavigationMenu/AboutAGMA/HistoryofAGMA/default.htm>.
- [18] **Bowers, George, Hawkins, Matt and Fox, Paul.** [interv.] B. Levi Haupt, Isaac Jones and Robert Todd. Indianapolis, June 11, 2008.

8. Appendix A

The Matlab .m file code containing the line of action model

```
%This file calculates the required adjustment of radius and angle
needed for
%the Line of Action Model
```

```
%Required Inputs:
```

```
% Npo Initial Pinion Number of Teeth
% Npf Final Pinion Number of Teeth
% Nr Ring Number of Teeth
% DP Diametral Pitch
% PhiG Pressure Angle at the Pitch Radius
% Ppco Initial Position of the Point of Contact
% Wp Angular Velocity of the Pinion
% Tstep (n-1) Number of Time Increments
```

```
function LofA(Npo,Npf,Nr,DP,PhiG,Ppco,Wp,Tstep)
```

```
if nargin==0
```

```
    Npo=12;
    Npf=24;
    Nr=36;
    DP=3;
    PhiG=22.5; %degrees
    Ppco=0;
    Wp=-12; %rad/sec
    Tstep=99;
```

```
end
```

```
%Standard Involutometry EQs
```

```
%Pinion (Driving) Gear
```

```
%Rpp Pitch Radius of Pinion
```

```
    Rpp_o=Npo/(2*DP)
```

```
%Rap Addendum Radius of Pinion
```

```
    Rap_o=Rpp_o+1/DP;
```

```
%Rbp Base Radius of Pinion
```

```
    Rbp_o=Rpp_o*cosd(PhiG)
```

```
%Tooth Thickness at Pitch Diameter
```

```
    Tp=pi/(2*DP);
```

```
%Involute function of Global Phi (Inv_g)
```

```
    Inv_g=tan(PhiG*pi/180)-PhiG*pi/180;
```

```
%Rppf Final Pitch Radius of Pinion
```

```
    Rpp_f=Npf/(2*DP);
```

```
%Rbpf Final Base Radius of Pinion
```

```
    Rbp_f=Rpp_f*cosd(PhiG);
```

```
%Rapf Final Addendum Radius of Pinion
```

```

        Rap_f=Rpp_f+1/DP
%Ring (Driven) Gear
    %Rpr Pitch Radius of Ring
        Rpr=Nr/(2*DP);
    %Rar Addendum Radius of Ring
        Rar=Rpr+1/DP;
    %Rir Inside Radius of Ring
        Rir=(Nr-1.2)/(2*DP);
    %Rbr Base Radius of Ring
        Rbr=Rpr*cosd(PhiG);
    %Tooth Thickness at Pitch Diameter
        Tpr=pi/(2*DP);
    %Initial Angular Velocity of Ring (Wr_o)
        Wr_o=Wp*Rpp_o/Rpr;
    %Final Angular Velocity of Ring (Wr_f)
        Wr_f=Wp*Rpp_f/Rpr;

%Angle from points of contact of Intitial Pinion w/ respect to the Ring
    %Angle to first point of contact (Eta)
        %Length along Line of Action (Arc Length of Engagement)
        La_o=Rpr*sind(PhiG)-sqrt(Rir^2-Rbr^2);
    EtaA_o=acos((-La_o^2+Rir^2+Rpr^2)/(2*Rir*Rpr));
    %Angle to Final point of contact (EtaA)
        %Length along Line of Action (Arc Length of Engagement)
        Lr_o=sqrt(Rap_o^2-Rbp_o^2)-Rpp_o*sind(PhiG);
        Rco=sqrt(Rpr^2+Lr_o^2-2*Rpr*Lr_o*cosd(PhiG+90));
    EtaR_o=acos((-Lr_o^2+Rco^2+Rpr^2)/(2*Rco*Rpr));
%Angle from points of contact of Final Pinion
    %Angle to first point of contact (Eta)
        %Length along Line of Action (Arc Length of Engagement)
        La_f=Rpr*sind(PhiG)-sqrt(Rir^2-Rbr^2);
    EtaA_f=acos((-La_f^2+Rir^2+Rpr^2)/(2*Rir*Rpr));
    %Angle to Final point of contact (EtaA)
        %Length along Line of Action (Arc Length of Engagement)
        Lr_f=sqrt(Rap_f^2-Rbp_f^2)+(Rpr-Rpp_f)*sind(PhiG)-
Rpr*sind(PhiG);
        Rcf=sqrt(Rpr^2+Lr_f^2-2*Rpr*Lr_f*cosd(PhiG+90));
    EtaR_f=acos((-Lr_f^2+Rcf^2+Rpr^2)/(2*Rcf*Rpr));

%Time Array of Initial Pinion
    Tfinal_o=(La_o+Lr_o)/(abs(Wr_o)*Rbr);%(EtaA_o+EtaR_o)/abs(Wr_o)
    t_o=[0:Tfinal_o/Tstep:Tfinal_o]'; %sec

%Time Array of Hybrid Pinion
    %Intitial Guesses of Apc and Tfinal_c
        Apc=500; %Raidans/s^2
        Tfinal_c=.02; %sec
    Time=[Apc, Tfinal_c]; %Radians
    %Function to find values of ThetaInm and Thetam
        [Time,fval]=fsolve(@MFunc,Time,[],La_o, Lr_f, Rbp_o, Rbp_f, Wp,
Ppco);
    %Position of Input
        Apc=Time(1);
    %Position of Output
        Tfinal_c=abs(Time(2)) ;
    t_c=[0:Tfinal_c/Tstep:Tfinal_c]'; %sec

```

```

%Time Array of Final Pinion
Tfinal_f=(La_f+Lr_f)/(abs(Wr_f)*Rbr);%(EtaA_f+EtaR_f)/abs(Wr_f)
t_f=[0:Tfinal_f/Tstep:Tfinal_f]'; %sec

%Psi
Psi=(PhiG-90)*pi/180; %rad
%PhiG in Radians
PhiG=PhiG*pi/180; %rad

%Initial Tooth Profile Radius of Contact (Ri_o)
%Initial Contact Velocity Vo
Vo_o=Wr_o*Rbr*i*exp(i*PhiG); %in/sec
%Velocity of the point of contact
Vpc_o=(abs(Vo_o)).*exp(i*Psi); %in/sec
%Position of the Point of Contact (Ppc)
Ppc_o=(abs(Vo_o).*t_o+Ppco).*exp(i*Psi); %in
%Radius of Contact Point on Ring (Rcr)
Rcr_o=Rir*exp(i*EtaA_o)+Ppc_o; %in
%Center Distance (CD)
CD_o=(Rpr-Rpp_o).*exp(i*0);
%Radius of Pinion at Point of Contact (Ri_o)
Ri_o=Rcr_o-CD_o;
%Eqs to determine Initial Involute profile (Ri_o)
%Pressure Angle
Phi_o = acos(Rpp_o.*cos(PhiG)./abs(Ri_o));
%Involute Function of Phi (Inv_i)
Inv_o=tan(Phi_o)-Phi_o;
%Arc Length of Tooth (T_i)
T_o = 2.*abs(Ri_o).*(Tp./(2.*Rpp_o)+Inv_g-Inv_o);
%Chordal Tooth Thickness
Tc_o = 2.*abs(Ri_o).*sin(T_o./(2.*abs(Ri_o)));
%X Coordinate
X_o=Tc_o./2;
%Y Coordinate
Y_o=sqrt(abs(Ri_o).^2-X_o.^2);
%Path of Contact (Ri_o)
Xp_o=abs(Ri_o).*sin(Phi_o-PhiG);
Yp_o=Rpp_o-abs(Ri_o).*cos(Phi_o-PhiG);
%Slope of the Path of Contact
PCslope_o=polyfit(Xp_o,Yp_o,1)

%Hybrid Tooth
%Initial Contact Velocity Vo
Vo_c=Wr_o*Rbr*i*exp(i*PhiG); %in/sec
MagVo=abs(Vo_c);
AngVo=angle(Vo_c);
%Velocity of the point of contact
Vpc_c=(Apc.*t_c+abs(Vo_c)).*exp(i*Psi); %in/sec
%Position of the Point of Contact (Ppc)
Ppc_c=(Apc/2.*t_c.^2+abs(Vo_c).*t_c+Ppco).*exp(i*Psi); %in
%Radius of Contact Point on Ring (Rcr)
Rcr_c=Rir*exp(i*EtaA_o)+Ppc_c; %in
%Angle between Rcr and Pitch Point (GammaR)
GammaR=angle(Rcr_c); %rad

```



```

%Angular Velocity of Ring (Wr)
Wr_c=abs(Vpc_c)./(abs(Rcr_c).*cos(PhiG-GammaR));%rad/sec
%Contact Velocity of Ring
Vcr_c=abs(Rcr_c).*cos(PhiG-GammaR).*exp(i*(Psi)).*Wr_c;%
in/sec
MagVcr=abs(Vcr_c);
AngVcr=angle(Vcr_c)*180/pi;
%Fundamental Law of Gearing (Rpp_fl)
Rpp_c=abs(Rpr.*Wr_c/Wp);
%Center Distance (CD)
CD_c=(Rpr-Rpp_c).*exp(i*0);
%Radius of Pinion at Point of Contact (Rip)
Ri_c=Rcr_c-CD_c;
%Angle between Rcp and Pitch Point (GammaP)
GammaP=angle(Ri_c);
%Velocity of the Point of Contact on the Pinion Vcp
Vcp=abs(Ri_c).*abs(Wp).*cos(PhiG-GammaP).*exp(i*Psi);
RipMag=abs(Ri_c);
%Eqs to determine the Involute profile
%Pressure Angle
Phi_c = acos(Rpp_c.*cos(PhiG)./abs(Ri_c));
%Involute Function of Phi (Inv_i)
Inv_c=tan(Phi_c)-Phi_c;
%Arc Length of Tooth (T_i)
T_c = 2.*abs(Ri_c).*(Tp./(2.*Rpp_c)+Inv_g-Inv_c);
%Chordal Tooth Thickness
Tc_c = 2.*abs(Ri_c).*sin(T_c./(2.*abs(Ri_c)));
%X Coordinate
X_c=Tc_c./2;
%Y Coordinate
Y_c=sqrt(abs(Ri_c).^2-X_c.^2);
%Path of Contact (Ri_o)
Xp_c=abs(Ri_c).*sin(Phi_c-PhiG);
Yp_c=Rpp_c-abs(Ri_c).*cos(Phi_c-PhiG);
PCslope_c=polyfit(Xp_c,Yp_c,1)
Growth=polyfit(abs(Rpp_c),abs(Ri_c),1)

%Final Tooth Profile Radius of Contact (Ri_f)
%Initial Contact Velocity Vo
Vo_f=Wr_f*Rbr*i*exp(i*PhiG); %in/sec
%Velocity of the point of contact
Vpc_f=(abs(Vo_f)).*exp(i*Psi); %in/sec
%Position of the Point of Contact (Ppc)
Ppc_f=(abs(Vo_f).*t_f+Ppco).*exp(i*Psi); %in
%Radius of Contact Point on Ring (Rcr)
Rcr_f=Rir*exp(i*EtaA_f)+Ppc_f; %in
%Center Distance (CD)
CD_f=(Rpr-Rpp_f).*exp(i*0);
%Radius of Pinion at Point of Contact (Rip)
Ri_f=Rcr_f-CD_f;
%Eqs to determine Initial Involute profile
%Pressure Angle
Phi_f = acos(Rpp_f.*cos(PhiG)./abs(Ri_f));
%Involute Function of Phi (Inv_i)
Inv_f=tan(Phi_f)-Phi_f;

```

```

    %Arc Length of Tooth (T_i)
    T_f = 2.*abs(Ri_f).*(Tp./(2.*Rpp_f)+Inv_g-Inv_f);
    %Chordal Tooth Thickness
    Tc_f = 2.*abs(Ri_f).*sin(T_f./(2.*abs(Ri_f)));
    %X Coordinate
    X_f=Tc_f./2;
    %Y Coordinate
    Y_f=sqrt(abs(Ri_f).^2-X_f.^2);
    %Path of Contact (Ri_o)
    Xp_f=abs(Ri_f).*sin(Phi_f-PhiG);
    Yp_f=Rpp_f-abs(Ri_f).*cos(Phi_f-PhiG);
    PCslope_f=polyfit(Xp_f,Yp_f,1)

%Plots of Involute Curves
figure(1)
subplot(221)
plot(Tc_f,t_f,'r',Tc_o,t_o,'g',Tc_c,t_c,'b')
grid;
axis ([-.65 .65 -.01 .07])
xlabel('Tc');
ylabel('Time');
title('Chordal Length vs Time');
legend('Final','Initial','Hybrid','location','SouthOutside')

subplot(222)
plot(Tc_f,abs(Ri_f),'r',Tc_o,abs(Ri_o),'g',Tc_c,abs(Ri_c),'b')
grid;
axis ([-2.5 2.5 1.75 4.35])
xlabel('Tc');
ylabel('Ri');
title('Chordal Length vs Ri');
legend('Final','Initial','Hybrid','location','SouthOutside')

subplot(223)
plot(X_o,Y_o+(Rpp_f-Rpp_o),'g',-X_o,Y_o+(Rpp_f-Rpp_o),'g',X_f,Y_f,'r',-
X_f,Y_f,'r',X_c,Y_c+(Rpp_f-Rpp_c),'b',-X_c,Y_c+(Rpp_f-Rpp_c),'b');
axis ([-.35 .35 3.75 4.35])
grid;
xlabel('X');
ylabel('Y');
title('Involute Profiles');

subplot(224)
plot(Xp_f, Yp_f,'r',Xp_o,Yp_o,'g',Xp_c,Yp_c,'b')
grid;
xlabel('Xp');
ylabel('Yp');
title('Path of Contact');

figure (2)
plot(X_o,Y_o+(Rpp_f-Rpp_o),'g',-X_o,Y_o+(Rpp_f-Rpp_o),'g',X_f,Y_f,'r',-
X_f,Y_f,'r',X_c,Y_c+(Rpp_f-Rpp_c),'b',-X_c,Y_c+(Rpp_f-Rpp_c),'b');
axis ([-.35 .35 3.75 4.35])
grid;
xlabel('X');
ylabel('Y');

```

```

title('Involute Profiles');
%legend('Initial','Initial','Hybrid','Hybrid','Final','Final','location
','SouthOutside')

figure (3)
plot(Xp_o,Yp_o,'g',Xp_c,Yp_c,'b',Xp_f,Yp_f,'r')
grid;
xlabel('Xp');
ylabel('Yp');
title('Path of Contact');
%legend('Initial','Hybrid','Final','location','SouthOutside')

%Function used for Fsolve of BCIm
function Time_c = MFunc(Time, La_o, Lr_f, Rbp_o, Rbp_f, Wp, Ppco);
    %Prep Equations
    Apc=Time(1);
    Tfinal_c=Time(2);
    Ppc=La_o+Lr_f;
    Vo=Wp*Rbp_o;
    Vf=Wp*Rbp_f;
    %System of Equations
    Time_c=[Vf-Apc*Tfinal_c-Vo,Ppc-Apc*Tfinal_c^2/2-Vo*Tfinal_c-
Ppco];

```